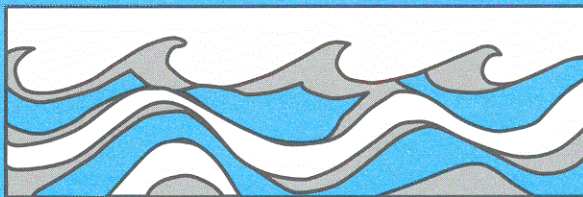


University of Washington
Department of Civil and Environmental Engineering



EFFECTS OF LAND COVER CHANGE ON THE HYDROLOGIC RESPONSE OF PACIFIC NORTHWEST FORESTED CATCHMENTS

James VanShaar



Water Resources Series
Technical Report No.165
October, 2002

Seattle, Washington
98195

Department Of Civil Engineering
University Of Washington
Seattle, Washington 98195

EFFECTS OF LAND COVER CHANGE
ON THE HYDROLOGIC RESPONSE OF PACIFIC NORTHWEST
FORESTED CATCHMENTS

by

James Vanshaar
Dennis P. Lettenmaier

Water Resources Series
Technical Report No. 165

April 2001

ABSTRACT

Extraction of natural resources, development of river systems, and conversion of desert-land to agriculture have changed the face of the Pacific Northwest. Quantification of the effects of these changes on the hydrology of the region is an ongoing challenge. Recent development of spatially distributed mathematical models provides a new laboratory for examination of complex interactions within the natural system. A previous assessment of the hydrologic effects of land cover change over the Columbia River Basin was made at a coarse spatial resolution of 1/4 degree. While broad patterns of change were identified, interpretation at the catchment scale was not possible. This study investigated the effects of land cover change on the hydrology of four catchments (97 to 1033 km²) within the Columbia River Basin (Mica Creek, Idaho, Swan River, Montana, Entiat River, Washington, and Mores Creek, Idaho). The Distributed Hydrologic Soil Vegetation Model (DHSVM) was applied using high resolution (20-30 m) current land cover data derived primarily from satellite imagery. Historical conditions were derived by transposing historical changes from 1900 to present using 1-km resolution land cover data developed by the Interior Columbia Basin Ecosystem Management Project (ICBEMP). This investigation infers increased average annual runoff 1900 of 19.2 and 6.1 percent in the Mores and Entiat catchments. Disparities between these results and those extracted from the macro-scale study are attributed to land-cover data preparation algorithms. Increases in average annual peak flows 20.6, 8.6, 6.0, and 0.9 percent were predicted for Mores, Entiat, Swan and Mica respectively, with maximum changes during the modeled period considerably longer. Fully-forested, fully-harvested, and road/no-road conditions were examined for all four catchments. Additional investigation was made using a 1-km aggregation of Mores current vegetation and a reconstruction of conditions in 1933 (shortly after extensive clear-cut harvest) for Mica. Aggregation of vegetation in Mores did not significantly affect the model predictions. For a fully-harvested condition, average increases in mean annual flow of 45.8 mm, 175 mm, 118 mm, and 423 mm were predicted for the Mores, Entiat, Swan and Mica catchments, respectively.

TABLE OF CONTENTS

	Page
LIST OF FIGURES.....	iii
LIST OF TABLES.....	vi
CHAPTER 1: INTRODUCTION.....	1
1.1 LAND COVER CHANGE IN THE COLUMBIA RIVER BASIN.....	2
1.2 HYDROLOGIC EFFECTS OF LAND COVER CHANGE.....	3
1.3 RESEARCH OBJECTIVES AND APPROACH.....	9
CHAPTER 2: BACKGROUND.....	12
2.1 PRECIPITATION AND VEGETATION.....	12
2.2 TRANSPIRATION.....	14
2.3 ENERGY BALANCE AND VEGETATION.....	14
2.4 FOREST ROADS AND WATER FLOW PATHS.....	16
2.5 CATCHMENT AND BASIN STUDIES.....	18
CHAPTER 3: CATCHMENT DESCRIPTIONS.....	21
3.1 APPROACH.....	21
3.1.1 <i>Stream Characteristics</i>	21
3.1.2 <i>Road and Culvert Mapping</i>	22
3.1.3 <i>Other Observations</i>	24
3.2 DIGITAL DATA ACQUISITION:.....	24
3.2.1 <i>Spatial Data:</i>	24
3.2.2 <i>Temporal Data:</i>	27
3.3 DESCRIPTION OF CATCHMENTS.....	28
3.3.1 <i>Mica Creek, Idaho</i>	28
3.3.2 <i>Swan River, Montana</i>	32
3.3.3 <i>Entiat River, Washington</i>	35
3.3.4 <i>Mores Creek, Idaho</i>	39
CHAPTER 4: DISTRIBUTED HYDROLOGIC SOIL AND VEGETATION MODEL (DHSVM).....	44
4.1 MODEL OVERVIEW.....	44
4.2 VEGETATION-CANOPY SUB-MODEL.....	55
4.2.1 <i>Attenuation of Above-canopy Forcings</i>	55
4.2.2 <i>Evapotranspiration</i>	56
4.3 APPLICATIONS OF DHSVM.....	57
CHAPTER 5: PARAMETER ESTIMATION.....	60
5.1 DEM.....	60
5.2 SOILS.....	61

5.3 STREAMS AND ROADS.....	63
5.4 CURRENT VEGETATION.....	66
5.5 SURFACE CHARACTERISTICS USED IN SENSITIVITY STUDIES.....	70
5.5.1 <i>Historical Approximation</i>	70
5.5.2 <i>Other Vegetation Scenarios</i>	93
5.6 METEOROLOGICAL DATA	94
5.6.1 <i>Time Series Preparation</i>	94
5.6.2 <i>Spatial Distribution</i>	97
CHAPTER 6: MODEL CALIBRATION	99
6.1 MICA CREEK.....	100
6.2 SWAN RIVER	114
6.3 ENTIAT RIVER.....	118
6.4 MORES CREEK	123
CHAPTER 7: RESULTS	129
7.1 ANNUAL WATER BALANCE	130
7.1.1 <i>Current vs. Historic Vegetation</i>	130
7.1.2 <i>Extremes, Special Cases, and Roads</i>	135
7.1.3 <i>Spatial patterns of ET</i>	137
7.2 ANNUAL PEAKS	141
7.3 STORAGE: SNOW AND SOIL MOISTURE.....	147
7.4 COMPARISON WITH VIC MODEL PIXEL(S)	159
LIST OF REFERENCES.....	175
APPENDIX A: VEGETATION CLASS DESCRIPTIVE PARAMETER ESTIMATION	184

LIST OF FIGURES

Number.....	Page
1-1 Distance between catchments vs. coincident peak flows	6
1-2 Columbia River basin and study catchment locations	10
2-1 Mechanisms of runoff interception by the road network	17
3-1 Mica Creek: Elevation, modeled streams and gages	29
3-2 Mica Creek: Roads and modeled streams	30
3-3 Swan River: Elevation, modeled streams and gages	33
3-4 Swan River: Roads and modeled streams	34
3-5 Entiat River: Elevation, modeled streams and gages	36
3-6 Entiat River: Roads and modeled streams.....	37
3-7 Mores Creek: Elevation, modeled streams and gages.....	40
3-8 Mores Creek: Roads and modeled streams	41
4-1 Schematic representation of DHSVM inputs, preprocessing requirements, outputs and interaction with GIS software.....	45
4-2 DHSVM: Model representation	47
4-3 DHSVM: One-dimensional vertical water balance.....	49
4-4 DHSVM: Snow model	51
4-5 DHSVM: Runoff production.....	53
4-6 Applications of DHSVM.....	58
5-1 Mica Creek vegetation	71
5-2 Swan River vegetation	73
5-3 Entiat River vegetation.....	75

5-4	Mores Creek vegetation	77
5-5	Historical vegetation development procedure.....	81
5-6	Mica Creek LAI	85
5-7	Swan River LAI	87
5-8	Entiat River LAI.....	89
5-9	Mores Creek LAI	91
6-1	Mica streamflow calibration and validation hydrographs.....	103
6-2	Mica SNOTEL SWE calibration / validation.....	105
6-3	Mica vegetation classification based on the University of Montana TM land cover classification	107
6-4	Mica Creek LAI: Current (Potlatch) - Current (UMT TM)	111
6-5	Mica Creek: Potlatch, UMT TM classification, and observed discharge hydrographs.....	113
6-6	Swan River streamflow calibration and validation hydrographs	116
6-7	Skylark Trail SNOTEL SWE calibration / validation.....	117
6-8	Entiat River streamflow calibration and validation hydrographs.....	122
6-9	Pope Ridge SNOTEL SWE calibration / validation	124
6-10	Mores Creek streamflow calibration and validation	128
7-1	Mean annual runoff depths for all investigation runs	132
7-2	Mean annual ET depths for all investigation runs.....	133
7-3	Catchment maps of residual ET	139
7-4	Annual peak flows: Mores Creek.....	142
7-5	Annual peak flows: Entiat River	143
7-6	Annual peak flows: Swan River.....	144

7-7	Annual peak flows: Mica Creek.....	145
7-8	Maximum flood during investigation: Flowrate and percent change	148
7-9	Range of percent change in annual maximum flood.....	149
7-10	Current maximum annual SWE vs. alternative vegetation maximum annual SWE.....	151
7-11	Catchment average annual SWE time-series	153
7-12	Spatial distribution of SWE: Mores Creek and Swan River	155
7-13	Spatial distribution of SWE: Mica Creek and Entiat River	157
7-14	Average seasonal spatial patterns of depth to water table: Mores Creek and Swan River	161
7-15	Average seasonal spatial patterns of depth to water table: Mica Creek and Entiat River	163
7-16	VIC ¼ degree pixels and catchment overlay.....	165
7-17	Average annual runoff: VIC & DHSVM	167
7-18	Average annual ET: VIC & DHSVM	168

LIST OF TABLES

Number.....	Page
3-1 Data sources by catchment.....	25
5-1 Catchment DEM attributes.....	61
5-2 DHSVM soil class parameters	62
5-3 Contributing area for stream initiation	64
5-4 Data sources by catchment.....	67
5-5 Vegetation species / stage classes	69
5-6 Vegetation class descriptive parameters	79
6-1 Mica Creek: Annual flow volumes	102
6-2 Swan River: Annual flow volumes	119
6-3 Entiat temperature lapses	120
6-4 Entiat River: Annual flow volumes.....	121
6-5 Mores Creek: Annual flow volumes	127
7-1 Meteorological data time periods.....	129
7-2 Current – Historic residual values.....	130
7-3 Annual water balance: VIC vs. DHSVM.....	170

ACKNOWLEDGMENTS

In a work of this nature there are many who contribute their time, expertise, and support in one way or another. Thanks to the United States Forest Service and United States Environmental Protection Agency for providing the funding for this work. Terrance Cundy, Brian Thomas and Brant Steigers of Potlatch Corporation and John Gravelle of Pine Orchard provided extensive information and resources for work in Mica Creek. Many at the Flathead National Forest and Swan Valley Visitors Center, Roly Redmond of the University of Montana and Brian Sugden of Plum Creek Timber Co. helped with Swan River. Many at the Wenatchee National Forest and Entiat Ranger District including Tom Robison, Patrick Murphy, Vickie Cunderla, Rick Edwards, and Claudia Narcisco and Brion Salter and John Lehmkul of the Pacific Northwest Research Station, and Scott Pattee of Natural Resources Conservation Service helped with the Entiat River. For help on Mores Creek, thanks goes to many folks at the Boise National Forest and Idaho City Ranger District including Cavan Maloney and Diane McConnaughey, Bob Smith of the Idaho Department of Lands, and Herb Manay, Jon Haufler, Chris Clay and Domini Glass of Boise Cascade. Thanks go to Greg Enstrom, Bernt Matheussen and Greg O'Donnel for help and information regarding the Matheussen, et al (2000) work. Thanks to Garry Schaefer of NRCS for extra details on SNOTEL gage locations, Iris Goodman of the EPA for getting me started on this project, and Tamara Yellin for assisting with preparation of this document. Special thanks go to my colleagues at the University of Washington for help too extensive to elaborate: Laura Bowling, Bart Nijssen, Pascal Storck, Serhad Atakturk, Ingjerd Haddeland, Ed Maurer, and Kyle Comanor. Thanks to Steve Burges and Rick Palmer who served on my Master's thesis committee and Dennis Lettenmaier for providing me with this opportunity and all the work that went with being my major professor.

Chapter 1: Introduction

Through history, man has developed an ever-increasing ability to modify his environment. In applying that ability, he has changed not only his immediate surroundings and circumstances, but also those that are more generally termed "nature." In some cases, he has not only changed the condition of the landscape, but the rates and processes that formed it.

The anthropogenic development of the Columbia River Basin precedes Anglo-European settlement. Native American peoples extracted natural resources such as fish, game, and berries and employed fire as a tool for enhancing the system for their benefit. In the mid-1800's Anglo-European influence took hold as migrants passed through the area, primarily on their way to Oregon and California farmlands. Shortly thereafter, gold, silver, and other precious minerals were discovered. Wagon roads, railroad, and in some cases, navigation of the rivers provided improved access to the region. Towns were built and other services developed to support the settlers.

Near the turn of the 20th century, the Newlands Reclamation Act promoted cooperative ventures in irrigated agriculture. Funds generated by the sale of federal lands were used to underwrite the construction of dams, canals and ditches (USDA Forest Service, 1996a). The Reclamation Service was established in 1908. New Deal projects introduced large dams, navigation

enhancements, and irrigation systems that have changed much of the Columbia River into a series of reservoirs and created productive farmland from arid lands.

As demands for land, timber, and water grew, the federal government took measures to preserve, protect, and otherwise manage the forested uplands of the West. National Forests were established with the intent that sale of timber would offset the costs of preservation. Places of extraordinary beauty were set aside as parks and monuments and the National Park Service was organized in 1916 to manage them. Beginning with these parks, an extensive system of recreational opportunities has been developed in accordance with the growing public demand for these services (USDA Forest Service, 1996a).

1.1 Land Cover Change in the Columbia River Basin

The development of the region's resources has greatly changed the face of the Columbia basin over the last 150 years. Basin-wide, only three percent of the current landscape pattern represents the historical conditions (USDA Forest Service, 1996a). Federally funded dams impound most of the flow of the Columbia and Lower Snake Rivers. The reservoirs provide water for navigation, irrigation, hydropower generation, and recreation, and have virtually eliminated major flooding within the main channels. They have also disrupted the natural flow of water, sediment, and populations of anadromous fish throughout much of the basin. Parts of the river system are now connected by canals with an extensive irrigated agricultural system. Federal and state irrigation projects have replaced the desert in parts of the mid-Columbia,

Yakima, and the Snake River plain. Farming and ranches have converted shrub land to dry farms while cattle have taxed the vegetative capacity of rangeland.

Over the last hundred years, forestry practices have also changed the face of the land by interfering with the natural successional sequence of wildland. Fire suppression and management practices have resulted in increased density, forest age, and forest extent (aforestation) in parts of the basin while selective and clear-cut harvesting and stand-replacing fire have reduced the average forest maturity elsewhere (deforestation).

Changes in forest characteristics arguably have had a greater impact on the hydrology of the Columbia River basin than have other land use changes. Generally, the forested uplands receive the largest amounts of precipitation and thus dominate the hydrology of the system (Matheussen, et al, 2000). According to the U.S. Forest Service, of the national forest land within the Columbia River basin, 29 percent occurs in reserve (or wilderness) areas where limited fire suppression occurs; 5 percent is in a condition similar to the historical condition, and the remaining 66 percent is managed for harvest.

1.2 Hydrologic Effects of Land Cover Change

Changes in forest maturity drive hydrological change in two primary ways. First, vegetation extracts water from a river catchment, either through transpiration or by interception and subsequent evaporation of precipitation. In general terms, increasing vegetation extent and/or

vegetation maturity increases evapotranspiration. Second, vegetation affects snow accumulation and ablation patterns. Snow intercepted by the forest canopy either evaporates, or falls to the forest floor as melt water or as saturated snow masses, thus reducing the under-canopy snow pack volumes (Storck and Lettenmaier, 1999; Kattleman, 1990; Berris and Harr, 1987).

Intercepted snow may be more susceptible to energy transfer, and thus melt (Miller, 1967) while snow beneath the canopy is shielded from the full effects of incoming radiation (Pomeroy and Dion, 1996; Black, et al 1991) and turbulent and latent heat transfers (Harr, 1981). In general, more vegetation and more mature vegetation: a) reduce the surface snow pack volumes and b) reduce the radiative and sensible heat transfers to the surface snow pack by attenuating the wind and short wave solar radiation by the canopy.

These two primary mechanisms may lead to secondary hydrologic changes. Reduced evapotranspiration may result in increased soil moisture, which in turn may increase the extent of saturation and lead to more runoff during snow melt or heavy rainfall events. Increased snowpack, associated with canopy removal, may melt more rapidly through enhanced heat flux into the pack (Wetherbee and Lettenmaier, 1996). Higher water tables and logging roads may result in interception of subsurface water and densification of the stream channel network through introduction of ditches (Bowling and Lettenmaier, 1997; La Marche and Lettenmaier, in press). This creation and rerouting of surface flow redistributes water spatially within a catchment and may change the natural timing of runoff by "short-circuiting" slower subsurface flow paths.

Various field experiments have examined the localized effects of land cover change at the plot or subcatchment scales (Rothacher, 1965, 1970; Megahan, 1972, 1983; Ziemer, 1981; Harr and McCorison, 1979; Troendle and King, 1985; Berris and Harr, 1987; Kattelmann, 1990).

Although these investigations have added understanding of the physical processes by which landscape disturbance affects local hydrologic response, extrapolation to the catchment scale is complicated, because a catchment integrates a variety of land use changes. There is also a question as to how changes at the plot scale are affected by their location within a catchment, which in turn partly determines the effect on catchment outlet hydrographs. These interactions between the plot and catchment scale, sometimes known as *cumulative effects*, are an important aspect of hydrologic change related to landscape disturbance.

Efforts to quantify the effects of land cover change on catchment hydrology date back at least ninety years as Bates and Henry (1928) reported on a study at Wagon Wheel Gap, Colorado. The approaches that have been used can be classified into one of three methods: 1) Paired catchment studies, in which one catchment is maintained as a control while the other nearby catchment(s) receive(s) some treatment. The discharge records before and after the treatment are compared, from which the significance of the treatment is deduced; 2) Retrospective studies, which are similar in nature to paired catchment studies, but use stream and land cover records which are not subject to careful scientific control. Statistical methods can be used to extract the *signal* from the records, which often will be smaller than if there were a true control, as changes in land

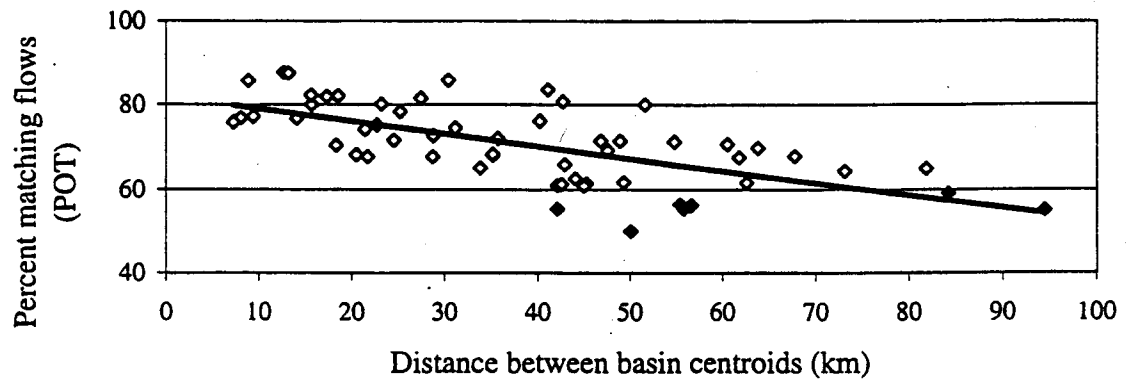


Figure 1-1: Distance between catchments vs. coincident peak flows
Source: Bowling, *et. al.*, 2000

cover occur simultaneously in all catchments (Jones and Grant, 1996; Bowling, et al, 2000); 3) Computer modeling, in which the output from a mathematical model of the natural system is compared with the output from an alternative land cover parameterization of the model. The difference between the two sets of output is attributed to the change in land cover. (Wetherbee and Lettenmaier, 1996, 1997; Bowling and Lettenmaier, 1997; Storck and Lettenmaier, 1999; Matheussen, et al, 2000; Storck, 2000; Bowling, et al, 2000; La Marche and Lettenmaier, in press).

Although much has been learned by applying the first two methods, there are certain limitations inherent in their application. The impossibility of isolating variables in the natural system limits the ability of these methods to determine cause and effect (see Eberhardt and Thomas, 1991). The catchments must be located near each other, which limits the possible range of variation of weather, climate, soils, and geology. Figure 1-1, taken from Bowling, et al. 2000, shows the relationship between the distance between catchments and the incidence of matching peak flows. The catchments must have divergent land use histories. This is controlled in paired catchment studies (which are mostly limited to relatively small catchments), but not in retrospective analyses (necessarily used for larger scale investigations). They must also have sufficiently long and coincident streamflow and weather records. Statistically, sample size limits the ability to identify effects. Furthermore, as disturbed vegetation is reestablished following the disturbance, the magnitude of the differential effect is reduced, so that the largest changes tend to occur during the few years of early re-growth. There is, therefore, an element of chance in the

occurrence of weather patterns that may or may not lead to altered response of treatment and control catchments during the period when land cover differences are the greatest. Finally, the number of possible study catchments diminishes rapidly as catchment size increases. Furthermore, interpretation of changes in large catchments is more confounded by cumulative effects.

The third method, use of a physically-based, spatially distributed hydrological model, addresses the shortcomings of the first two methods. Such models describe the hydrologic processes that are related to land cover in such a way that individual variables can be isolated and modified, allowing direct interpretation of the effects.

Matheussen, et al (2000) investigated the effects of historical land cover change on the hydrology of the Columbia River basin using a macro-scale hydrological model. The Variable Infiltration Capacity (VIC) model of Liang, et al (1994) was parameterized at 1/4 degree spatial resolution (subsequently, the work was repeated using 1/8 degree pixel resolution, although the results have not been published as of the time of this writing). Matheussen, et al (2000) quantified the effects of land cover change within the basin between 1900 and 1990. The 1900 land classification was derived from an estimation of historical conditions for the federal Interior Columbia Basin Ecosystem Management Project (ICBEMP), as described by Quigley and Arbelide (1997); Losensky (1994); Menakis, et al (1996); Hann, et al (1997); Hardy, et al (1996); and Thornton and White (1996). The 1990 land cover classification was derived from remotely

sensed Advanced Very High Resolution Radiometry (AVHRR) visible satellite imagery at 1-km resolution (Loveland, et al, 1991; Loveland and Ohlen, 1993; Menankis, et al, 1996; Hardy, et al, 1996; Thornton and White, 1996; Hann, et al, 1997; Quigley and Arbelide, 1997). The model was forced using 10 years of meteorological data, beginning in 1979. In the land cover experiments, only the vegetation description varied between model runs; the same historical climatological forcings were used in all scenarios and all other parameters remained consistent.

Matheussen, et al (2000) found that the trend toward less mature vegetation within the Columbia River basin (due to extensive logging) resulted in modeled annual average increases of runoff ranging from 4.2 to 10.7 percent for various large sub-basins (the 567,000 km² Columbia River basin, comprises 9 sub-basins). Modeled annual average evapotranspiration decreases ranged from 3.1 to 12.1 percent. While this assessment was sufficient to identify patterns of change over large sub-basins, it is insufficient for interpretation of the texture of the changes and their implications at the catchment scale. Generally speaking, it is at the smaller catchment scale (typical drainage areas 10-500 km²) where individual management decisions are made.

1.3 Research Objectives and Approach

This thesis describes application of the Distributed Hydrology-Soil-Vegetation Model (DHSVM) (Wigmosta, et al, 1994) to four catchments distributed throughout the United States' portion of the Columbia River Basin (Figure 1-2). The purpose of this investigation was to interpret the possible effects of land cover change at the catchment scale. The "current" land cover

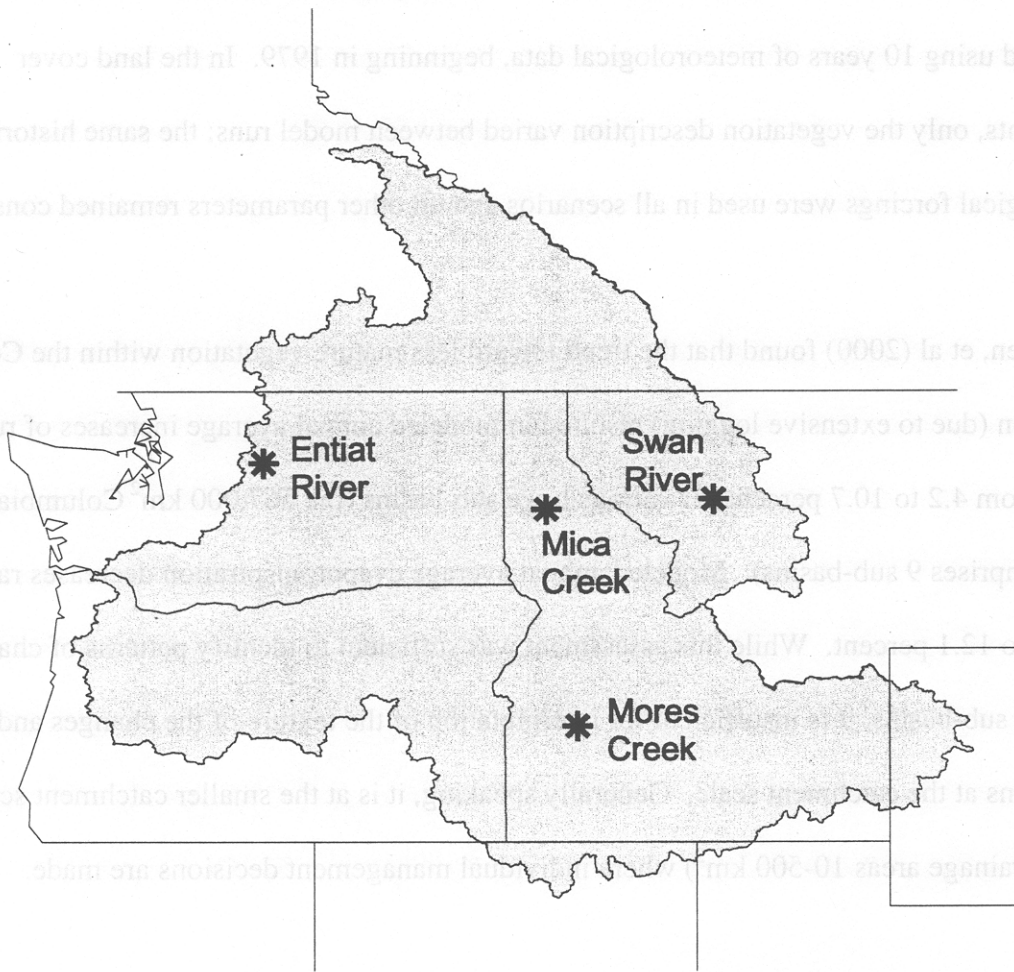


Figure 1-2: Columbia River basin and study catchment locations

classifications were developed for each catchment based on best available land classifications at high spatial resolution (~30 m), which was consistent with spatial resolution of the topographic data used to drive DHSVM. The specific objectives of the analysis were:

- 1- Investigate the effects of land cover change on catchment scale hydrology over the last century.
- 2- Investigate hypothetical extremes to identify limits on land cover influence on hydrologic response.
- 3- Investigate the influence of spatial scale of land cover descriptions on resulting predictions of hydrologic response.

To address these objectives, a series of hydrologic modeling experiments evaluated the model-predicted effects of changes from estimated 1900 land cover conditions (and, in the case of one catchment, inferred 1930's land cover) to the present. Subsequently, these changes were compared to the larger scale results of Matheussen, et al (2000).

Chapter 2: Background

This chapter reviews the mechanisms by which land cover change affects catchment hydrology, with particular emphasis on vegetation and forest road pathways. It also reviews recent research in this area.

2.1 Precipitation and Vegetation

In this thesis, only one-way interactions between land cover and hydrologic response are considered. That is, land cover change is assumed not to affect precipitation or other surface meteorological inputs. Therefore, the volume of precipitation passing through a flat surface overlying the land cover is assumed to be unaffected by vegetation change. On the other hand, the effects of land cover on the interception of precipitation by vegetation, and its transfer to the land surface, are represented.

As precipitation falls through a hypothetical horizontal surface, it first encounters the vegetation canopy. Depending on the nature of the canopy and the state of the precipitation, some portion of the precipitation is intercepted and stored in the canopy. Although the amount of precipitation intercepted varies, on an annual average basis Calder (1993) and Calder, et al (1982) report that 26 to 33 percent was intercepted by coniferous forest vegetation at Plylimon, Wales and subsequently re-evaporated. This range applied to an area where average annual snowfall was only about five percent of annual precipitation. In areas with greater snowfall the fraction of intercepted precipitation would be expected to be larger.

Other investigations have studied interception, focusing on winter precipitation (Miller, 1964; Satterlund and Haupt, 1967, 1970; Storck and Lettenmaier, 1999; Storck, 2000). Storck and Lettenmaier found up to 60 percent of snowfall was intercepted by the forest canopy in a southwestern Oregon site, with mature conifer forest storing as much as 40 mm of snow water equivalent.

Although precipitation, whatever its form, can be stored for some time in the vegetation canopy, eventually it leaves by one of two pathways. The precipitation may exit via state change to water vapor (sublimation from snow, or evaporation from liquid water). Alternatively, the stored water can be transferred by gravity to the underlying (soil or snow) surface. This transfer occurs through windblow, drip of rain or snow melt water, or mass release of clumps of a snow-water mixture. Liquid water is usually stored in the canopy for shorter periods than is snowfall. Intercepted liquid water that does not contribute to throughfall eventually evaporates at a rate determined by meteorological conditions. For snow, Storck and Lettenmaier (1999) found sublimation rates in a Pacific maritime climate to be less than 1 mm/day, with 72 percent of the remainder falling as melt water drip and 28 percent dropping from the canopy to the underlying surface still in solid form.

2.2 Transpiration

Precipitation that reaches the ground is stored in the ground snow pack, in ponds on the surface, in the soil column following infiltration, or contributes directly to runoff. Changes in the effectiveness by which soil moisture can be extracted by vegetation and ultimately transpired, is likely the most significant way that land cover affects hydrologic response of a catchment.

Transpiration depends on a variety of factors including available soil moisture, atmospheric vapor pressure, availability of heat and its rate of exchange with the canopy, and plant physiology. The details of transpiration biophysics are available in a variety of sources (e.g. Monteith, 1965), so plant physiology is discussed only briefly here. The root system influences how much soil moisture is available (in both a horizontal and vertical context) for extraction by the plant. Leaf area defines the region available for exchange of water vapor to the atmosphere. Stomatal structure defines the ease with which this exchange occurs. Overall plant structure influences the rate of heat exchange necessary for liquid to gaseous state change.

2.3 Energy Balance and Vegetation

Land cover has a significant influence on the rates at which the moisture evaporates or melts. These influences are both direct and indirect. The sources of heat available to drive evaporation or melt include radiation (short wave, long wave), sensible heat, advected heat (rain water), and latent heat (ET, condensation). The vegetation canopy attenuates incoming short wave radiation according to the density of the canopy. A portion of direct beam insolation is intercepted while

the percentage of the sky seen—representative of indirect short wave availability—may also be attenuated. Wind speeds are reduced through the canopy by vegetation roughness, which affects the efficiency of sensible heat transfer. Energy is advected by canopy melt water drip and snow mass wasting. Latent heat transfer may also be affected in a secondary fashion, as the vapor pressure deficit beneath the canopy is dampened.

In general, intercepted precipitation remains more fully exposed to atmospheric conditions than does precipitation that reaches the ground. Long wave radiation, sensible and latent heat inputs can occur laterally as well as vertically (Miller 1967).

While some of the more direct influences of vegetation on the energy balance have been mentioned here, the interaction of these influences with the forest canopy can be significantly more complex. The overall effect of these adjustments may vary in magnitude and direction depending on time scales and periods. Some processes which tend to reduce heat exchange with the surface water (liquid or solid) may be counteracted to various degrees by processes increasing the heat exchange. For example, removal of canopy in a localized area will increase the radiative heat transfer with the ground snowpack while reducing the amount of sensible heat that would have been transferred to the snow had it been intercepted by the canopy.

2.4 Forest Roads and Water Flow Paths

As water travels laterally, either at the surface or sub-surface, vegetation has some influence on its micro-scale pathways (see Seyfried and Wilcox, 1995). As observation scale increases, however, the details of these processes no longer require deterministic description. For our purposes, therefore, the larger scale effects of forest roads (a type of land cover) are likely to be more significant.

Roads affect the hydrologic response of a forested catchment in three major ways: 1) conversion of subsurface flow to surface flow; 2) reduced infiltration rates on the road's surface itself; and 3) concentration and rerouting of surface flow in road ditches. Figure 2-1, from Bowling and Lettenmaier (1997), shows these processes schematically. Conversion of subsurface flow to surface flow by the road cut slopes has been observed and investigated extensively (Megahan, 1972; King and Tennyson, 1984; Bowling and Lettenmaier, 1997; La Marche and Lettenmaier, in press). Sullivan and Duncan (1981), Luce and Cundy (1994), and Ziegler and Giambeluca (1997) described infiltration rates significantly lower than surrounding soils. Wemple (1994), Bowling and Lettenmaier (1997) and La Marche and Lettenmaier (in press) described the extension of the natural drainage structure through connectivity of road ditch culvert outflow to streams and redistribution of water by non-connected culvert outfalls.

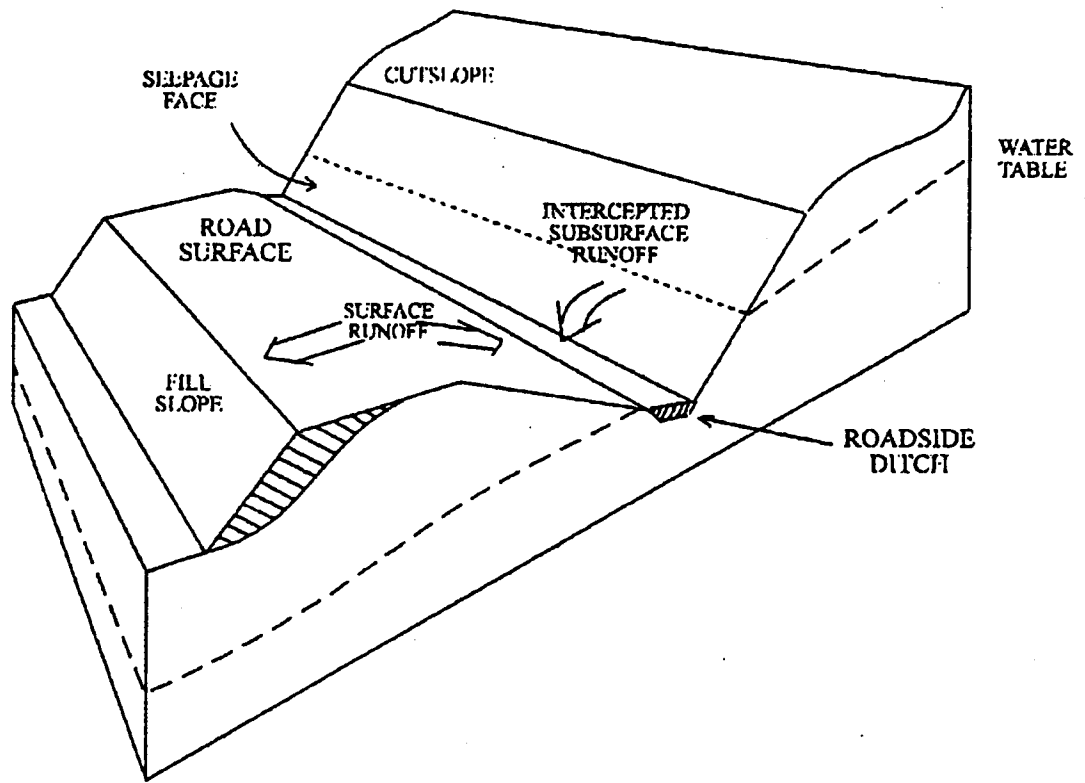


Figure 2-1: Mechanisms of runoff interception by the road network
Source: Bowling and Lettenmaier, 1997

2.5 Catchment and Basin Studies

As the processes described above are integrated over an entire catchment, the interaction of varying land cover changes with characteristics inherent in soil and topography clouds the picture. Due to the cumulative effects of this variation within the catchment, the results of a given treatment cannot be predicted entirely through use of the simple models described earlier in this chapter. On the other hand, the effects of land cover change at the catchment scale have been investigated for nearly 100 years; the first documented study in the U.S. began at Wagon Wheel Gap, Colorado in 1909 (Bates and Henry, 1928).

Because of the need to synthesize the number of studies conducted, the literature reporting on individual studies has periodically been reviewed and summarized (Hibbert, 1967; Bosch and Hewlett, 1982; Sahin and Hall, 1995; Stednick, 1995). Each of these reviews has built on the information presented by the previous studies and has attempted to uncover additional studies. Hibbert (1967) generalized that "reduction of forest cover increases water yield" and "establishment of forest cover on sparsely vegetated land decreases water yield."

Bosch and Hewlett (1982) added 55 catchments to the 39 considered by Hibbert (1967). They inferred that "coniferous forest, deciduous hardwood, brush and grass cover have (in that order) a decreasing influence on water yield." Although highly variable, the data analyzed suggested that for each 10 percent reduction in conifer forest cover, an increase of about 40 mm of water yield

accompanied the change. The authors concluded that the hydrologic effects of reductions in forest cover of less than 20 percent could not be determined by examining streamflow and meteorological records alone. Examining the influence of annual precipitation on the sensitivity of a catchment to land cover disturbance, they concluded that changes in yield were greatest where mean annual precipitation was greatest. The results for these wetter catchments were relatively insensitive to the year by year variation from the mean in precipitation. In dryer areas, year by year variation in precipitation appeared to greatly affect the findings. Mean annual precipitation also controls the length of the recovery period.

In a summary of 95 paired catchment studies in forested areas throughout the United States, Stednick (1996) investigated the effects of timber harvest on annual water yield. He attempted to classify results by region. For the Rocky Mountain / Inland Intermountain region which appears to include southern Idaho and eastern Washington and Oregon of the Columbia River basin, 35 studies were reviewed. The data suggest a threshold harvest rate of about 15 percent for a measurable change to occur. Harvest of 50 percent resulted in increased runoff of 25 to 250 mm. Full clear-cut harvest resulted in 0 to 350 mm of additional runoff. Stednick's regression slope of annual water yield increase versus percent harvest area for this region was the lowest of the series of studies reviewed, with a value of 0.94. Stednick also pointed out that no studies existed for the Continental / Maritime Province region including northeast Washington, the Idaho panhandle and northwestern Montana.

Sahin and Hall (1996) applied fuzzy linear regression to the data from 145 catchment experiments, which included most of the 95 reviewed by Bosch and Hewlett (1982). Their results suggested that conifer forest removal affected water yield more than any other type of vegetation change. Full vegetation removal resulted in a 330 mm increase in annual yield, with 23 mm increase for each 10 percent reduction in cover inferred (this represents a reduction from the earlier estimate by Bosch and Hewlett (1982)). His findings were recommended only for use in cases where treatments exceeded 20-25 percent, and included a preference for 40 percent or more.

Jones and Grant (1996) addressed the effects of clear-cutting and roads on peak flows in large and small catchments. They found that treatment of 10 to 25 percent of the catchment could produce "significant, long-term increases in peak discharges." These increases were attributed primarily to changes in flow paths associated with roads and secondarily to changes in soil moisture associated with vegetation removal. Small catchments experienced up to 50 percent increases in peak discharges with patch cutting and road building. Changes in timing of peak flows were more persistent in roaded than in non-roaded catchments. In large catchments, peak discharge was found to be related to cumulative area harvested, although their attempts to quantify the change could not be reproduced when untransformed residuals are used in the statistical analysis (Thomas and Megahan, 1998).

Chapter 3: Catchment Descriptions

Chapters 1 and 2 discuss historical land cover change in the Columbia River basin. This chapter introduces the data sources used in the hydrologic modeling study which is designed to evaluate the possible hydrologic manifestations of these changes. Subsequent chapters describe the hydrologic model and the details of its parameterization for each of the catchments studied.

3.1 Approach

For each of the four catchments, field reconnaissance was conducted to help provide basic background information that could later be used in the modeling aspect of the study. Some limited mapping of features such as road locations and drainage systems was made using Geographic Positioning System (GPS) equipment. The purpose of the field reconnaissance, which for most of the catchments was conducted during one or two visits of several days each, was to assure that the dominant processes affecting runoff generation in each of the catchments was reflected properly in the model implementations. In addition, the validity of maps of road locations and other catchment attributes was spot-checked.

3.1.1 Stream Characteristics

Stream attributes provided on U.S. Geological Survey (USGS) maps (and corresponding Geographic Information System (GIS) layers) consist of so-called *blue lines*, which indicate the location of streams but include no reference to width, depth, or channel roughness. Due to the map scale, the upstream terminus of the blue lines generally do not accurately represent channel

initiation as observed in the field. During the field reconnaissance, stream attributes were observed to the extent possible. In particular, stream road crossings were located, and width, depth and channel roughness were visually estimated at or near road crossings. In some cases, the location of channel initialization was observed and recorded. This information was subsequently used to specify model channel parameters. Although detailed measurements were not possible, the data collected augmented other estimated or indirectly obtained model features.

3.1.2 Road and Culvert Mapping

GIS map layers for all but the most recently constructed roads are available through the U.S. Forest Service or from the U.S. Census Bureau's TIGER (Topologically Integrated Geographic Encoding and Reference) database. At present, however, none of the National Forest Districts has developed GIS information specifying locations and other attributes of stream and ditch relief culverts. Also, information is lacking in existing databases that allows updating of maps to reflect abandoned roads or those removed following logging operations. In attempting to parameterize the road network realistically, rough estimates of the spacing of culverts and the connectivity of ditches, culvert outfalls, and the stream network were made based on calculated spacing from road segments observed in the field. In addition, the accuracy of information about road attributes from old maps was assessed.

Each catchment was unique with respect to the number of roads and culverts as well as the extent to which mapping was feasible. In Mica Creek, which is the smallest of the catchments, each

road, culvert, hydrologic divide, and waterbar structure (small mound of soil used to divert running water off the road surface) was mapped. Many of the culvert outfalls were followed to determine explicitly their connectivity to the stream network.

The size of the other catchments restricted the extent to which detailed mapping of road and drainage features was feasible. To maximize the utility of data collected, certain roads and streams were identified as being of particular significance hydrologically, and attempts to map these were made. Priority was given to road segments which intersect streams, those located at mid-slope, as opposed to ridge and valley bottom roads, and those found in wetter parts of the catchment. Examination of roads which intersect streams allowed investigation of both road and stream segments at one time. Also, connectivity of the road runoff into the stream is most likely at these intersections. Mid-slope roads, as suggested by previous investigations, (Bowling and Lettenmaier, 1997; La Marche and Lettenmaier, in press) have the greatest potential for modifying catchment hydrologic response. One would expect a greater amount of water in the soil column at mid-slope, as compared to the ridges. Also, greater distances may be short-circuited by changes in the drainage network related to roads, such as conversion of subsurface to overland flow, at the mid-slope as compared to valley bottoms. These priorities were adjusted due to time and access constraints in an attempt to acquire as much data as possible during the limited field visits.

3.1.3 Other Observations

During the field visits, other observations were made which, although qualitative in nature, provided important background for the modeling study. These observations included information about: 1) topology, geology and soil / rock make-up of the catchment—information that may or may not be readily available or understandable from maps; 2) appearance, types, density, ages and spatial patterns of vegetation; and 3) location and condition of meteorological and stream gaging stations.

3.2 Digital Data Acquisition:

Significant amounts of digital data had to be compiled and / or created, quality checked, and scaled in space or time in preparation for the modeling work described in Chapters 4 through 6. The cooperation of various government agencies and private organizations, and subsequent application of GIS software and other computer algorithms facilitated this effort. The data can be classified into two major types, spatial and temporal. The sources of the data described below are shown in Table 3-1.

3.2.1 Spatial Data:

Digital Elevation Model (DEM)

Digital topographic data are the backbone of spatially distributed hydrologic models like DHSVM. Elevation and related topologic features were derived from 30m digital

Table 3-1: Data sources by catchment

	Mores	Entiat	Swan	Mica
DEM	NED	NED	NED	USGS NMP
Vegetation	UMT: Redmond et al & USU: Intermtn. Region Land Cover Characterization	U.S. Forest Service: Wenatchee National Forest	UMT: Redmond, et al	Potlatch Corp. & UMT: Redmond, et al
Soils	STATSGO	STATSGO	STATSGO	STATSGO
Roads	USFS Boise NF	USFS Wen. NF	USFS Flathead NF & Plum Creek	Field Data
Temperature	NRCS	NRCS	NRCS	NRCS
Precipitation	NRCS	NRCS	NRCS	NRCS
Wind	NCEP/NCAR	NCEP/NCAR	NCEP/NCAR	NCEP/NCAR & Potlatch Corp.
Stream flow	USGS	USGS	USGS	USGS
NED	National Elevation Database			
UMT	University of Montana			
USU	Utah State University			
Statsgo	State Soil Geographic database			
USFS * NF	United States Forest Service * National Forest			
NRCS	Natural Resources Conservation Service			
NCEP/NCAR	National Center for Environmental Prediction /			
	National Center for Atmospheric Research reanalysis data			
USGS	United States Geologic Survey			
NMP	National Mapping Project			

elevation models obtained from the United States Geological Survey Mapping Program (USGS, 1993) and the National Elevation Database (USGS, 1999). The DEM was aggregated using bilinear resampling, and processed according to catchment size and characteristics. In general, DEMs were aggregated so that each of the catchments could be represented with roughly 100,000 pixels or less. This number was selected primarily on the basis of computational constraints. The aggregated DEMs were then used to delineate the catchments, to derive the

stream and road networks, to distribute meteorological forcings and to derive downhill surface and subsurface flow paths. (The discussion of network derivation is included in Chapter 5.)

Vegetation

The model study design (Chapter 7) involves comparison of the predicted effects of vegetation change over the last century using various vegetation scenarios derived from two or more vegetation data sets for each of the four catchments studied. Model implementation and calibration was performed for a high resolution (approximately 30 m) current vegetation data set. The current vegetation data sets were developed primarily from land cover classifications applied to satellite imagery. Field investigation and aerial photographs were also involved, especially for Mica Creek. The alternate land cover scenarios that were investigated include fully forested, open range land, no roads, and an historical approximation of 1900 vegetation. These are derivatives of the current vegetation, although the historical scenario is also based on a large scale historical land cover classification (see Mattheussen, et al, 2000). The methods used to develop the current and alternative vegetation scenarios are described in Sections 5-4 and 5-5.

Soils, Roads and Observation Station locations

The U.S. Department of Agriculture (USDA) - National Resource Conservation Service's (NRCS) State Soil Geographic (STATSGO) database (USDA, 1994) was the primary source of the soils information used in the model. National Forests and private forest product companies provided the road coverages, while most culvert information was mapped in the field or

extrapolated from field and other data through various algorithms. NRCS and USGS provided location information for meteorological and stream gaging stations respectively.

3.2.2 Temporal Data:

Meteorological Records

The primary meteorological data required for the modeling were daily records of precipitation and maximum and minimum temperatures. In some cases, higher temporal frequency observations, and observations of other variables like wind were acquired. The source for most of the meteorological data was the National Climatic Data Center (NCDC), with data access provided via commercial vendors on electronic media. Missing daily data were manually estimated by comparing with nearby observing stations. In addition to NCDC stations, daily precipitation and temperature data were acquired for some NRCS SNOTEL gages, which are typically located at high elevations. Wind data were extracted from the National Center for Environmental Prediction / National Center for Atmospheric Research (NCEP / NCAR) reanalysis data (Kalnay, et al, 1996). Additional processing of these data was performed as described in Section 5-6.

Streamflow and Snow Water Equivalent

Streamflow and snow water equivalent time-series were also acquired and used to evaluate model performance in the calibration process. Streamflow records were obtained from the USGS. Generally, these are average daily discharges calculated from the measured stage and

converted to discharge by the USGS using stage-discharge relationships. Snow pillows, which measure snow water equivalent, are available at NRCS SNOTEL stations. These data were used in the model calibration process as described in Chapter 6.

Vegetation

Although vegetation attributes in fact vary temporally, the study catchments are mostly forested, and conifers are the dominant vegetation cover type. Therefore, over the course of the model simulations, vegetation characteristics were treated as fixed.

3.3 Description of Catchments

3.3.1 Mica Creek, Idaho

Mica Creek is a tributary of the St. Joe River in Northern Idaho. It drains 26.9 km² of forested mountainous terrain (Figures 3-1 and 3-2). Potlatch Corporation, which owns most of the catchment, has instrumented the catchment heavily in preparation for a paired watershed experiment. Most of the data records began in 1991, although wind observations were not initiated until late 1997. The Mica Creek catchment contains 7 flume weirs at which discharge is observed, multiple meteorological stations, as well as a SNOTEL gage. For this study, data for the period from October 1990 through September 1999 were used.

The Mica Creek catchment ranges in elevation from 1005 m at the stream gage to 1611 m at Renfro Peak, on the western edge of the catchment. Slopes calculated from the

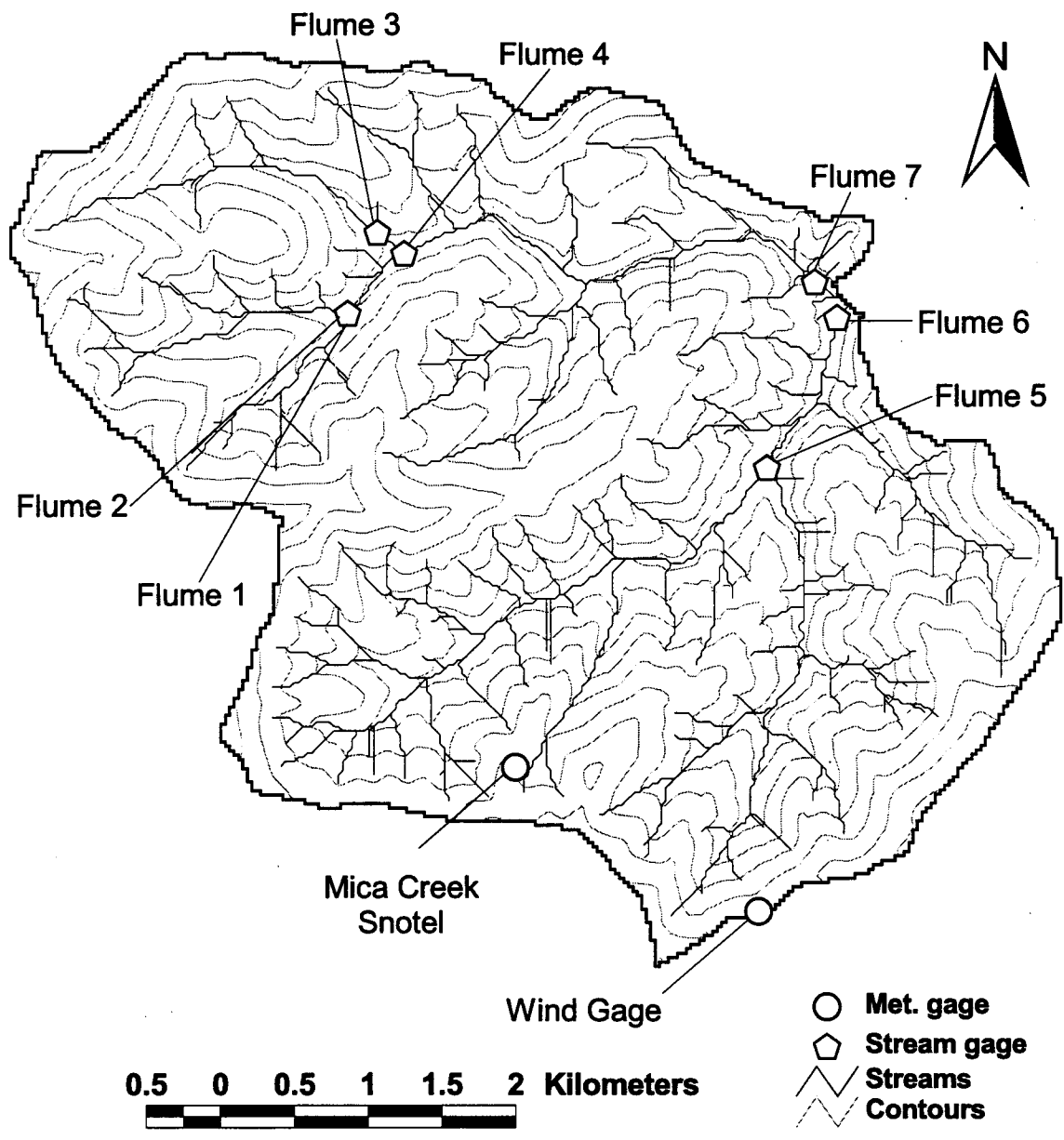


Figure 3-1: Mica Creek: Elevation, modeled streams and gages
(Contour interval = 50 m)

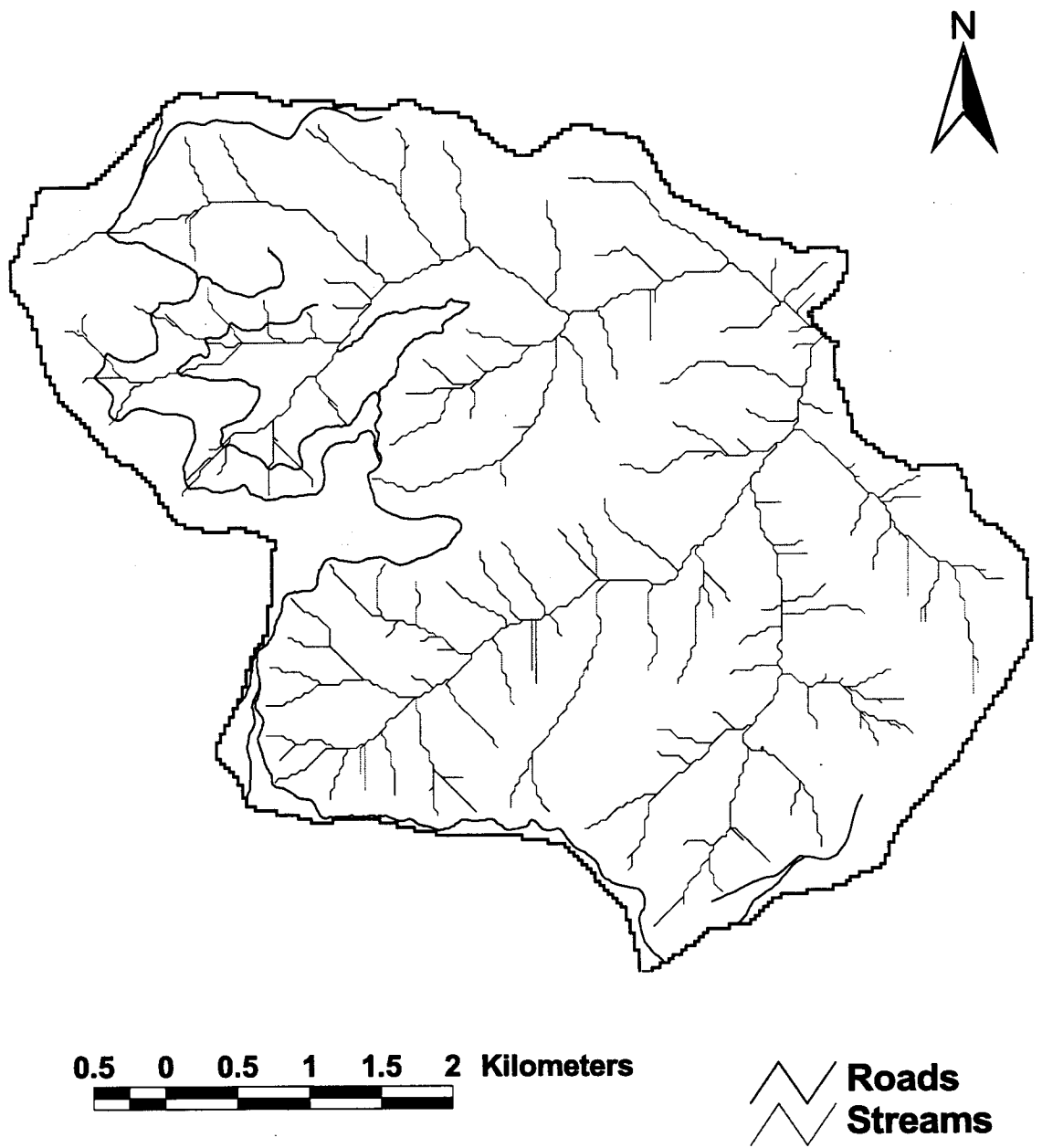


Figure 3-2: Mica Creek: Roads and modeled streams

DEM range from 0 to 88 percent with a mean and standard deviation of 31.4 and 10.3 percent respectively. The geology is metamorphic, consisting of unweathered gneiss and quartzite beltseries, covered by deep volcanic ash.

The catchment receives about 1500 mm of precipitation annually, as estimated from the SNOTEL gage. Over the period from October 1990 through September 1999, the range was 930 to 2090 mm. Most precipitation falls as snow in the winter months, and melts in April through early June. Temperatures range from an average maximum of 23.9 °C in August to an average minimum of -7.0 °C in December. Occasional warm periods occur in early to mid winter which can melt part or all of the accumulated snow in the lower portions of the catchment.

Temperature inversions during dry winter weather are common, as ridges shade valleys from the sun and protect them from wind patterns that normally would advect the cold air from the catchment.

The average annual runoff ratio is approximately 47 percent. Over the period of observation, discharge from the catchment ranged from 0.05 to 10.1 m³/s.

The catchment has undergone extreme changes in land cover. Although most of the catchment is now covered with mature second growth forest (less than 10 percent is old growth), in the late 1920's and early 1930's, the catchment was almost entirely clear-cut logged. Subsequent to the

logging, much of the catchment burned (Cundy, 1998). The catchment currently has a road linear density of about 1.1 km/km², or 0.72 percent of the catchment area.

3.3.2 Swan River, Montana

The Swan River drains the valley between the Mission and Swan Mountain Ranges of western Montana. The river flows through Swan Lake and discharges to Flathead Lake (Figures 5-3 and 5-4). The catchment, as defined by this study, includes 179 km² of the headwaters draining from at Lowary Peak in the west to USGS gage #12369200 near Condon on the northeast edge of the catchment. This spectacularly glaciated terrain ranges in elevation from 1220 m at the gage to 1830 m Lowary Peak. Slopes calculated from the DEM range from 0 to 165 percent with a mean and standard deviation of 28.6 and 22.9 percent respectively. The terrain includes cirques, kettles, glacial trough valleys, and deposited till. The catchment is not as instrumented as Mica Creek. One long-term precipitation and temperature gage (1960-present) exists near the outlet of Lindburgh Lake and three SNOTEL gages have operated near the catchment boundaries over at least part of the study period, although the record lengths are much shorter (approximately 10 years). Air temperatures at Lindburgh Lake range from average minima of -9.7 °C in the winter to average maxima of 26.5 °C in the summer. The Lindburgh Lake gage receives an average of 686 mm of precipitation annually, ranging from 438 mm in 1987 to 923 mm in 1975. These measurements are much lower than the catchment average, as the gage is located at low elevation in the driest part of the catchment.

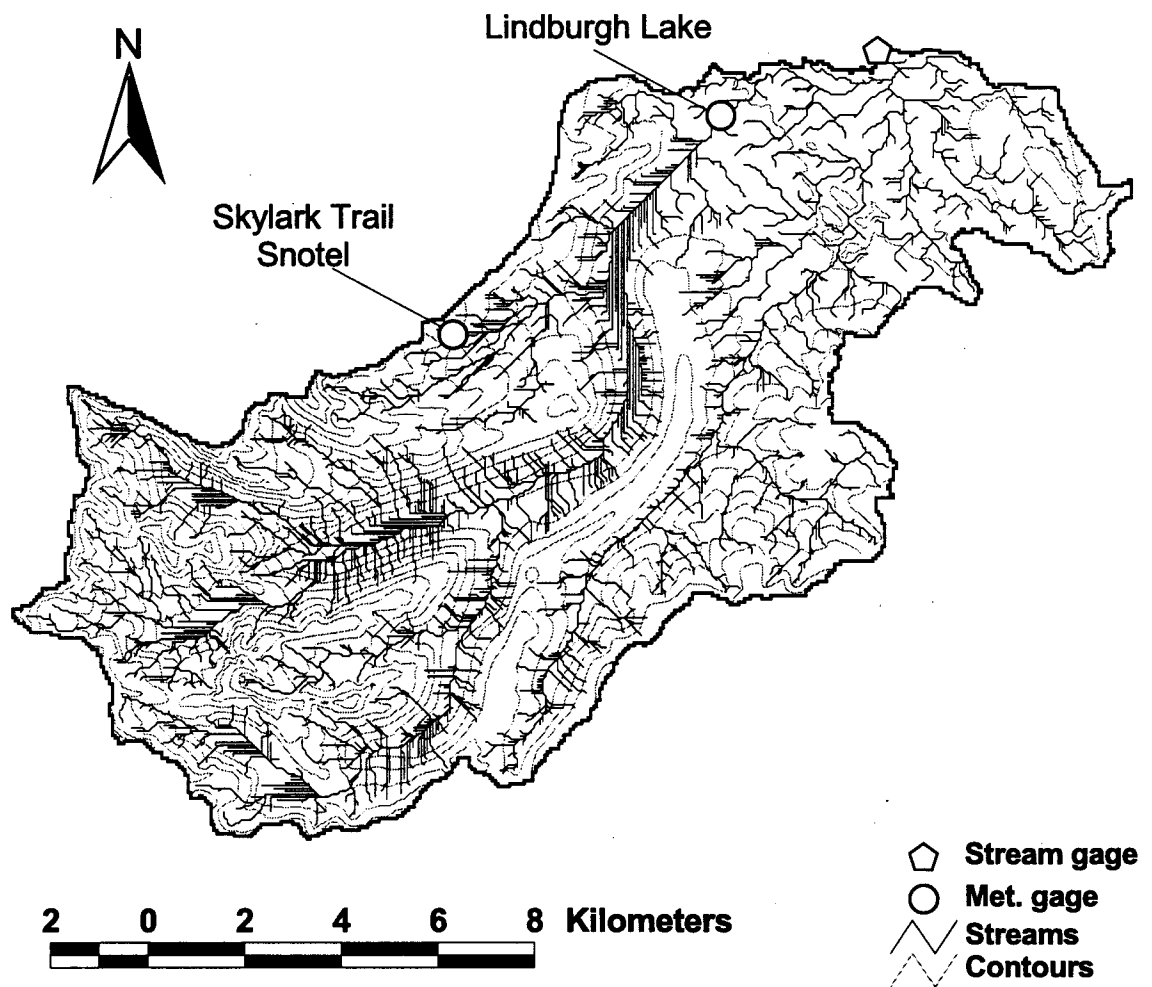


Figure 3-3: Swan River: Elevation, modeled streams and gages
(Contour interval = 100 m)

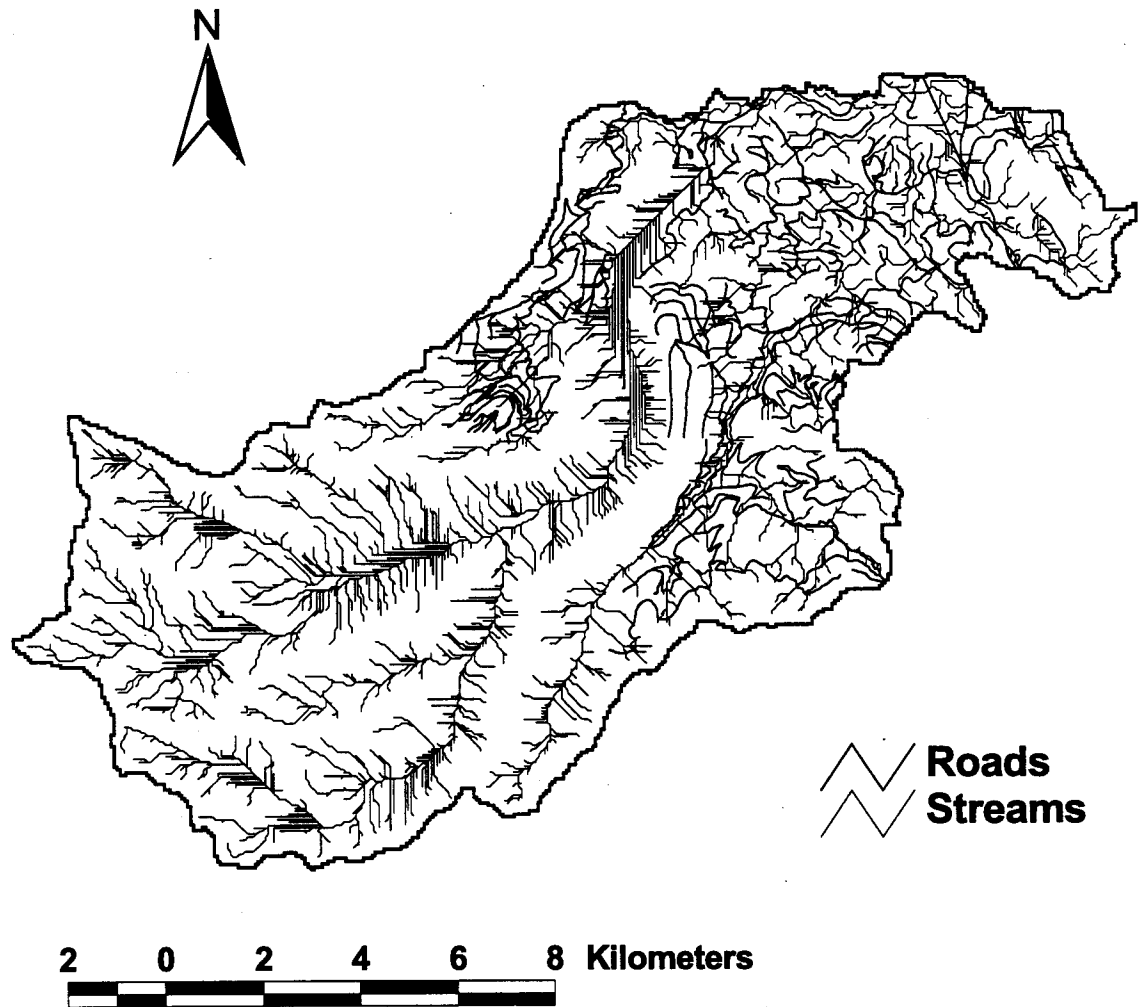


Figure 3-4: Swan River: Roads and modeled streams

Snow accumulation and ablation dominate the hydrology of the Swan River headwaters, although glacial lakes attenuate flows somewhat. The annual average runoff ratio is 55 percent. Daily average discharge at the gage has ranged from a maximum of 42.6 m³/s in June 1974 to a minimum of 0.481 m³/s in September 1988.

Although approximately 40 percent of the catchment is now protected as part of the Mission Mountain Wilderness, the catchment's land cover has undergone significant change over the last century. Large fires in the early part of the 20th century burned most of the lower portion of the catchment. Also, the National Forest and private lands within the catchment are actively managed with timber production as a major objective. The result is a patchwork of harvest and various stages of re-growth through the lower (non-wilderness) portion of the catchment. Catchment-wide, roads have a density of approximately 1.2 km/km² or 0.78 percent of the catchment area. Only about 50 percent of the basin contains roads.

3.3.3 Entiat River, Washington

The Entiat River drains the east slope of the Cascade Mountains, flowing into the Columbia River north of Wenatchee, Washington (Figures 3-5 and 3-6). The 527 km² catchment is defined for this study by the USGS gage near Ardenvoir, Washington. The high point in the catchment is Mount Maude (2747 m), from which the flow is generally southeasterly, eventually reaching the gage at 479 m elevation. Slopes calculated from the DEM range from 0 to 164 percent with a

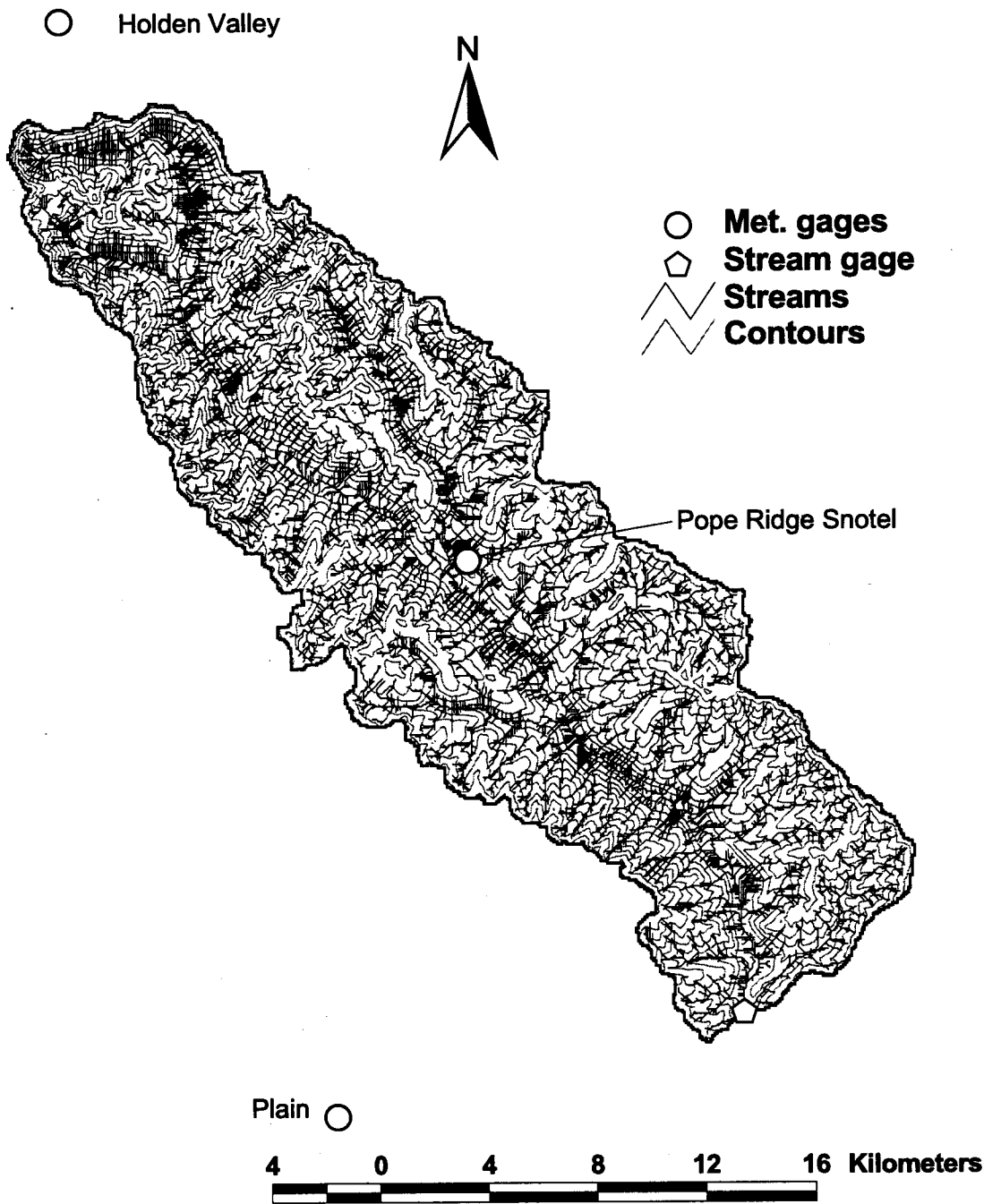


Figure 3-5: Entiat River: Elevation, modeled streams and gages (Contour interval = 150 m)

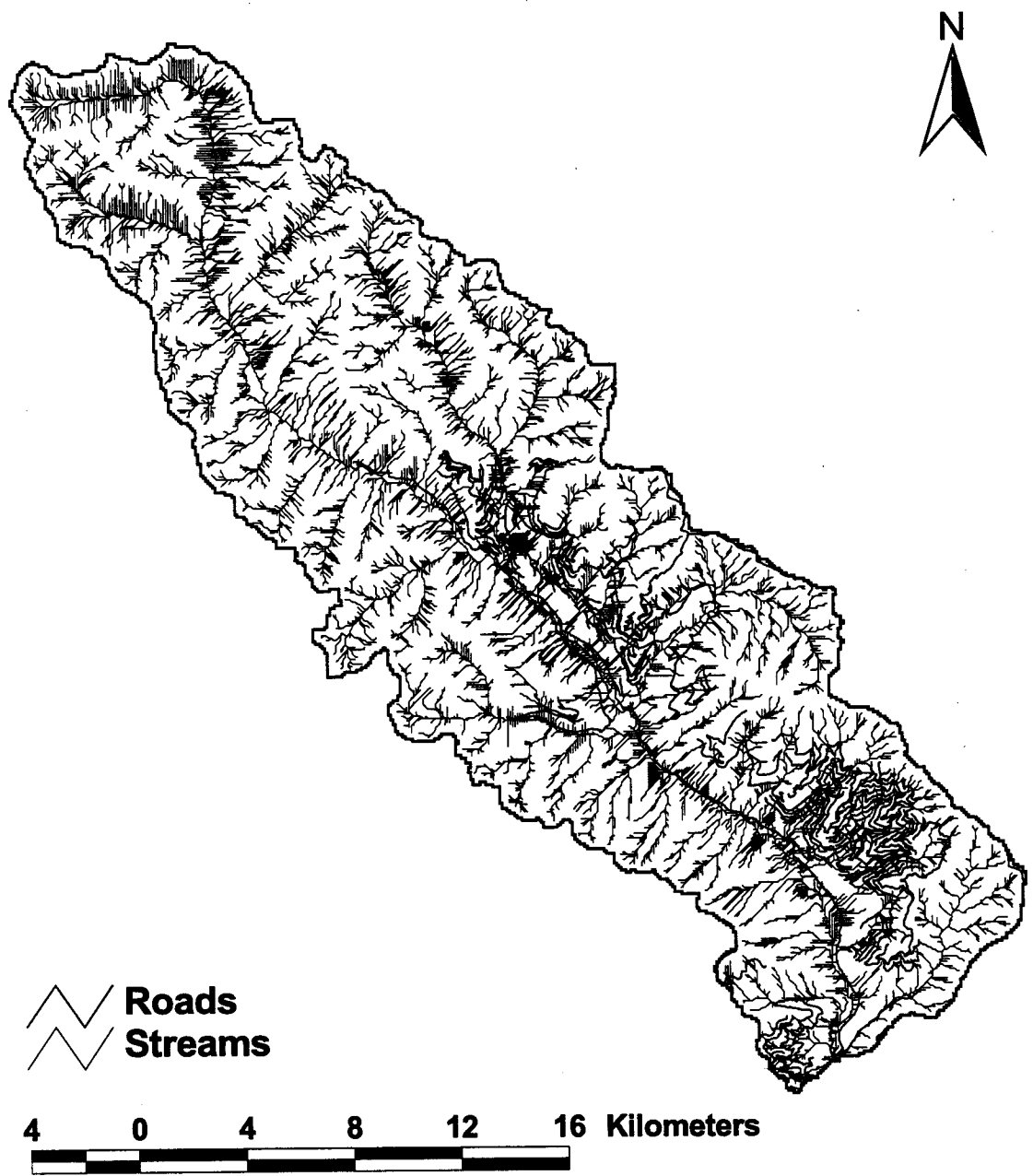


Figure 3-6: Entiat River: Roads and modeled streams

mean and standard deviation of 43.4 and 20.0 percent respectively. The river valley is long with many features from its history of glaciation.

The catchment contains only one precipitation gage, at the Pope Ridge SNOTEL site. Gages at Plain and Holden Village, slightly outside the catchment, were also used extensively. Other gages were used to fill in missing data. Because of the length of the catchment and the rain shadow effect of the high ridges to the west and south, a wide range of precipitation and temperatures exist within the catchment. Studies conducted by the USDA (1978, 1996) estimate that annual average precipitation ranges from a maximum of 2300 mm to as low as 250 mm near the river's mouth at the Columbia River (which is, however, considerably downstream of the Ardenvoir gage).

Snow accumulation and ablation patterns dominate the hydrology of the Entiat River. The annual average runoff ratio is about 66 percent. Over the 1950-1997 period of record, observed flows at Ardenvoir have ranged from 0.57 m³/s in August 1984 to 182 m³/s in December 1955.

Although approximately 20 percent of the catchment now lies within the Glacier Peak Wilderness Area, the catchment's land cover has undergone significant change over the last century (USDA Forest Service, 1996b). In the late 1800's and early 1900's, the catchment was intensively grazed and logged. Logging continues although often in the form of salvage logging,

as wildfire periodically burns portions of the catchment. Catchment-wide the road density is approximately 0.85 km/km^2 , or 0.55 percent of the catchment area, although less than 60 percent of the catchment is roaded. Floods and sedimentation associated with land use change have been long standing problems in the Entiat River catchment (USDA Forest Service, 1996b). A portion of the catchment was instrumented by the U.S. Forest Service for a paired watershed study in the 1960's which was originally designed to include paired sub-catchments representing logging and forest road effects. However, the study area was burned in 1970 before the treatments could be made and studied. Some analysis of the data collected following the fire is reported by Helvey (1973, 1980).

3.3.4 Mores Creek, Idaho

Mores Creek drains 1033 km^2 of the Boise Mountains to USGS gage #13200000, northeast of Boise, in Southern Idaho. The catchment ranges in elevation from 2467 m at Pilot Peak to 955 m at the gage (2.7 km upstream from Robie Creek near the head of Lucky Peak Reservoir), and includes all of the Grimes Creek catchment. A short distance below the gage, Mores Creek drains into Lucky Peak Reservoir (Figures 3-7 and 3-8). Slopes calculated from the DEM range from 0 to 72.5 percent including some broad valleys in the central portion of the catchment. The mean slope in the catchment is 23.0 percent with a standard deviation of 12.2 percent.

There is one meteorological gage within the catchment (Idaho City), and four more close to the catchment boundary (Moores Creek Summit SNOTEL (Mores Creek is

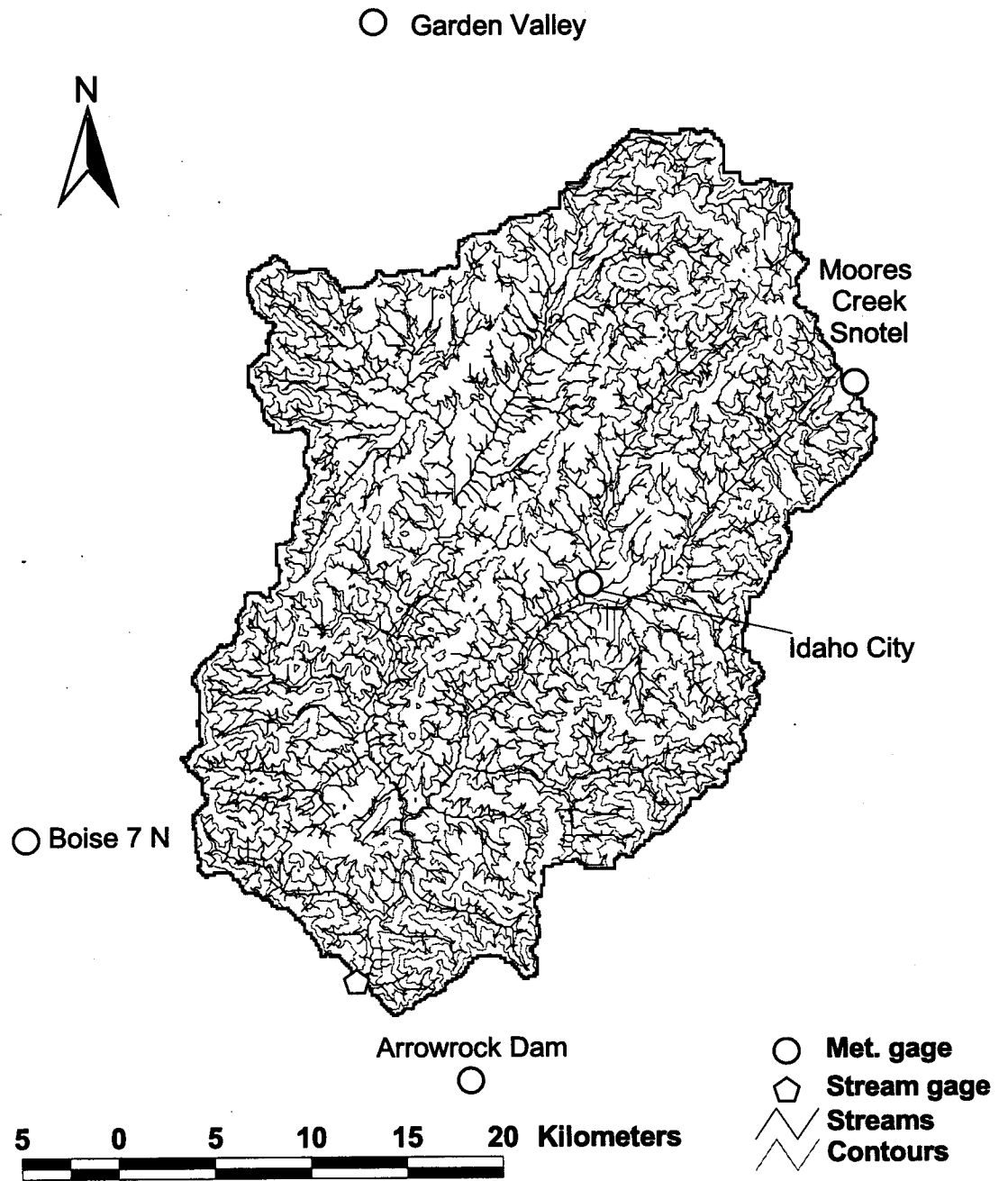
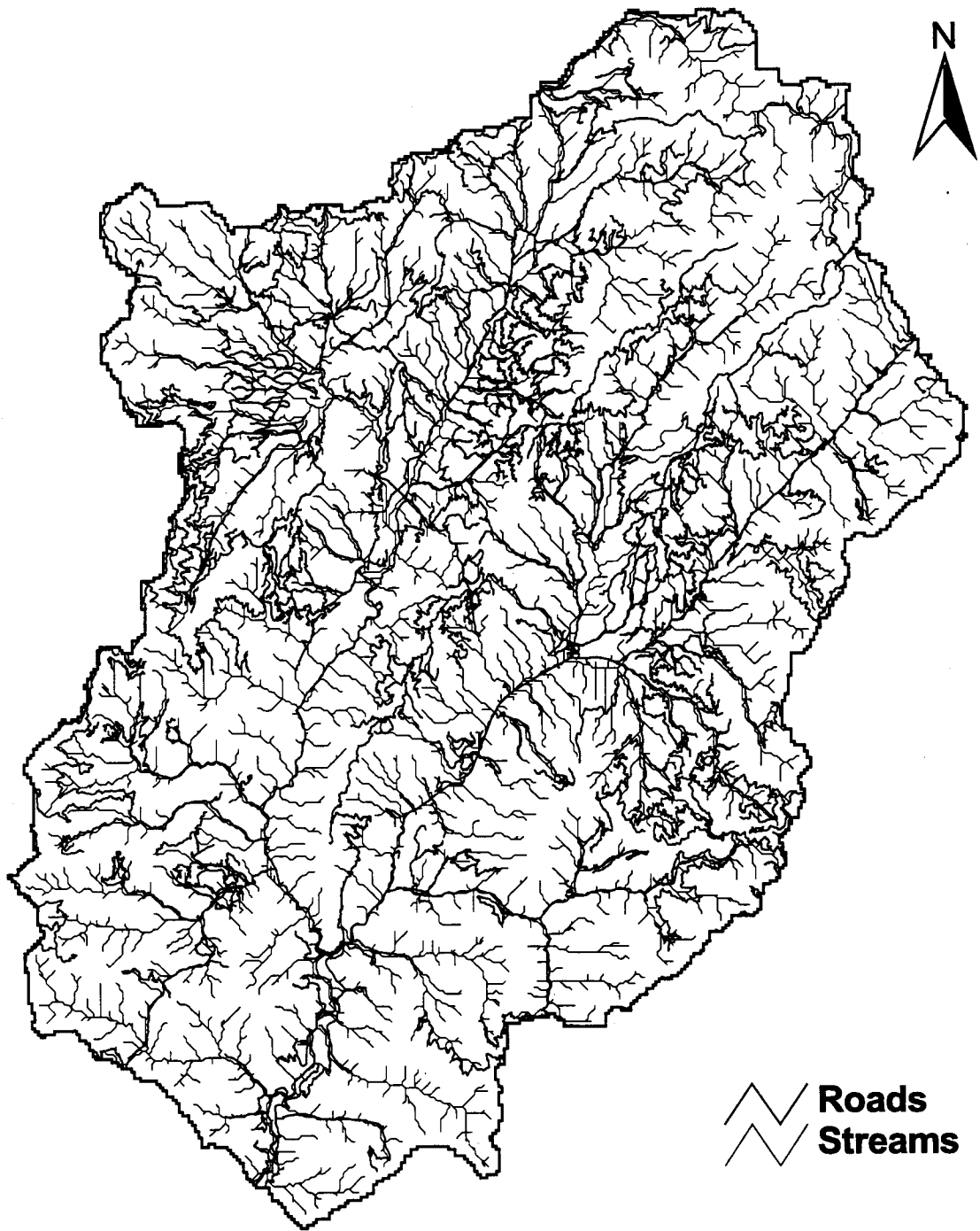


Figure 3-7: Mores Creek: Elevation, modeled streams and gages
 (Contour interval = 150 m)



4 0 4 8 12 16 Kilometers

Figure 3-8: Mores Creek: Roads and modeled streams

spelled "Moore's" Creek in NRCS records), Garden Valley, Boise 7 N, and Arrowrock Dam). Several other gages have operated both inside and outside the watershed for relatively short periods. At Idaho City, the average monthly maximum temperature ranges from 31.6 °C in July to 2.6 °C in January. Average annual precipitation at Idaho City is 606 mm. The lower part of the catchment lies in the transient snow zone, although most of the snowpack lasts through the winter.

Mores Creek and its tributaries have been monitored by various gages, although most have very short records, and many were operated prior to 1950. Based on the USGS gage #13200000 (above Robie Creek, Near Arrowrock Dam), average annual discharge is 15.86 m³/s, with measured historical maximum and minimum of 154 in December 1955 and 0.10 m³/s in August 1994.

While Mores Creek cannot boast of striking glacial beauty, its history is by far the most eventful of the four study catchments. In 1862, gold was discovered near the current location of Centerville. This began a decade of boom in the western gold rush tradition (Hart, 1986). Since that time, most if not all of the lower valleys have been completely disturbed through placer mining operations and much of the forested area has been logged. Many of the valleys have been mined and re-mined as technology improved and as gold prices merited the effort. The last major mining operations dredged the mainstem of the creek to a depth of approximately 12 m in the 1940's and 1950's. Since that time, there has been a period of afforestation as fire suppression

and logging limitations have been observed. The catchment is mostly within the US Forest Service Boise National Forest, with significant ownership also by the State of Idaho Department of Lands and the Boise Cascade Corporation. The catchment has a road density of 1.6 km/km², or 1.04 percent of the catchment area.

Chapter 4: Distributed Hydrologic Soil and Vegetation Model (DHSVM)

This section describes the Distributed Hydrologic Soil-Vegetation Model (DHSVM) which was used in this study. A general overview of the model is provided first, followed by a more detailed discussion of the model's representation of vegetation. Finally, previous studies and applications of the model are reviewed briefly.

4.1 Model Overview

DHSVM (Wigmosta, et al. 1994; Wigmosta and Lettenmaier, 1999; Wigmosta, et al. 2000) is a physically-based, spatially-distributed, hydrologic model that simulates the effects of soil, vegetation, and topography on the movement of water at and near the land surface. The model consists of four major elements: 1) a two-layer vegetation / canopy model, 2) a multi-layer unsaturated soil moisture model, 3) a saturated subsurface flow model, and 4) a surface channel flow network for simulation of ditches and streams. A DEM, with typical spatial resolution (pixel size) ranging from several tens to several hundreds of meters, forms the foundation of the model structure. Other catchment surface attributes, such as vegetation and soil characteristics, are defined at each pixel. The model is forced with time series of meteorological variables: precipitation, temperature, solar radiation, relative humidity, and wind. Figure 4-1 shows DHSVM inputs and outputs, including off-line data processing.

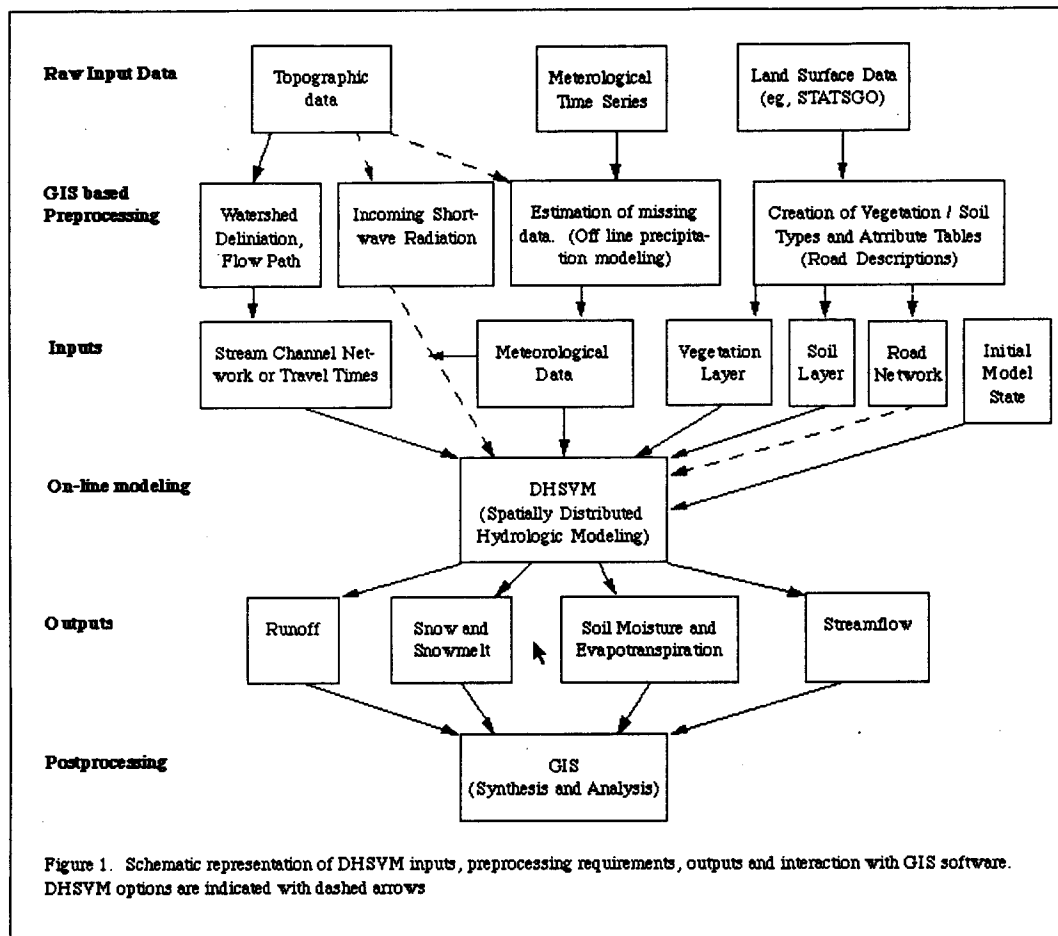
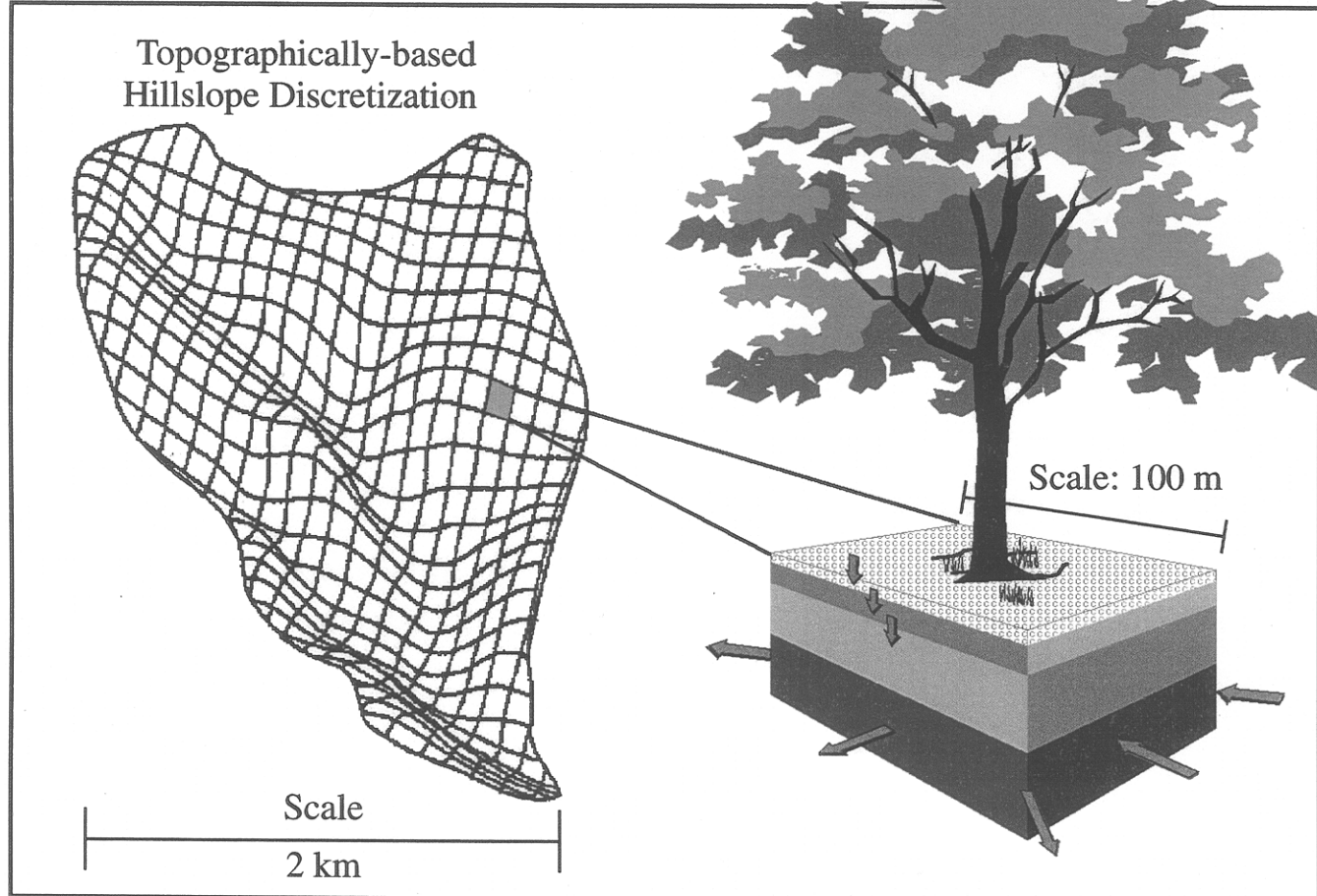


Figure 4-1: Schematic representation of DHSVM inputs, preprocessing requirements, outputs and interaction with GIS software
 Source: Storck, 2000

Once the land surface attributes have been assigned (Figure 4-2), meteorological forcings are applied to each grid cell. DHSVM solves the water and energy balance at each pixel for multiple vegetation and soil layers (Figure 4-3). Precipitation is partitioned into rain or snow on a pixel by pixel basis given the estimated local air temperature. Temperature, radiation, relative humidity and wind drive evapotranspiration, snow melt and sublimation on the vegetation and soil surface. A vegetation-canopy sub-model (Storck, 2000) represents the attenuation of wind and solar radiation and interception, storage conditions and fate of both solid and liquid incident precipitation (Figure 4-4).

Beneath the vegetation canopy the model tracks the fate of precipitation as direct runoff, infiltration and subsequent sub-surface storage and contribution to runoff or extraction as evapotranspiration. Surface water is transferred to neighboring pixels as controlled by the DEM (Figure 4-5). Subsurface moisture is redistributed laterally in the saturated zone according to Darcy's Law using a downslope / down-gradient algorithm (Wigmosta and Lettenmaier, 1999). Where the water table intersects an incised road or stream channel, or surface water moving horizontally encounters a channel, water is transferred into the channel. Channel water is routed using an algorithm described by Perkins, et al (1996) through the system according to a linear storage reservoir algorithm described by Storck (2000) until reaching an outlet (either the catchment outlet or a culvert).

DHSVM Model Representation



Surface / Subsurface Flow
Redistribution to / from
Neighboring Pixels

Figure 4-2: DHSVM: Model representation
Source: Adapted from Wigmosta, *et al*, 1994

1-D Vertical Water Balance

Evaporation (E)

Interception (E_{io} E_{iu})

Soil (E_s)

Evapotranspiration (E_t)

Overstory (E_{to})

Understory (E_{tu})

Storage (S)

Overstory (S_{io})

Understory (S_{iu})

Soil layer 1 ($\theta_1 d_1$)

Soil layer 2 ($\theta_2 d_2$)

Rooting Zones

$$S_s = \theta_1 d_1 + \theta_2 d_2$$

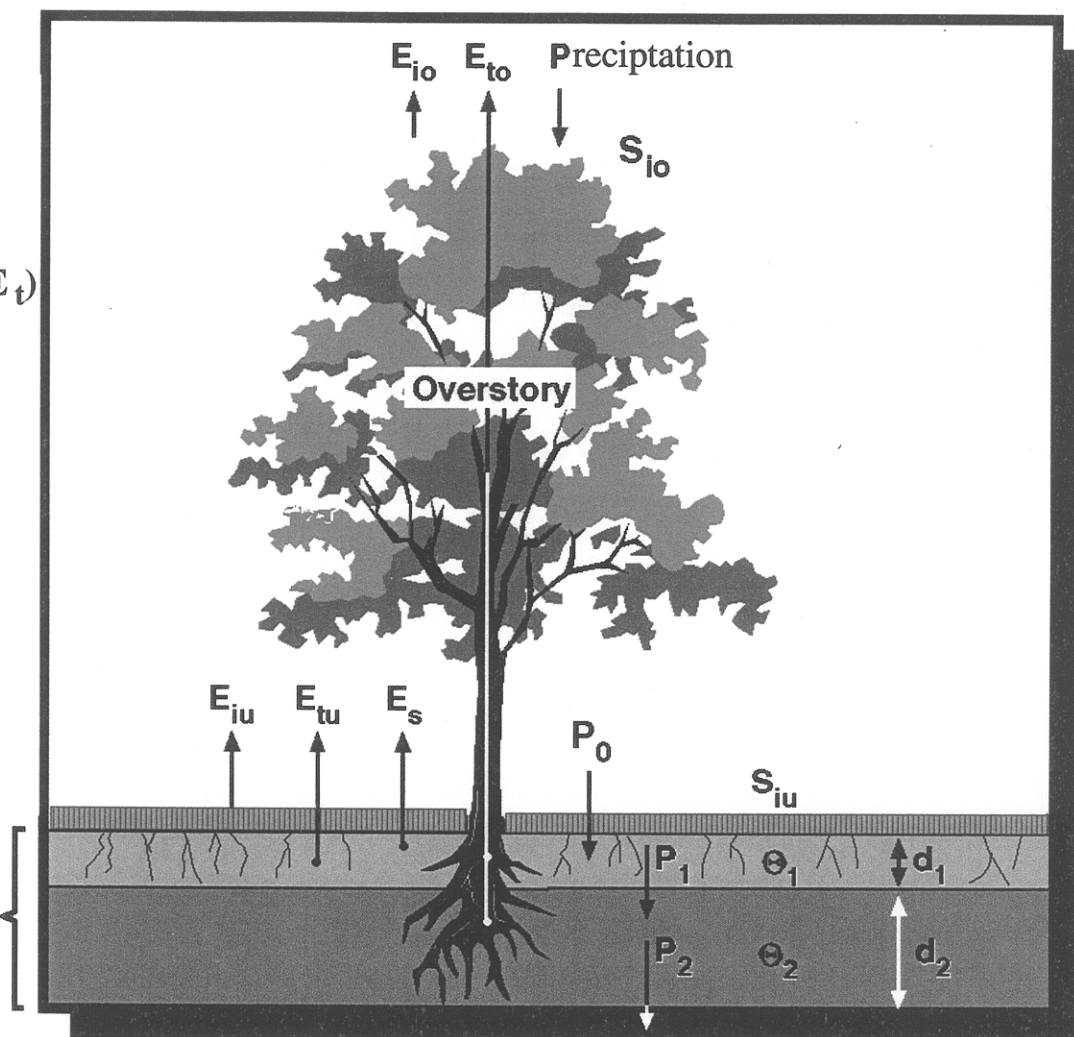


Figure 4-3: DHSVM: One-dimensional vertical water balance

Source: Adapted from Wigmosta, *et al*, 1994

DHSVM: Snow Model

Required Forcings: Above-canopy meteorology

- Air Temperature
- Relative Humidity
- Windspeed
- Shortwave Radiation
- Longwave Radiation
- Precipitation

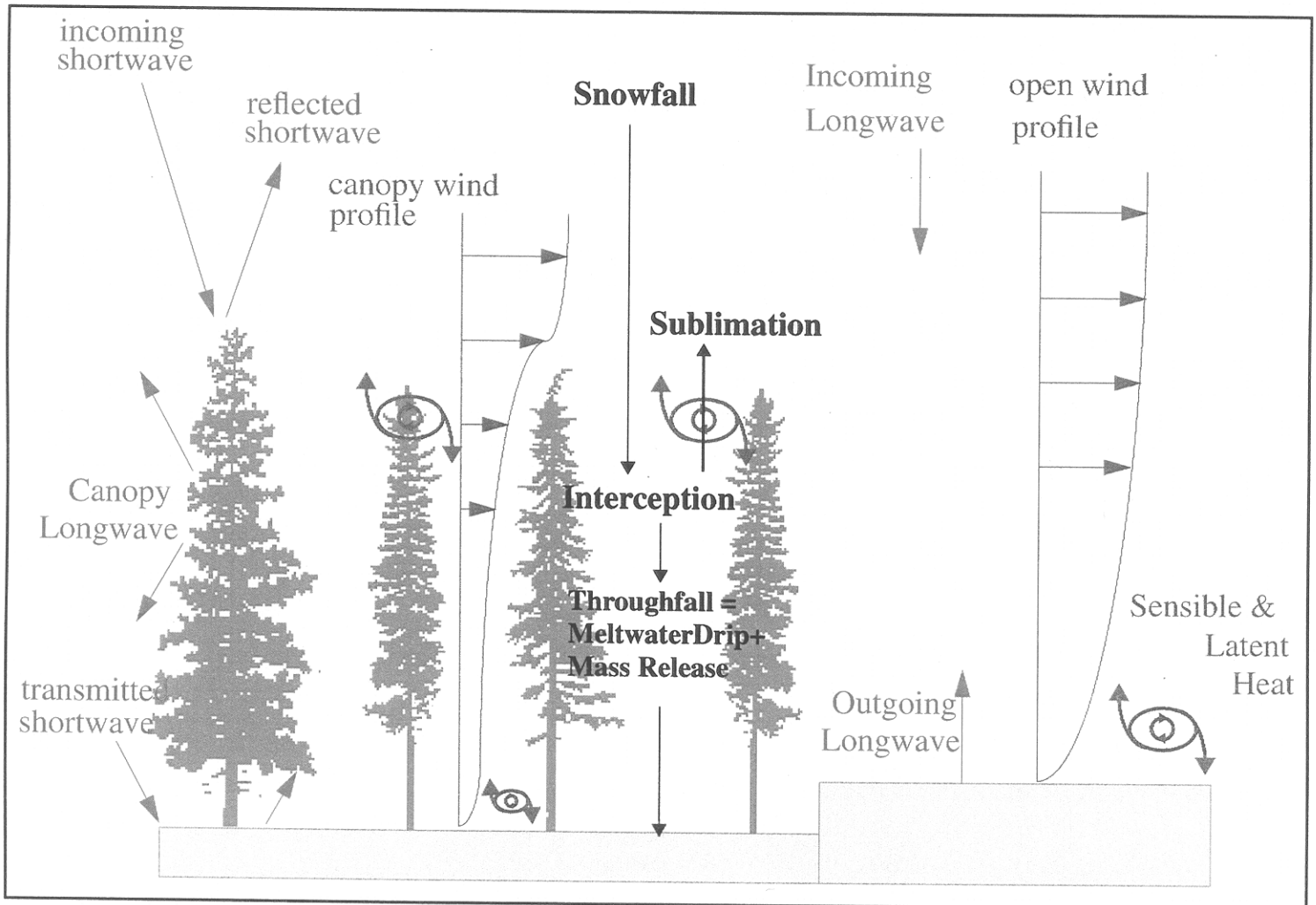


Figure 4-4: DHSVM: Snow model
Source: Adapted from Storck, 2000

Surface - Subsurface Flow Routing and Runoff Generation

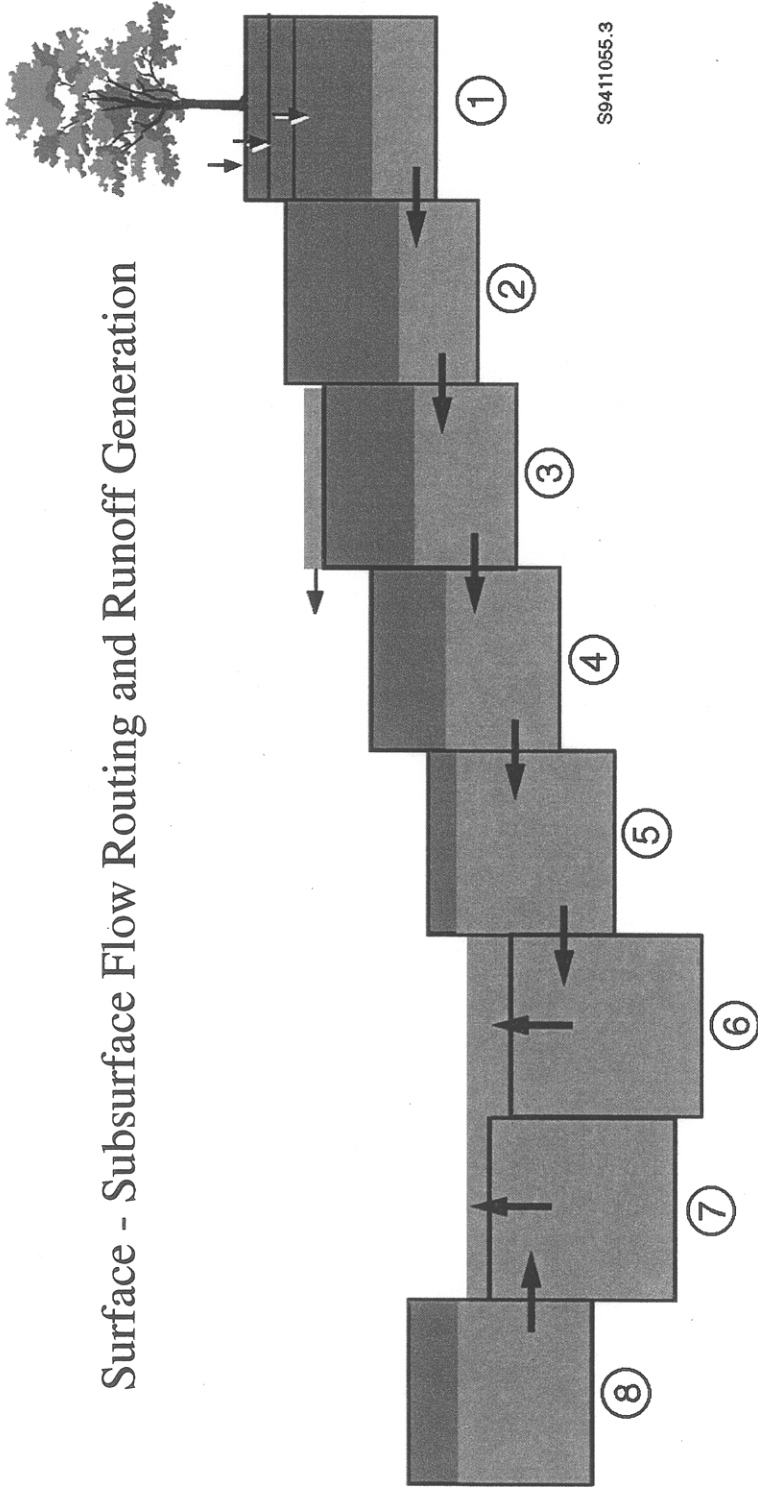


Figure 4-5: DHSVM: Runoff production. Source: Wigmosta and Perkins, 1997

Pixels (1-5 and 8): Subsurface flow redistribution based on local water table slope

Pixels (6, 7): Runoff Production (Saturation Excess)
Surface water routed to downslope neighbor

Pixel (3): Runoff Production (Infiltration Excess)
Surface water routed to downslope neighbor

Channel Network Segments (including road ditches)
May intercept subsurface flow (depends on channel depth)
Intercept all surface flow
Route water between segments using linear reservoir scheme

4.2 Vegetation-Canopy Sub-Model

The DHSVM vegetation-canopy sub model is described by Wigmosta, et al (1994) and Storck, et al (1995), (see also Storck, 2000). A few details of the model warrant more discussion than is included in these references. The reader is also referred to Wigmosta and Perkins (2000).

4.2.1 Attenuation of Above-canopy Forcings

The two-layer vegetation parameterization consists of optional overstory and understory descriptions. Attenuation of meteorological variables occurs in the vertical profile through the canopy. A percentage of the falling precipitation volume as large as the fractional coverage percentage may be intercepted in the overstory as a function of leaf area index (LAI), temperature (partitioning rain and snow) and remaining storage capacity. Snow stored on the overstory can sublimate or be transferred downward at a later time—either as meltwater drip, mass wasting, or by wind. Precipitation not intercepted in the overstory (or storage transfer from the overstory) continues downward where it may be intercepted by the understory, if in liquid state. The model assumes that solid precipitation (snow and ice) fully cover the understory when present. Interception is a function of LAI and storage capacity. Precipitation that is not intercepted is added to the under-canopy snowpack, if snow is present. Otherwise it reaches the soil surface where it either infiltrates or contributes to runoff.

Downward solar (short wave) radiation may be attenuated or reflected by the vegetation (Figure 4-4). Absorption and reflection of the short wave radiation is a function of albedo, LAI, and

precipitation storage. As in the case of precipitation, the maximum percentage of intercepted and reflected radiation equals the fractional coverage percentage. Short wave radiation transferred to the understory is also attenuated or reflected by the understory before reaching the underlying soil. Reflected solar radiation returns to the overstory to be absorbed or transferred from the system. Long wave radiation follows a path similar to the short wave radiation with two notable differences. First, long wave radiation is not reflected. Second, the vegetation (both over and understory) and soil or snowpack emit long wave radiation in addition to absorbing incoming long wave radiation at the top of the canopy.

Wind is also attenuated by the vegetation. Attenuation above and below the overstory canopy follows a logarithmic profile (Figure 4-4). Attenuation within the overstory canopy follows an exponential profile. These profiles are functions of the resistances of the vegetation layers and soil or snow. The estimation of the resistances is documented in Wigmosta, et al (1994). Wind acts as a mechanism for turbulent heat transfer and overstory snow storage removal (which is a linear function of wind speed and snow storage). Temperature and relative humidity, used in calculation of turbulent convective sensible and latent heat transfers respectively, are not attenuated through the vegetation layers.

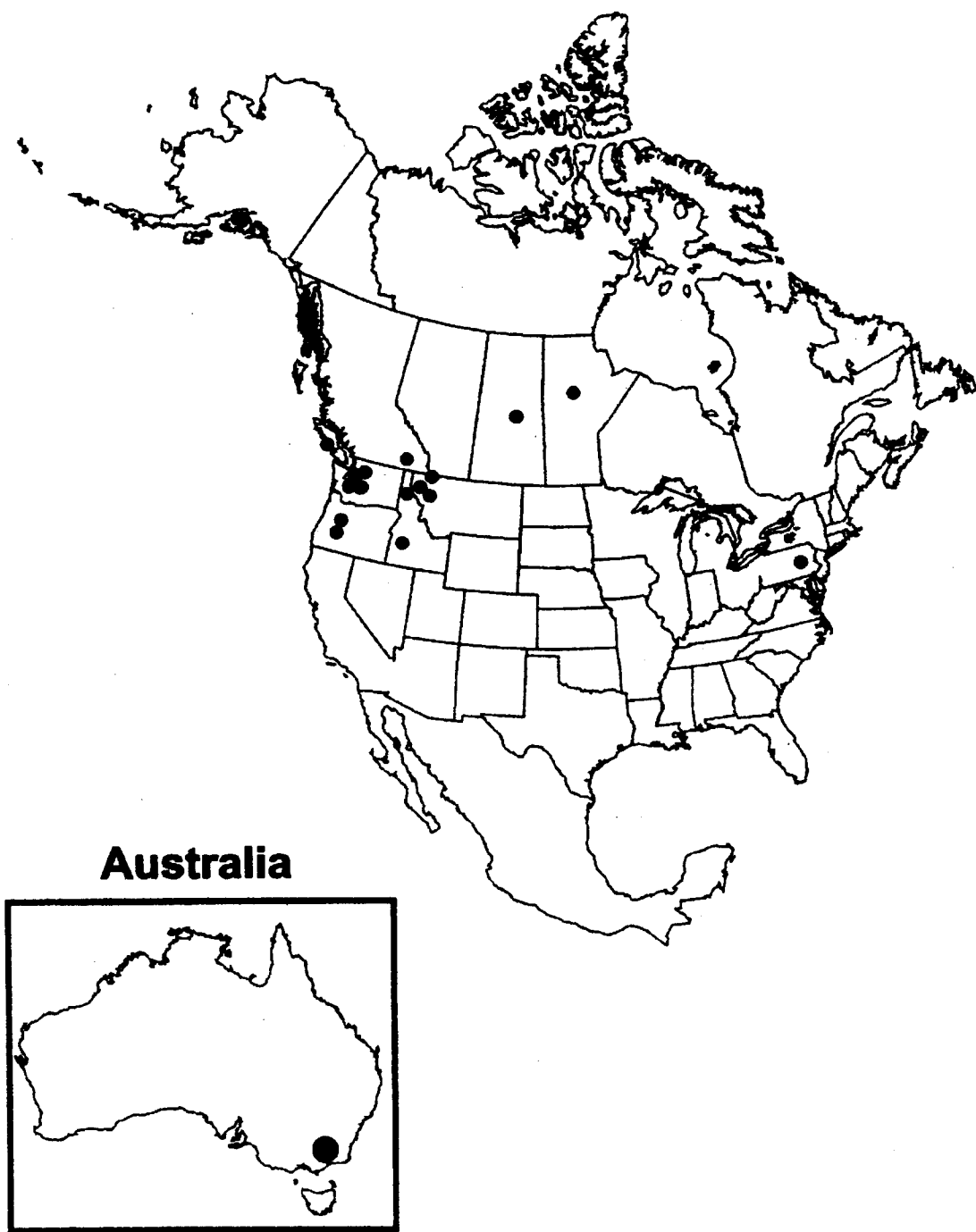
4.2.2 Evapotranspiration

The previous discussion of precipitation, radiation and wind attenuation provides a foundation for discussing evapotranspiration formulation. DHSVM uses a Penman-Monteith approach.

While water is stored on the canopy (either in liquid or solid state) all heat input is used to eliminate the storage through sublimation, melt, or evaporation. When the entire canopy (either over or understory) is dry, transpiration may take place. Evaporative demand is calculated based on atmospheric conditions. Stomatal resistance is calculated using atmospheric conditions and a species-dependent minimum resistance. Water for transpiration is extracted from one or more root zones in accordance with soil moisture presence and fraction of canopy roots in each zone (Figure 4-3).

4.3 Applications of DHSVM

DHSVM was first applied to the Middle Fork Flathead catchment in Montana (Wigmosta, et al 1994). Since then it has been applied to a number of catchments with a variety of objectives (Figure 4-6). Perkins, et al (1996) applied it to Carnation Creek, British Columbia to test its road network algorithm. The model was applied to the Boreal forest in Canada as part of the Boreal Ecosystem-Atmospheric Study (Boreas) by Haddeland and Lettenmaier (1995) and Nijssen, et al (1997). Kenward, et al (2000) studied the required accuracy of DEMs for hydrologic modeling using DHSVM in Mahantango Experimental Forest, in Pennsylvania. Bowling and Lettenmaier (1997) used the model to study the effects of forest roads in Hard and Ware Creeks, Washington. Storck, et al (1998) used DHSVM to investigate two rain-on-snow floods



Australia

Figure 4-6: Applications of DHSVM

on the North Fork Snoqualmie and on the Little Naches River (both in Washington) to investigate spring snow melt. Dubin and Lettenmaier (1999) studied the effect of DEM resolution and accuracy on runoff predictions for two catchments in Victoria, Australia using DHSVM. Storck (2000) applied DHSVM to the Snohomish River, Washington in a study on snow accumulation and melt. LaMarche and Lettenmaier (in press) applied DHSVM to the Deschutes River to investigate the hydrologic impact of forest roads.

Chapter 5: Parameter Estimation

Estimation of DHSVM parameters can be broadly classified into two major steps. The first is to assemble surface characteristics data, including digital elevation data, soil characteristics, vegetation, and stream and road network information. The model requires attributes derivable from surface characteristics data for each model pixel. This step is facilitated by use of a GIS, with appropriate overlays for each of the attributes. The second step is to assemble the model forcing data, which consists of time series of meteorological variables and spatial overlays used to distribute these forcings from observing (gaging) stations throughout the catchment. This chapter discusses the sources and processing of these data.

5.1 DEM

Elevation data taken directly from the DEM are used by DHSVM, as are various other topographic attributes (like surface slope and drainage patterns) that are derived from the DEM. DEMs for all four catchments were obtained from the USGS National Mapping Program (USGS, 1993) for Mica and the National Elevation Database (NED) (USGS, 1999) at 30 m spatial resolution. The DEMs were aggregated, using bilinear resampling, according to catchment size so that each of the catchments could be represented with roughly 100,000 pixels or less (see Section 3.2.1). Table 5-1 shows the area, level of aggregation, and number of pixels for each catchment. The aggregated DEMs were then used to delineate each of the catchments (that is, to identify all of the area draining to each of the stream gages). This procedure, which was implemented

Table 5-1: Catchment DEM attributes

	Mores	Entiat	Swan	Mica
Area (km ²)	1028	527	180	27
Pixel Size (m)	120.0	90.0	60.0	30.0
Number of Pixels	71358	65022	50102	29874

using an algorithm described by Jensen and Domingue (1988), is coded in most GIS programs, including Arc/INFO routine FLOWDIRECTION which was used here. Additional processing was performed to preserve general flow characteristics as seen in USGS 7.5 minute map blue lines.

5.2 Soils

The soil data used by DHSVM are based on STATSGO (USDA, 1994) digital soil type and depth maps, and tables describing physical characteristics of each soil type. STATSGO soil units were used to delineate the spatial extent of each soil class used by the model. While these units are at considerably larger scale (30 arc-seconds or about 1 km) than the model resolution (30-120 m), they represent the best currently available data. The STATSGO soil units provide the starting point for estimation of the most sensitive soil parameters which are subsequently varied in the calibration process.

Each DHSVM soil class is described by 13 parameters. Nine of these may vary for each of three model soil horizons (corresponding to rooting zones described later in Section 5.4) as defined in

Table 5-2. For each soil unit, STATSGO specifies the predominant soil texture (sand, loam, clay, and mixes), and bulk density for multiple

Table 5-2: DHSVM soil class parameters

Parameter	# of Values	Description
Lateral Conductivity	1	Lateral saturated hydraulic conductivity (m/s). Used as a calibration parameter.
Exponential Decrease	1	Exponent for decrease in conductivity with depth. Used as a calibration parameter.
Maximum Infiltration	1	Maximum infiltration rate (m/s). Fixed at 1.0E-5 as a large value. (Pacific Northwest soils are generally not infiltration limiting.)
Surface Albedo	1	Soil surface albedo. Fixed at 0.1.
Porosity	3	Soil porosity. Estimated from Table 5.3.3 in Maidment (1992).
Pore Size Distribution	3	Pore size distribution. Estimated from Table 5.3.3 in Maidment (1992).
Bubbling Pressure	3	Bubbling Pressure (m). Estimated from Table 5.3.3 in Maidment (1992).
Field Capacity	3	Soil moisture content at field capacity. Estimated as moisture retained at -33 kPa from Table 5.3.3 in Maidment (1992).
Wilting Point	3	Soil moisture content at wilting point. Estimated as moisture retained at -1500 kPa from Table 5.3.3 in Maidment (1992).
Bulk Density	3	Soil bulk density (kg/m ³). Taken as weighted average of soil horizons from STATSGO.
Vertical Conductivity	3	Vertical saturated hydraulic conductivity (m/s). Fixed at 1.0E-5.
Thermal Conductivity	3	Effective solids thermal conductivity (W/(m*K)). Calculated as the weighted average of the thermal conductivity of the sand and clay fractions.
Thermal Capacity	3	Dry soil thermal capacity (J/(m ³ *K)). Fixed at 1.4E6.

soil horizons. A table created by Rawls (1983) as presented in the Handbook of Hydrology (Maidment, 1992) provides mean values and standard deviation ranges based on soil texture for

most of the required parameters. The other parameters were estimated via calibration or assigned values from previous DHSVM applications.

STATSGO mean rock depth data associated with each soil unit were used as initial estimates of average soil depth. These values were adjusted during the calibration process, however, and were reset to values greater than the total depth of the root zones, if this was not initially the case. For instance, the Swan and Entiat catchments contain a significant area of glacially scoured rock at high elevations. The mean soil depths and some of the other parameters were necessarily adjusted upward to provide subsurface water storage required to produce acceptable matches to observed hydrographs. These changes serve as surrogates for infiltration into fractured rock, which is not directly represented by the model.

Mores Creek required some adjustments of the initial STATSGO-based values as well. Despite being the largest of the study catchments, only three soil units were present in the STATSGO data (likely due to the history of disturbance by mining within the catchment). One of these did not contain useful data. Therefore, the region of the third unit was assigned the values of the second unit.

5.3 Streams and Roads

The DHSVM stream network is based on three types of information: a mapping table which locates a portion of a stream reach within its appropriate grid cell and describes the depth, width,

and aspect of the channel cut into the soil; a reach table describing the length, slope, and class of a reach while connecting it to the next reach downstream; and a class file which assigns routing characteristics of width, depth, and roughness for each stream class. These files are derived from the DEM using an algorithm described by Wigmosta and Perkins (in press).

In essence, the DEM topology defines the stream locations, while the extent of the network is specified by the model user via a given support area (minimum area below which a stream channel is assumed to exist). For the Swan River, Entiat River, and Mores Creek catchments, channel initiation was defined solely through the specification of a source area, which was based in part on field observations. Table 5-3 shows the contributing areas used. For Mica Creek, the channel network extent was estimated by imposing a threshold value such that the inferred channel density was slightly greater than inferred from the blue lines from the USGS 7.5-minute quadrangle. However, the small size of the catchment allowed for the streams to be clipped or extended manually as needed to match field observations. Calibration adjustment of soil conductivity resolves some issues caused by modest mis-specification of the channel network.

Table 5-3: Contributing area for stream initiation

	Mores	Entiat	Swan	Mica
Number of Pixels	3	5	11	15
Area (ha)	4.32	4.05	3.96	1.35

Stream order was defined for use in an initial classification of reaches into a manageable number of types to which channel characteristics could be indexed. Some manual adjustment based on limited field observation was conducted. Class characteristics were defined according to field observations (where available) and the relative descriptive size of the classes. The channel depth, width, and roughness were imposed according to the reach classifications using GISWA algorithms (Wigmosta and Perkins, 1997). Reach mean slope was calculated from the DEM.

The DHSVM road network specification requires information about drainage ditches which are similar to the stream network in construct. The main difference between roads and channels is that the constructed road network is imposed on the DEM as a GIS (arc and node) data layer. Sinks, divides, and stream crossing breaks are present throughout the system, because the road network is not forced to (and generally does not) coincide with local minima in the DEM. The DEM determines the slope and direction of flow along roads. Ditch width, depth and roughness were defined using estimates observed in the field. Proximity of road sinks and modeled culvert discharge to the stream reaches were used to determine connectivity of the road and stream networks. For Mica Creek, direct observations were incorporated in the road attributes. The size and limited number of observations in the other catchments required that some assumptions be used in the development of the road drainage network. Storck (2000) provides a thorough discussion of plausible assumptions used to extrapolate from road observations to parameterize the unobserved portions of the road network. These assumptions were followed in this study as well.

5.4 Current Vegetation

Vegetation information was derived from various sources, and subsequently was processed to be similar in form to the data sets used by Kirschbaum (1997) and Matheussen, et al. (2000).

Current vegetation data were extracted from classified satellite imagery (generally Landsat Thematic Mapper), U.S. Forest Service records, and proprietary records of landowners. Table 5-4 shows the source of vegetation data by catchment. In addition to land classification type, these sources often provided

Table 5-4: Data sources by catchment

	Mores	Entiat	Swan	Mica
DEM	NED	NED	NED	USGS NMP
Vegetation	UMT: Redmond et al & USU: Intermtn. Region Land Cover Characterization	U.S. Forest Service: Wenatchee National Forest	UMT: Redmond, et al	Potlatch Corp. & UMT: Redmond, et al
Soils	STATSGO	STATSGO	STATSGO	STATSGO
Roads	USFS Boise NF	USFS Wen. NF	USFS Flathead NF & Plum Creek	Field Data
Temperature	NRCS	NRCS	NRCS	NRCS
Precipitation	NRCS	NRCS	NRCS	NRCS
Wind	NCEP/NCAR	NCEP/NCAR	NCEP/NCAR	NCEP/NCAR & Potlatch Corp.
Stream flow	USGS	USGS	USGS	USGS
NED	National Elevation Database			
UMT	University of Montana			
USU	Utah State University			
Statsgo	State Soil Geographic database			
USFS * NF	United States Forest Service * National Forest			
NRCS	Natural Resources Conservation Service			
NCEP/NCAR	National Center for Environmental Prediction B4/			
	National Center for Atmospheric Research reanalysis data			
USGS	United States Geologic Survey			
NMP	National Mapping Project			

additional information such as crown closure and vegetation height. Where possible these supplemental data were incorporated into the model representations of vegetation characteristics.

The basic method used to create the DHSVM vegetation parameters was as follows:

- 1- Each species or land cover type present in the catchment was reclassified into one of 36 basic land cover types including the 30 used by Matheussen, et al (2000) using species and size information (such as height, or diameter at breast height) where available. Six classes were

added to the 30 from Matheussen, et al (2000) to describe seasonally bare needleleaf forest (such as Western Larch). Table 5-5 lists the categories. The Matheussen, et al classifications make no distinction for stage or size for single story vegetation (shrubs and meadows).

- 2- These classes were then subdivided based on canopy closure. This deviates from Matheussen, et al who used canopy closure values ("open", "closed") in the original data as a measure of stage in the derived data set. The thematically mapped data quantified the extent of closure enabling its direct use as fractional coverage estimates parameterized in DHSVM vegetation tables.
- 3- Adjacent grid cells (at the native resolution of the vegetation data—generally 30 m) with identical vegetation classifications were combined and transformed into polygons, representing stands.
- 4- The polygons were then converted to a grid at the model resolution (see Table 5-1). Where more than one type existed within a modeling cell, the dominant type was

Table 5-5: Vegetation species / stage classes

CLASS	ABBREVIATION	Name
1	CFI-early	Conifer, low drought tolerance, early
2	CFM-early	Conifer, moderate drought tolerance, early
3	CFT-early	Conifer, high drought tolerance, early
4	CFVT-early	Conifer, very high drought tolerance, early
5	DFI-early	Cottonwood/willow, early
6	DFM-early	Aspen, early
7	DFT-early	Oregon white oak, early
8	CFI-middle	Conifer, low drought tolerance, middle
9	CFM-middle	Conifer, moderate drought tolerance, middle
10	CFT-middle	Conifer, high drought tolerance, middle
11	CFVT-middle	Conifer, very high drought tolerance, middle
12	DFI-middle	Cottonwood/willow, middle
13	DFM-middle	Aspen, middle
14	DFT-middle	Oregon white oak, early
15	CFI-late	Conifer, low drought tolerance, late
16	CFM-late	Conifer, moderate drought tolerance, late
17	CFT-late	Conifer, high drought tolerance, late
18	CFVT-late	Conifer, very high drought tolerance, late
19	DFI-late	Cottonwood/willow, late
20	DFM-late	Aspen, late
21	DFT-late	Oregon white oak, early
22	SI-shrub	Herbaceous wetland/shrub, shrub
23	SM-shrub	Mountain shrub, shrub
24	ST-shrub	Sage shrub, shrub
25	G/F-shrub	Grassland/forbs, shrub
26	W-shrub	Herbaceous wetland, shrub
27	T-shrub	Alpine tundra, shrub
28	A-shrub	Agriculture, shrub
29	N/A	Barren, shrub
30	N/A	Water,
31*	CFMS-early	Conifer, Moderate Drought Toler., Early, Seasonal
32*	CFMS-middle	Conifer, Moderate Drought Toler., Middle, Seasonal
33*	CFMS-late	Conifer, Moderate Drought Toler., Late, Seasonal
34*	CFMSM-early	Conifer, Moderate Drought Toler., Early, Seasonal, Mixed
35*	CFMSM-middle	Conifer, Moderate Drought Toler., Middle, Seasonal, Mixed
36*	CFMSM-late	Conifer, Moderate Drought Toler., Late, Seasonal, Mixed

used. Figures 5-1, 5-2, 5-3, and 5-4 show the current vegetation classification for the Mica, Swan, Entiat, and Mores catchments.

5- The detailed description of the characteristics of each land class (Table 5-6) was developed by using the descriptive parameters used by Matheussen, et al and vegetation descriptions available from previous DHSVM applications. Some of the parameters overlap while others were not available. Where necessary, estimates of parameters were made based on the author's understanding of tree species, literature values, and experimentation with the model. Appendix A includes a more complete summary of this procedure.

5.5 Surface Characteristics used in Sensitivity Studies

Alternate land classification descriptions were developed for each of the catchments for the sensitivity runs. Four states were developed for each catchment: 1- A "historical" condition derived using current vegetation variability and a 1-km historical data set; 2- A mature overstory condition; 3- No overstory (clear-cut); and 4- No roads. In addition, vegetation scenarios representing 1933 post-harvest Mica Creek and Mores Creek current land cover aggregated to 1-km resolution were prepared.

5.5.1 Historical Approximation

Historical vegetation data (corresponding to the 1900 condition from Matheussen, et al (2000)) were not available for any of the catchments at the same level of detail as was the current vegetation information. Therefore, it was necessary to estimate historical vegetation conditions using the best available information, combined with a consistent

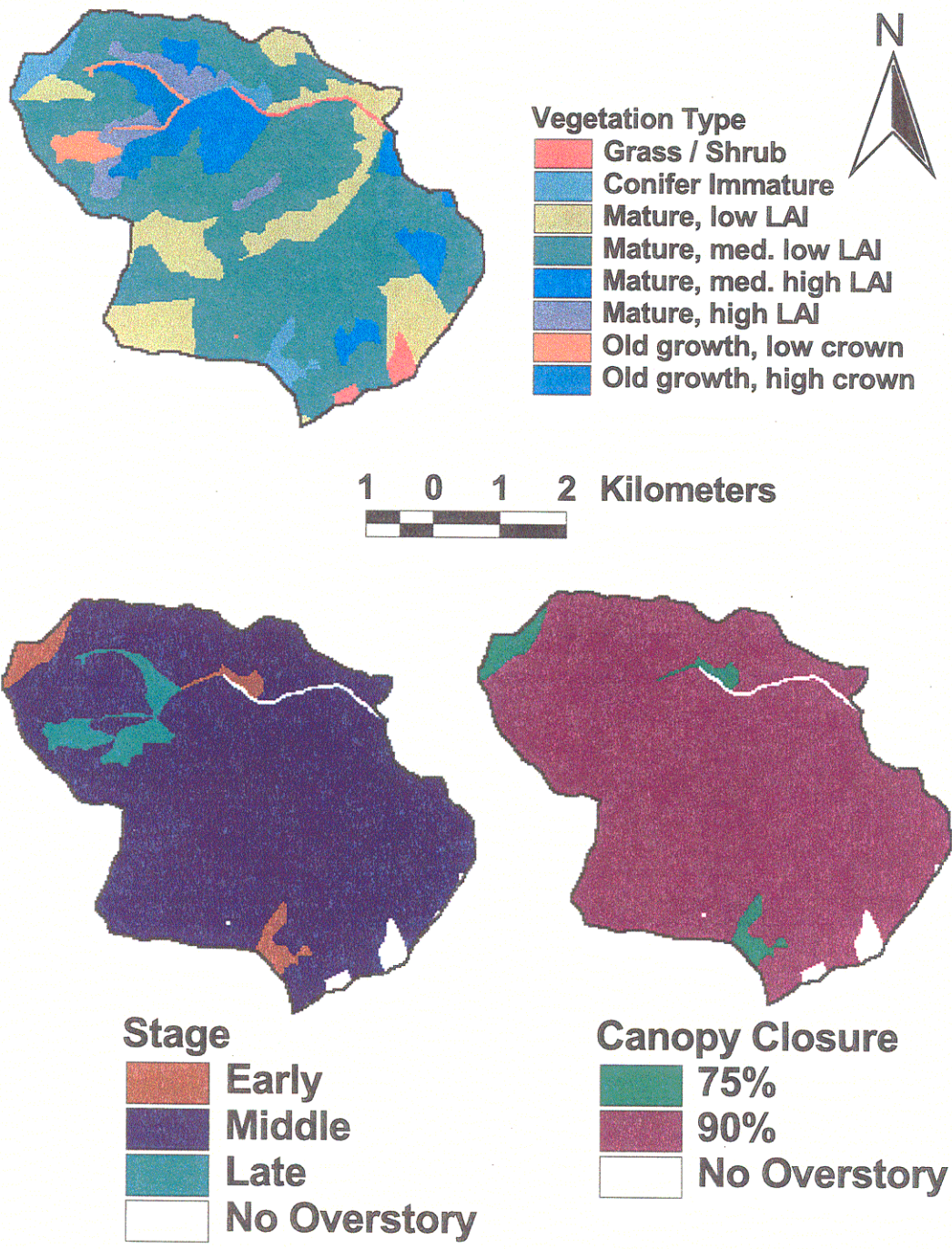


Figure 5-1: Mica Creek vegetation. Three characteristics were used to classify the vegetation into 108 types: 1) species group (top); 2) stage—estimation of age and size of overstory vegetation (bottom-left); and 3) overstory canopy closure or density (bottom-right).

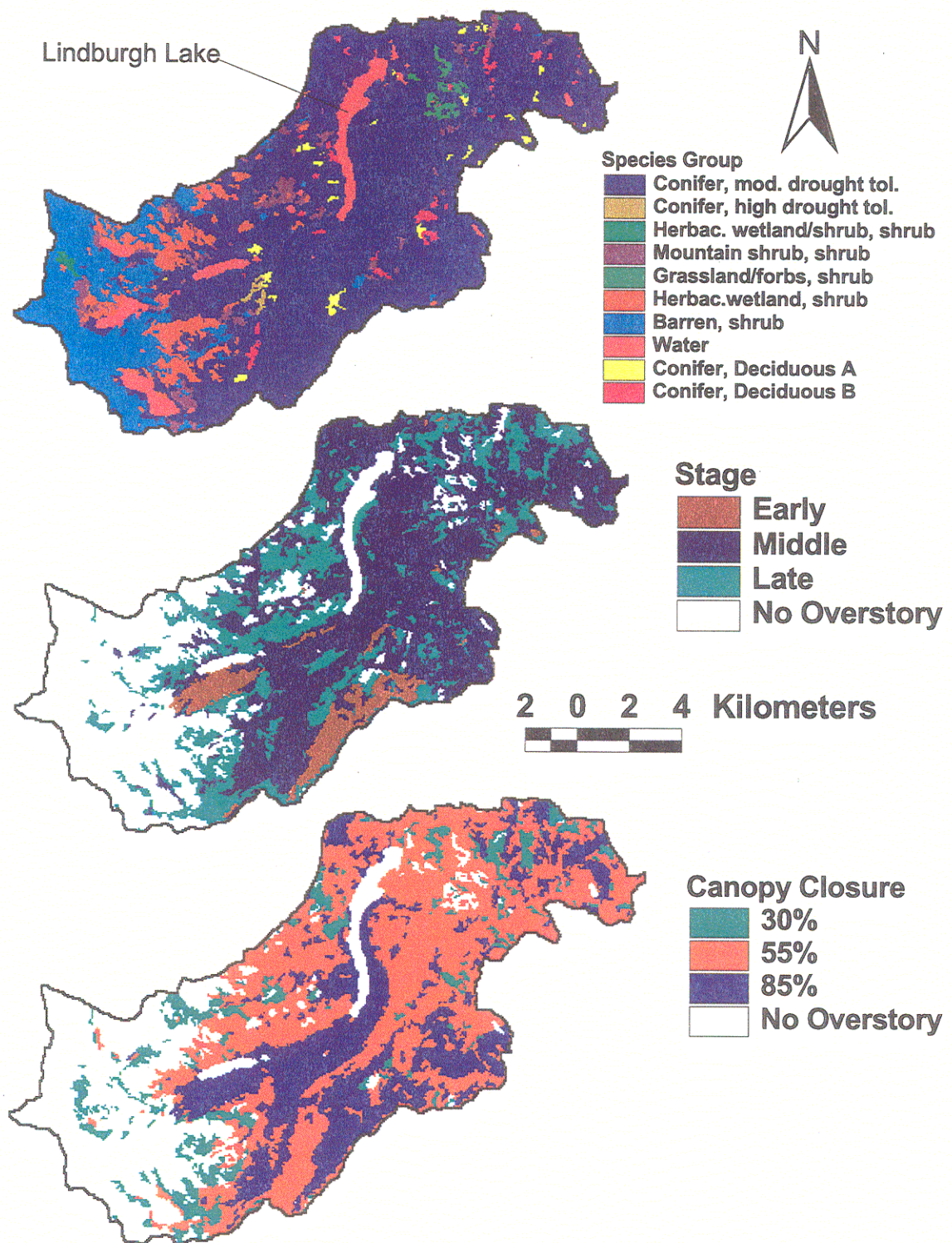


Figure 5-2: Swan River vegetation. Species group (top), stage (middle), canopy closure (bottom) are the characteristics of each of 108 vegetation types.

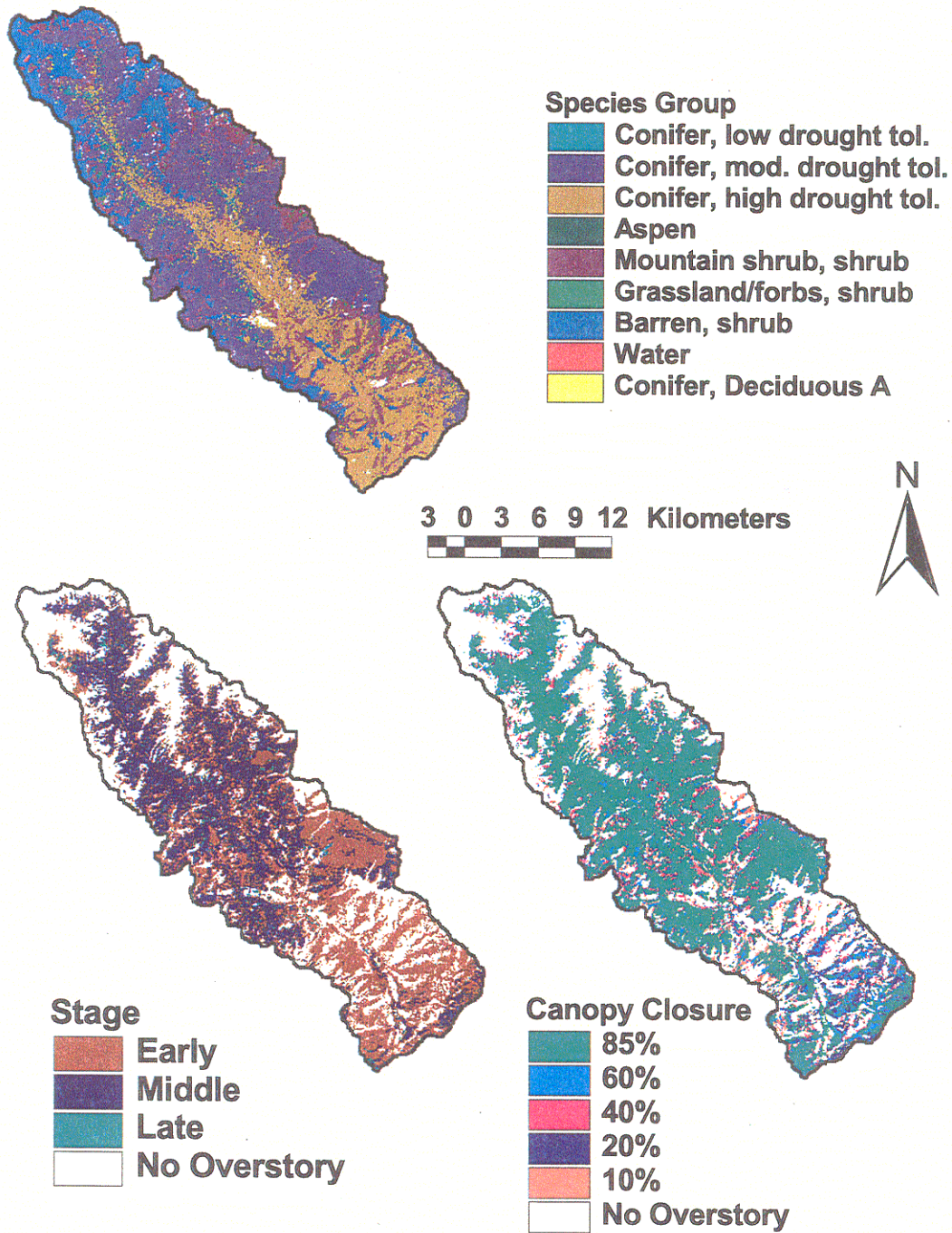


Figure 5-3: Entiat River vegetation. Species group (top), stage (middle), canopy closure (bottom) are the characteristics defining each of 108 vegetation types.

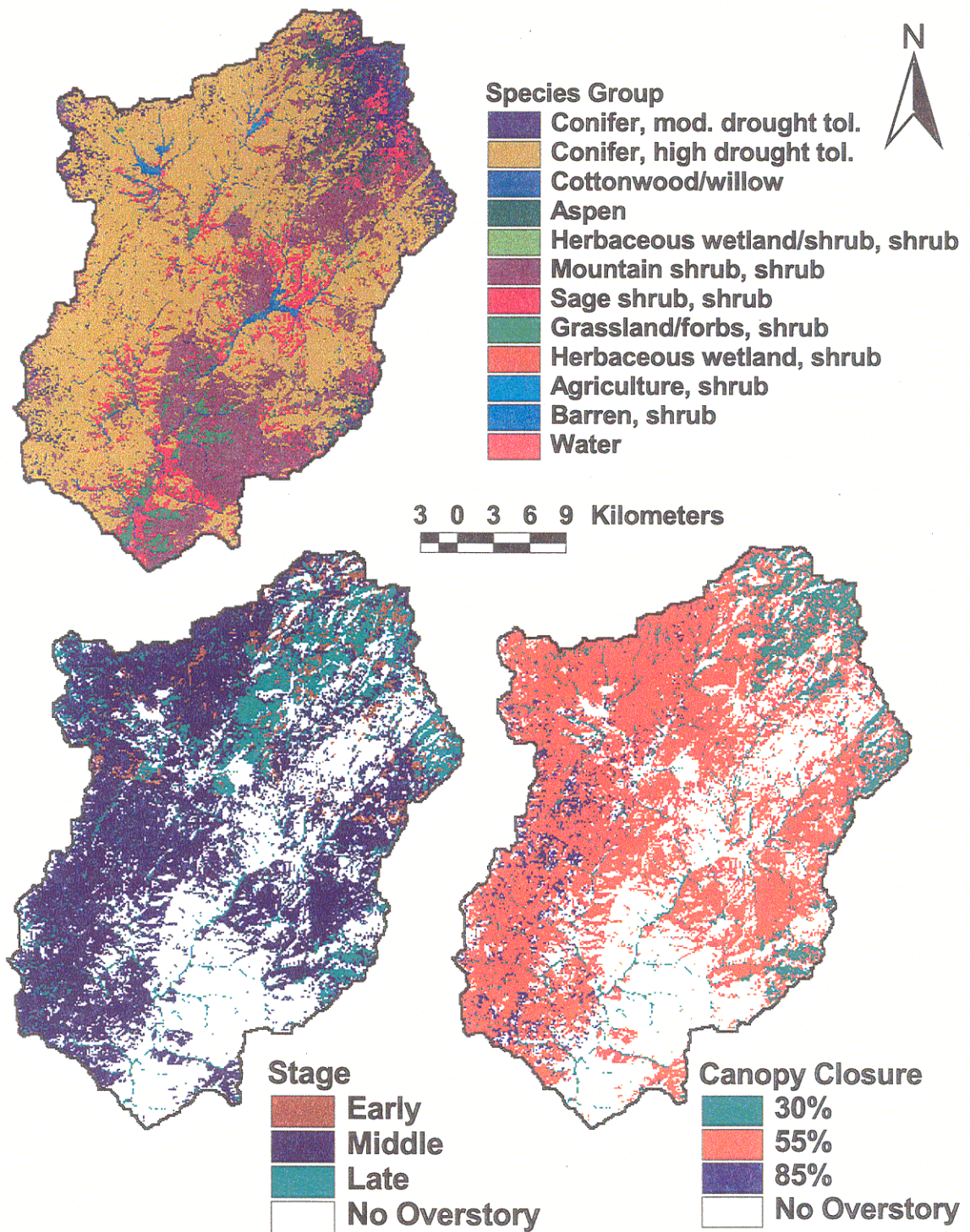


Figure 5-4: Mores Creek vegetation. Species group (top), stage (middle), canopy closure (bottom) are the characteristics defining each of 108 vegetation types.

Table 5-6: Vegetation class descriptive parameters

Overstory Present	Vegetation has an overstory (TRUE or False)
Understory Present	Vegetation has an understory (TRUE or False)
The following set of properties only applies to the overstory layer (if there is one)	
Fractional Coverage	Fractional coverage of the overstory (0-1)
Trunk Space	Height of the trunk space as a fraction of the overstory height
Aerodynamic Attenuation	Aerodynamic attenuation for wind through the overstory
Radiation Attenuation	Attenuation coefficient for radiation through the canopy
Max Snow Int Capacity	Maximum snow interception capacity of canopy under wet snow conditions (i.e. near freezing); below -5C value is 25% of given (m of SWE)
Snow Interception Eff	(0-1) Efficiency of snow interception
Mass Release Drip Ratio	(0-1) Ratio of mass release to meltwater drip
The following set of properties varies with the layer (overstory, understory).	
Height	Vegetation Height (m)
Summer LAI	One-sided summer LAI
Winter LAI	One-sided winter LAI
Maximum Resistance	Maximum stomatal resistance (s/m)
Minimum Resistance	Minimum stomatal resistance (s/m)
Moisture Threshold	Soil moisture threshold below which transpiration is restricted
Vapor Pressure Deficit	Vapor pressure deficit above which transpiration is restricted
Rpc	
Albedo	Albedo of vegetation
The following provides root zone information for the current vegetation type	
Number of Root Zones	Number of root zone layers.
Root Zone Depths	Depth of root zones (m)
Overstory Root Fraction	Fraction of overstory roots in each root zone layer
Understory Root Fraction	Fraction of understory roots in each root zone layer

method for estimating the historical condition at the same resolution as was available for current conditions. As was the case in developing the current vegetation data for each of the catchments, the relative mix of direct information and assumptions varied between the catchments.

Two data sets form the basis for the construction of historical land cover. The first is the current land cover data set for each catchment as described in Section 5.5. The second is a land cover classification representative of 1900 conditions at 1-km resolution produced by the Interior Columbia Basin Ecosystem Management Program (ICBEMP -- Hardy, et al, 1996; Thornton and White, 1996) which was used by Matheussen, et al (2000). The ICBEMP data do not include information about canopy closure, although stand stage is included and the transformation to these classes did use density, which was specified in the ICBEMP data.

The procedure used to develop historical land cover data sets is shown in schematic form in Figure 5-5. In the figure, regions are labeled with letters, vegetation species / stage types are identified by color. Canopy closure is labeled by colored letters A, O, and X or empty cells.

The algorithm consists of the following steps:

- 1- The 1-km grid cells used in the ICBEMP vegetation (B) were defined and labeled uniquely (A).
- 2- The high-resolution land cover types were spliced into two grids, one representing the species and stage (C), and the other representing canopy closure (D), or absence of canopy for understory-only vegetation.
- 3- For a given 1-km cell, the corresponding high-resolution grid cells were identified (E).
- 4- The species / stage types within the region were extracted into a histogram of occurrences (F).

- 5- The bins were ordered from most populous to least populous, with the exception of rock and water types. These were considered “least populous” independent of their count because they were assumed not to have changed within the 100-year time frame (see the maroon portion in Figure 5-5).
- 6- Using the pseudo-cumulative probability distribution completed in step 5 above, the location of the 50th percentile was identified.
- 7- Beginning with the most populous, all bins up to the 50th percentile were earmarked for change. If a bin was selected, all cells within the bin were to be changed, even if more than 50 percent of the region was selected. If a majority of the region was rock and / or water, then the percentage for change was less than 50 percent.
- 8- All cells belonging to non-earmarked bins were copied directly into the historical grid (1 & G).
- 9- All cells belonging to earmarked bins were reassigned the vegetation class present in the 1-km ICBEMP grid cell (2 & G). In some cases, this class is no different from the original high-resolution class.
- 10- Because no canopy closure information is available in the 1-km vegetation class, the high-resolution cells were then stamped with canopy closure from the original current vegetation (3 & G). If a forested type (w/ overstory, and canopy closure > 0) transforms to a non-forested (understory only) type, canopy closure information is not applicable and hence discarded. If a non-forested type transforms to a forested type, the canopy closure type defaulted to 85 percent.

The procedure described above was developed with the intention of maintaining spatial patterns and variability of similar species and stages to represent plausible stand progressions.

Assumptions were made where there simply was not sufficient information available to specify species and age definitively. The resultant high resolution historical vegetation descriptions are plausible approximations of what could have been. Results and conclusions must be considered within this context. Furthermore, every effort has been made to document the decisions that were made with the intention that any subsequent studies may be able to use improved representations.

Maps of Leaf-Area Index (LAI) were produced for the current and historical vegetation data sets and are shown in Figures 5-6, 5-7, 5-8, and 5-9. The LAI values shown were calculated using the overstory summer LAI multiplied by the canopy closure and added to the understory summer LAI. The residual LAI values (current LAI – historical LAI) are also shown in the figures.

In addition to the 1900 historical approximation, a parameterization representing Mica Creek 1933 conditions was prepared. Aerial photographs were provided by the Potlatch Corporation, and are dated 1933—shortly after most of the catchment was clear-cut harvested. The extent of harvest covered more than eighty percent of the catchment.

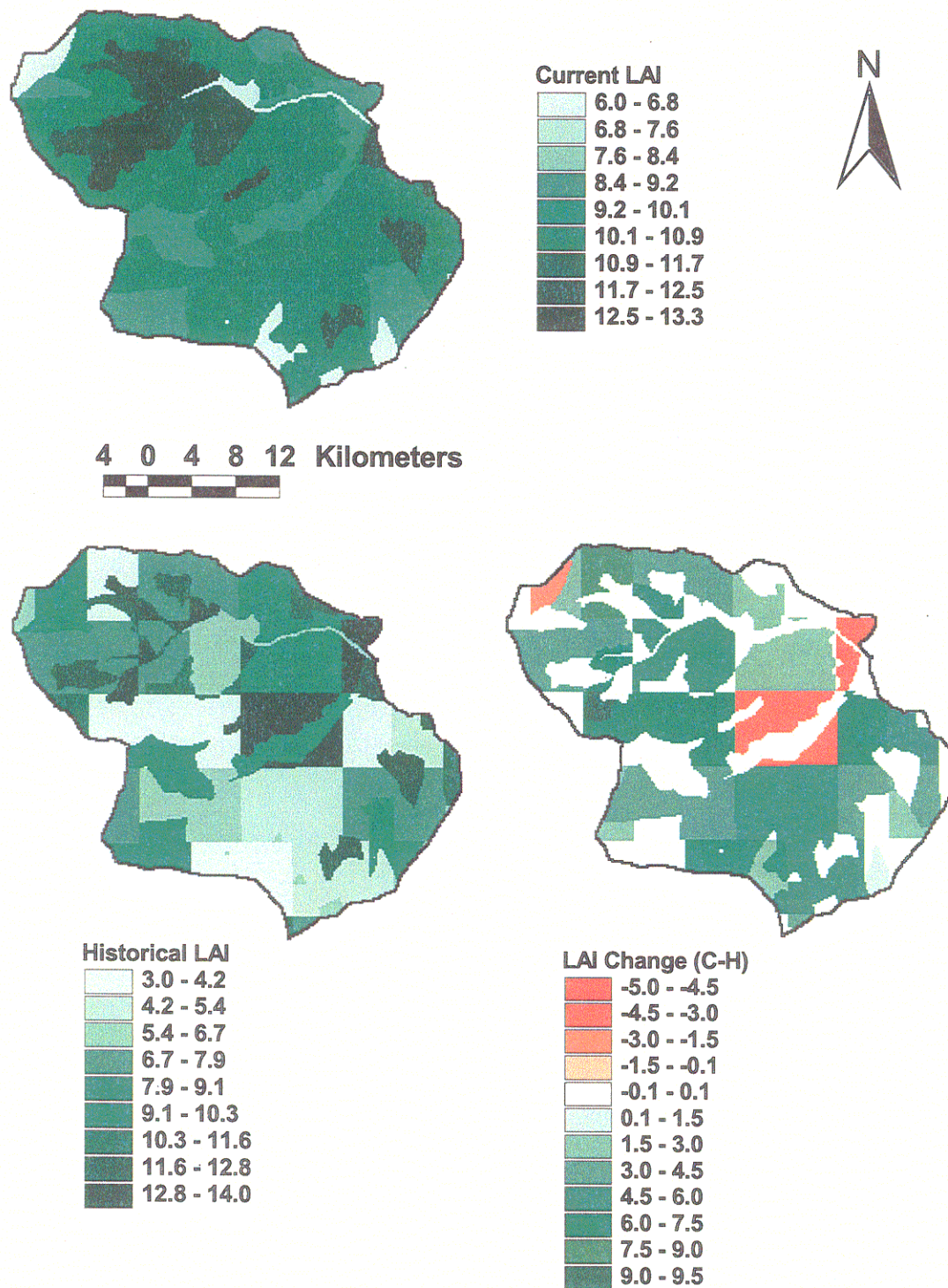


Figure 5-6: Mica Creek LAI. Calculated from current vegetation based on Potlatch data (top), historical vegetation (bottom-left), and the change (current – historical) in LAI (bottom-right)

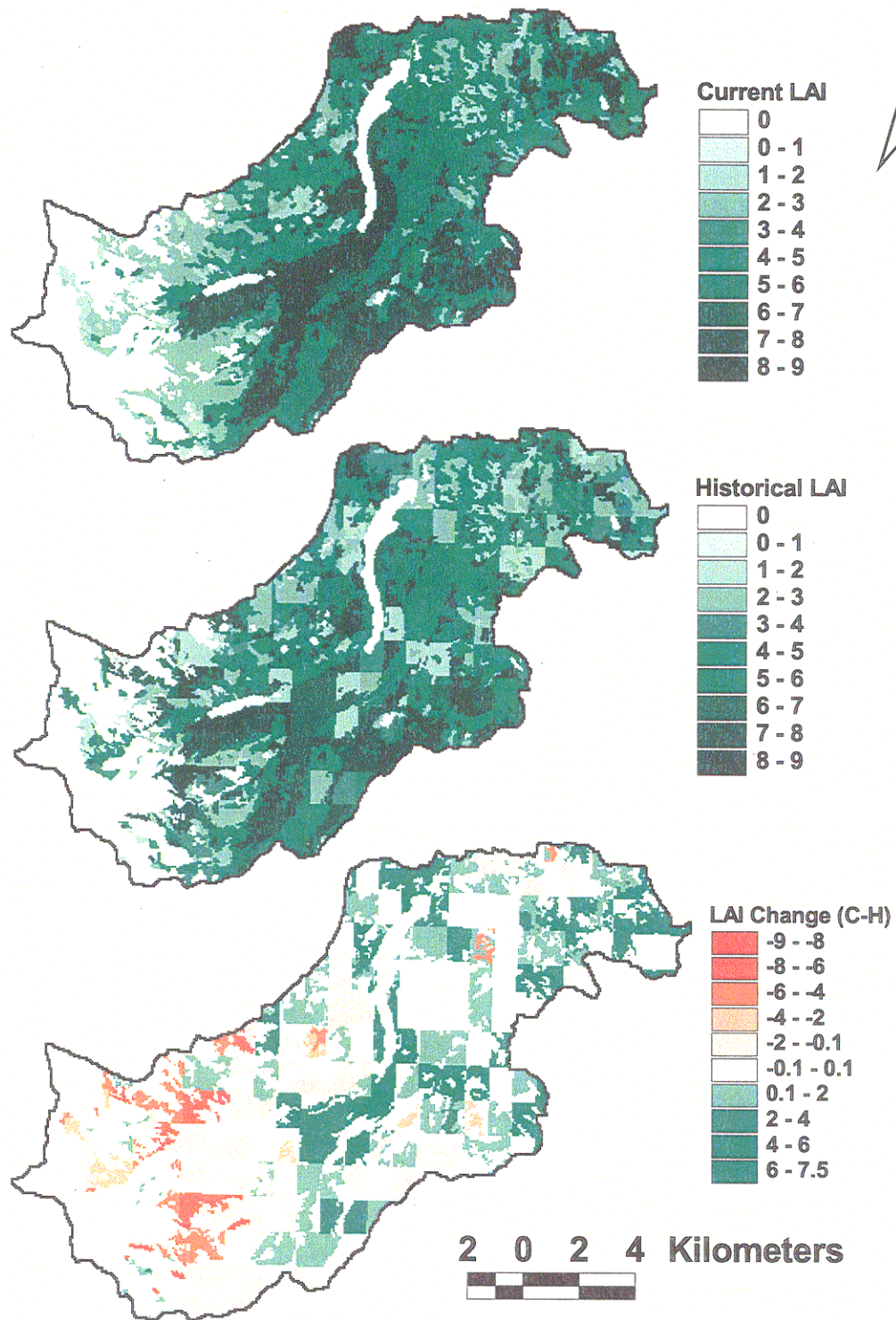


Figure 5-7: Swan River LAI. Calculated from current UMT (top), historical vegetation (middle), and the change (current – historical) in LAI (bottom)

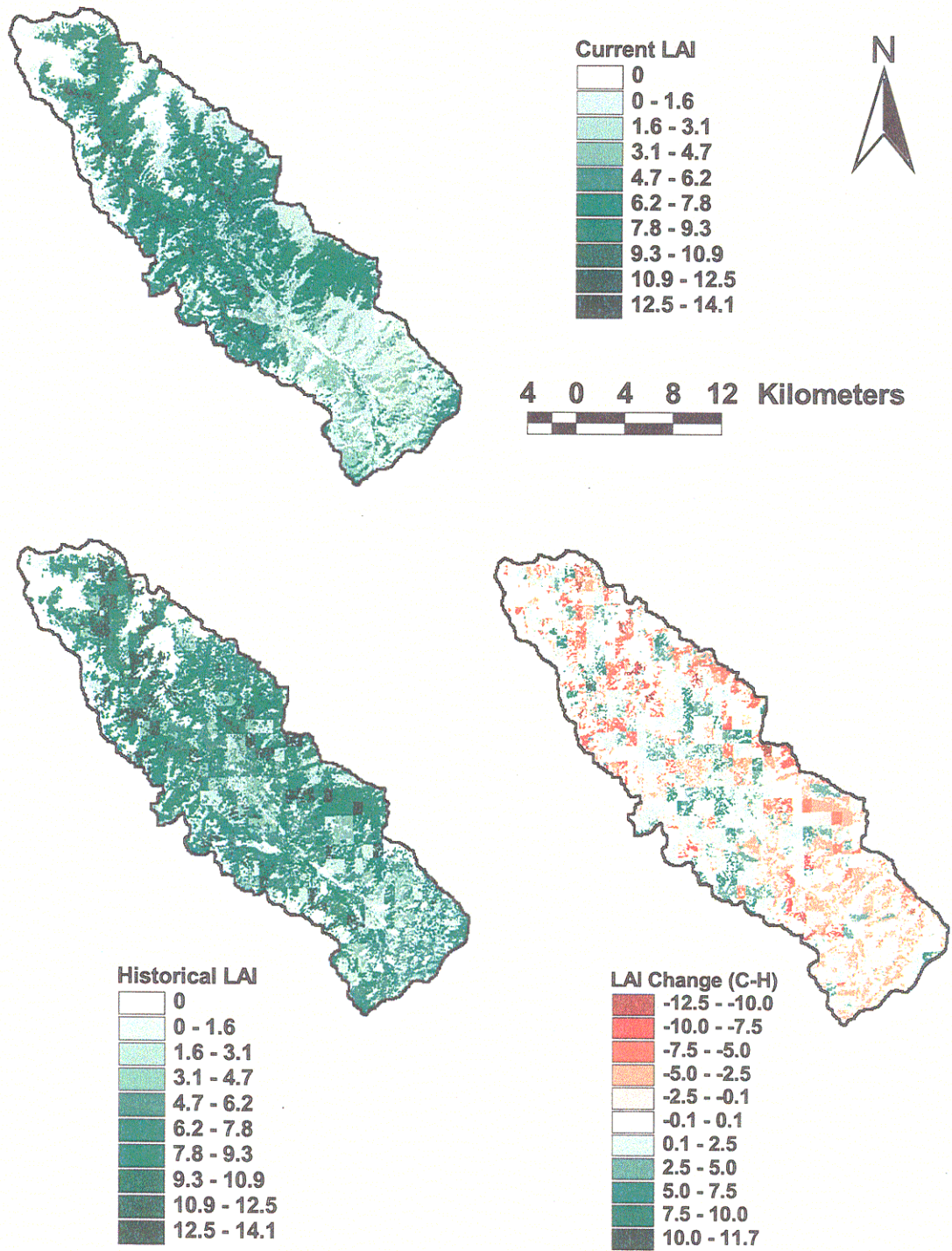


Figure 5-8: Entiat River LAI. Calculated from current vegetation (top), historical vegetation (middle), and the change (current – historical) in LAI (bottom)

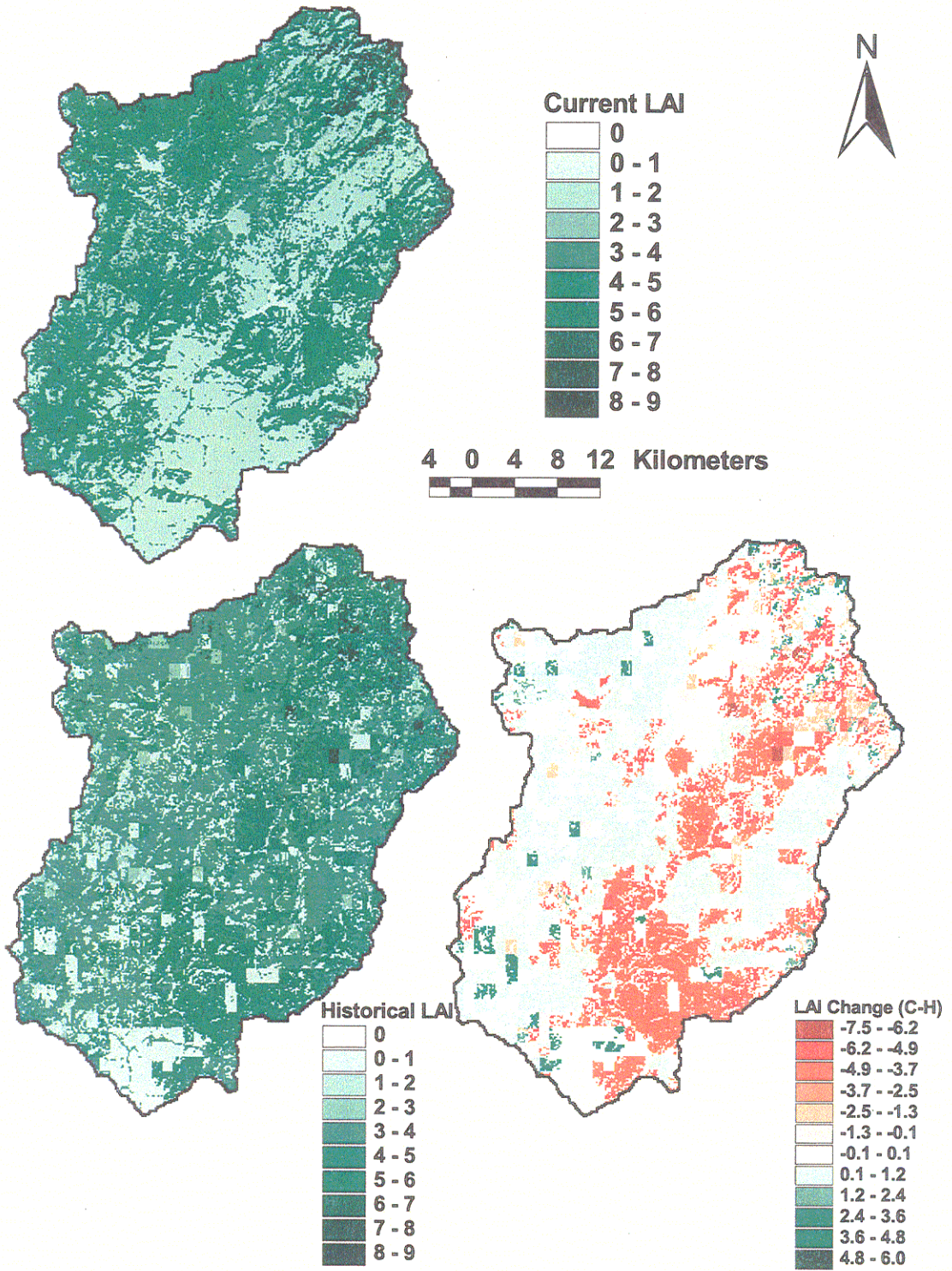


Figure 5-9: Mores Creek LAI. Calculated from current vegetation data (top), historical vegetation (bottom-left), and the change (current – historical) in LAI (bottom-right)

Uncut patches retained the old-growth classification described in the current Potlatch vegetation grid. Cut patches were assumed to contain only understory vegetation.

5.5.2 Other Vegetation Scenarios

For the fully mature condition, all pixels other than water were assigned to the late stage, 85 percent canopy closure, low drought tolerance, conifer land cover type. This represents the most water demanding, highest LAI vegetation class developed for the study, and should provide an upper envelope for canopy evapotranspiration for fully forested conditions.

For the no overstory condition, all forested pixels were reassigned to the mountain shrub-shrub land cover type. Non-forested pixels (barren, herbaceous, water) were unchanged.

Road effects were assessed by removing the road network in the model. This is accomplished simply by switching off roads in the main input file. Generally, the roads are not visible in the land cover classifications themselves.

The 1-km parameterization of Mores Creek current vegetation was developed using the 1-km regions described in Section 5.5.1. For each of these regions, the dominant vegetation type (of the 36 described in Table 5-5) was determined. The dominant level of canopy closure was also found. The combination of the type and canopy closure was assigned for all 120 m cells within the region. If the type was understory vegetation only, the canopy closure was not used.

5.6 Meteorological Data

DHSVM is forced with meteorological time series data for a variety of variables measured or estimated at a given point in or near the catchment. The time series values are distributed spatially during model execution. The model is sensitive to the meteorological variables, especially precipitation and temperature. In developing the input time series, careful attention was given to identification of data errors (James and Burges, 1982), estimation of missing data, and to adjustment for differences in elevation and other topographic effects. Errors and limitations in the data often become apparent in calibration of the model. All four catchments are topographically complex, and in most cases observation locations are remote from at least part of the catchment. Nevertheless, the nature of the investigation—sensitivity of the catchment to variations in land cover—allows for these limitations since all model runs are forced with identical data and only differences in model simulations are considered.

5.6.1 Time Series Preparation

Meteorological time series development began with daily observations of precipitation and maximum and minimum temperatures. The time series available for gages within the basin and nearby were assembled, and missing data were estimated from nearby reporting stations. Two techniques were used to estimate missing data. First, individual values or short gaps in data were filled by hand using comparisons of the previous and subsequent observed values, observed values at nearby gages, estimates of local (in a spatial and temporal sense) lapse rates, and precipitation ratios. Longer data gaps were filled by applying a monthly temperature lapse or

precipitation volume ratio to data from the nearby gage with the highest correlation to the gage in question for the particular month. Records of filled dates and data were kept as a reference in case the forcing data appeared to be problematic during model calibration.

Hourly temperatures were then derived through interpolation using Hermite polynomials as described in Conte and de Boor (1980). The maximum temperature was fixed at the hour during which the angle of the sun (with respect to the horizon) decreases most rapidly. The minimum temperature was set to the hour before sunrise.

Because relatively few of the gages used in this study record hourly precipitation, daily precipitation was disaggregated to hourly values by applying an hourly to daily depth ratio calculated at a nearby station to the observed daily precipitation data. Although the calculated timing of storms may be in error due to the geographic location of the gages, the pattern of storm intensity is preserved. This timing affects solid-liquid precipitation partitioning (as determined by coincident temperature) and is occasionally apparent in the simulations. Over the course of a winter, however, these effects tend to cancel. For most of the catchments (all of which are snowmelt-dominant), spring runoff is determined primarily by total winter snow accumulation. When no hourly precipitation record was available (due to missing data), or was zero during a period of precipitation at the gage in question, the precipitation was distributed uniformly over the 24-hour period.

Observed wind data were not available within any of the catchments for the full length of investigation. In fact, Mica Creek is the only catchment for which any wind data were available within the catchment. Initially, wind was extrapolated from the closest airport for Swan River and Mores Creek, which in both cases is a considerable distance from the catchments. There are no data within reasonable proximity of the Entiat River. Therefore, wind data from the lowest model layer in the NCEP/NCAR Reanalysis (Kalnay, et al, 1996) were used. For Mica Creek, observations were used when available (post-1996). The reanalysis data were processed using methods described by Bowling and Lettenmaier (1997). In all cases, daily average wind speeds were used because 6-hour interval data were not complete over the entire period of investigation. The wind speed was adjusted to the reference height of DHSVM (from ground to 75 m) using a power function and estimates of vegetal roughness lengths.

Relative humidity was taken from observations or was estimated using the method of Kimball, et al (1997). For Mores Creek, relative humidity observed at the Boise International Airport was used. Kimball's method was applied in Mica Creek, Swan River, and Entiat River catchments due to the absence of relative humidity data. In the case of the Swan River, Missoula was found to be unrepresentative because it is considerably dryer. This method uses annual precipitation, estimates of daily potential evaporation, and daily air temperature to estimate the dew point. This improves on the assumption that the dew point is equal to the daily minimum temperature. The hourly temperatures derived as described above were used to produce hourly values of relative humidity.

Downwelling long wave radiation was calculated for each hour using the hourly temperatures according to the method outlined in Bras (1990) as taken from Tennessee Valley Authority (1972) and Bristow and Campbell (1984). Bowling and Lettenmaier (1997) and La Marche and Lettenmaier (1998) provide details of application of this method for DHSVM. The hourly values were aggregated to the 3-hour model time step.

Short wave radiation was calculated at each meteorological gage based on the solar calendar and an estimate of atmospheric transmittance (Gates, 1980; Bras, 1990; Curtis and Eagleson, 1982; Tennessee Valley Authority, 1972). Hourly estimates were aggregated to the 3-hour model time step as was the long wave radiation. The estimated value was later partitioned (internally by DHSVM) into direct beam and diffuse radiation, and scaled according to topographic shading of each pixel. Details of the approach are provided by Dubayah (1990) and Arola (1993).

5.6.2 Spatial Distribution

Precipitation interpolation was accomplished using either maps of monthly average precipitation or through use of elevation lapse rates. For Mores Creek and the Entiat River (the two largest catchments) PRISM maps (Daly, et al, 1994) were used for spatial adjustment. The approach was to interpolate the precipitation at the gages to the given pixel using standard inverse-distance squared methods. Next, the long-term monthly means for the stations (PRISM value of the station cell) were interpolated to the pixel. The interpolation of the current precipitation was

then scaled by the ratio of the pixel's long-term monthly mean (PRISM value at the pixel) and the interpolated long-term monthly mean. The PRISM maps, originally produced at 2.5 minute (~5km) spatial resolution, were re-projected from the geographic coordinate system to UTM, and resampled to the modeling pixel size using a bilinear interpolation scheme.

Because of its small size, Mica Creek used a monthly average precipitation lapse rate based on the averages of the elevation lapses between the SNOTEL site (Figure 3-1) within the catchment and four meteorological stations operated by the Potlatch Corporation. For the Swan River, a monthly lapse rate was back-estimated from Lindburgh Lake (Figure 3-3) monthly means and model output to approximate the monthly catchment average precipitation depths achieved with the PRISM. While maintaining PRISM volumes, precipitation was distributed entirely according to elevation. This procedure was found to produce the most reasonable results during the calibration process.

For each catchment, variable (by month) temperature lapse rates were estimated using daily maximum temperatures. Using this concept as a general rule, each basin required individual treatment based on the number of temperature gages within (or near) the basin. The specifics are discussed in Chapter 6.

Chapter 6: Model Calibration

Chapter 5 discussed the general approach to model implementation. This chapter summarizes the estimation of model parameters for the four study catchments. The objective of the parameter estimation procedure (often referred to as calibration) was to identify a set of parameters for each catchment that produced model results consistent with observations while maintaining appropriate relationships between parameter values and watershed characteristics (James and Burges, 1982).

There is extensive literature on the topic, much of which deals with application of optimization techniques for calibration of hydrologic models (see e.g. Duan, et al, 1994; Gupta, et al, 1998; Yapo, et al, 1998; Gupta, et al, 1999).

In general, optimization procedures, however, are inappropriate to complex spatially distributed models like DHSVM. The computational time required (hours to days) for a multi-year, catchment-wide simulation precludes the use of techniques that require many such simulations to estimate relationships between individual parameters and an objective function related to model “fit” (ability to reproduce observations). For this reason, manual trial and error approaches (which are much more common in hydrologic practice) were used. The manual approach proceeded as follows. First, point simulations (at SNOTEL gages, for example) were used to obtain an initial indication of the effect of adjusting individual parameters. A “fast track”

sensitivity analysis was conducted by simulating a small representative fraction (typically about 5 percent) of the catchment. Catchment-wide runs are also made to produce simulated streamflow for comparison with recorded hydrographs at the catchment outlet. In all cases (point, representative subcatchment, and catchment) an iterative calibration process was used, in which selected parameters (identified from previous DHSVM studies in similar environments) were adjusted within pre-specified ranges, until a parameter set was identified that reproduced the observed streamflow. Hydrograph peaks, recession and general shape, annual water balance quantities, and snow accumulation and ablation patterns were used in comparison of simulated and recorded values. Once this process was complete, simulations were made for an additional period of record. Comparison of the simulated and observed values for this period (termed "validation") demonstrates how well the model performed under conditions that may not have been present in the calibration period. Application and results of this approach are described for each catchment in the remainder of this chapter.

6.1 Mica Creek

Mica Creek was initially identified by the Potlatch Corporation for use in a planned, paired catchment study and was included here for that reason. Land cover classifications were based on proprietary data provided by Potlatch. Calibration for this basin required adjustment of temperature lapse rates, lateral saturated hydraulic conductivity (K_s), exponential decrease of K_s with depth, precipitation lapse rates, stream cut depths, and rain / snow threshold temperature. It was also decided during this process to force the model using meteorological observations from

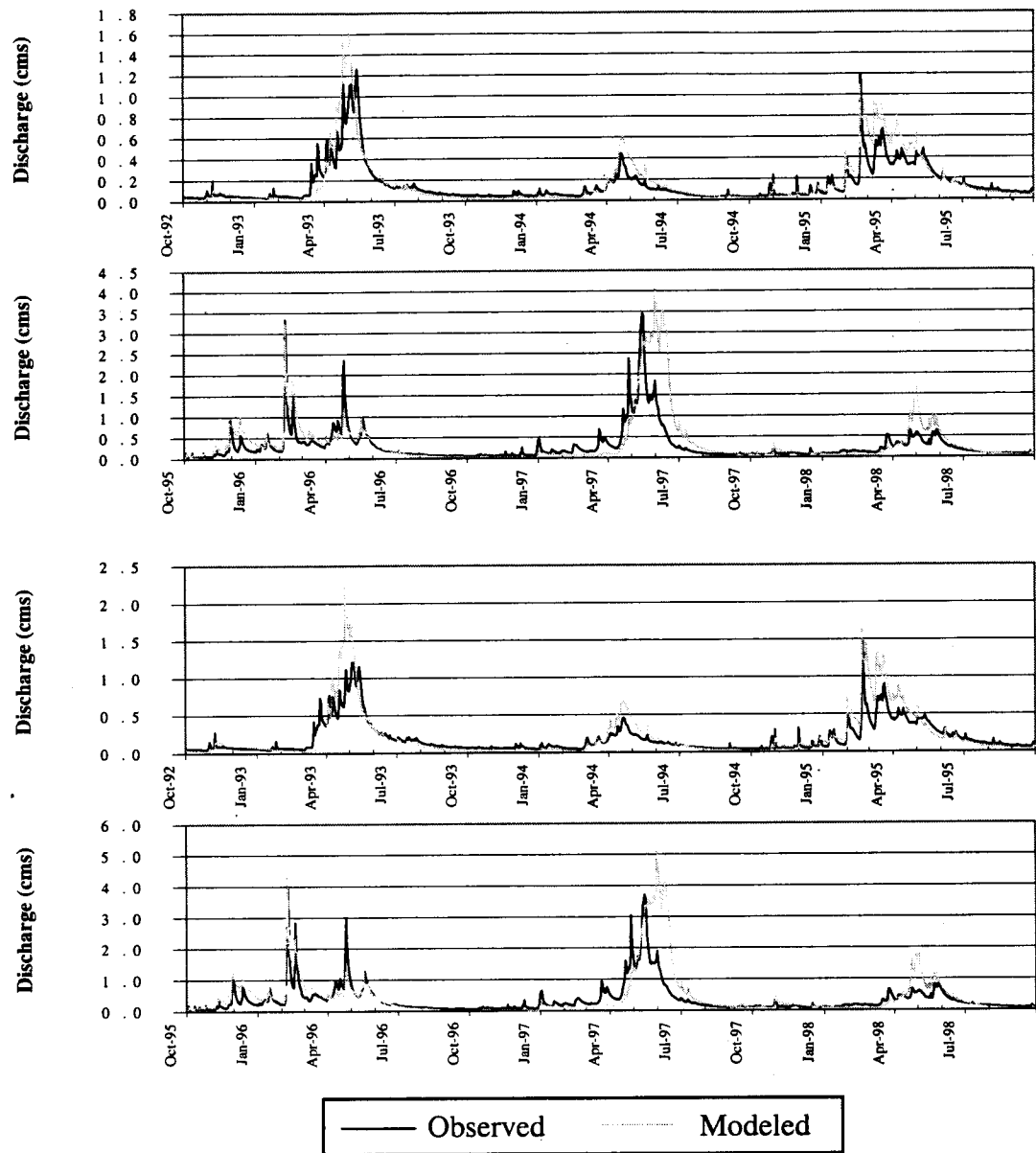
the SNOTEL gage only (see Figure 3-1), as various data quality problems were experienced using data from the other sites. Calibration was performed for the no-road condition, as the roads that most affected the hydrology of the catchment were not built until after the calibration period (October 1992 through September 1995).

Time series temperature lapse rates were estimated using constructed 3-hourly data from the SNOTEL site and flumes 1, 4, 5 and 7 (see Figure 3-1). If temperatures at the flumes were either all warmer or all cooler than the SNOTEL gage, a lapse rate was calculated as the average lapse of SNOTEL and gages 1 and 5. The lapse rates were bracketed by extreme values of -5.5 °C/km and 5.5 °C/km, with calculated values reset to these limits if they were outside the range. If a lapse rate could not be calculated in this fashion it was initially assigned to 0 °C/km. If precipitation was recorded at flumes 1, 5 or 7, an inversion was considered unlikely and initial lapse rates greater than or equal to 0 °C/km were reassigned the moist adiabatic lapse rate of -5.5 °C/km. Precipitation lapse rates were calculated as monthly values averaged over the entire gage record. An undercatch of 10 percent for each precipitation event was assumed in accordance with ranges provided by Legates and DeLiberty (1993) at each of the flume precipitation gages, although a larger value for snow could be justified. Lapse rates from each flume to the SNOTEL gage were calculated on a daily basis. Averaging the rates for each gage by month, the monthly value with magnitude closest to zero was used. This method attempted to provide an elevation lapse rate without magnifying the errors associated with precipitation gages that were inoperable in the winter months (only the SNOTEL precipitation gage is all-weather).

Calibration was achieved by comparing the modeled and observed streamflow for the gages within the basin. Figure 6-1 shows the daily time series for gages 6 and 7. From these figures, several things are apparent. First, although the peaks are over-simulated in most cases, the timing of the peak flows is reasonably well estimated. Some of the peak flows appear to be displaced due to early melt, and early spring flows are often under predicted—particularly in the years with large, late modeled flows. The recession slopes are consistent with observations. The annual simulated and observed flow volumes for the sum of flumes 6 and 7 are shown in Table 6-1, and are in reasonable agreement with observations for the calibration years. Somewhat larger discrepancies between predicted and observed annual flows are apparent in the verification years.

Table 6-1: Mica Creek: Annual flow volumes

Water Year	Observed Runoff (m)	Modeled Runoff (m)	Prec. (m)	ET (m)
Calibration				
1993	0.463	0.496	1.045	0.464
1994	0.207	0.228	0.471	0.440
1995	0.455	0.578	0.570	0.354
Totals	1.125	1.302	2.086	1.259
Validation				
1996	0.843	0.985	0.745	0.495
1997	0.900	1.231	0.668	0.469
1998	0.418	0.537	0.563	0.399
Totals	2.161	2.752	1.977	1.363



Graphs from the top are: Flume 7 calibration, Flume 7 validation, Flume 6 calibration, Flume 6 validation

Figure 6-1: Mica streamflow calibration and validation hydrographs (cms)

Comparisons of snow accumulation and ablation at the SNOTEL gage were also made and are shown in Figure 6-2. Rain / snow threshold temperature and snow roughness were adjusted between -1 and 3 °C (USACE, 1956) to improve the calibration for water years 1993-1995. An increase in the threshold resulted in more precipitation falling as snow. While the peak snow volumes for the calibration years are consistent with observations, the ablation is slightly early, and melt rates are too high for the model as compared with observations. This can be attributed to the sheltering from wind and insolation experienced by the snow pillow due to trees surrounding the clearing in nature which is not present in the vegetation description for the SNOTEL model pixel. The SNOTEL pixel, specified as a clearing, is treated independently from neighboring pixels, with lateral transfer allowed only for surface water and subsurface soil moisture. The volumes during the validation periods vary from too low to too high. Because the SNOTEL precipitation gage provides the model forcing for the SNOTEL pixel (without adjustment), the total precipitation volume at this location should be represented without spatial interpolation (or extrapolation) error. Discrepancies in snow pack accumulation, therefore, should arise primarily from the rain-snow partitioning of precipitation in the model.

Following calibration, an alternative land cover description, derived from the University of Montana (Redmond, et al., 1996) land cover classification, was tested (Figure 6-3). The intent in using this alternative classification was to maintain consistency with the other catchments. Comparison of the two classifications, however, showed

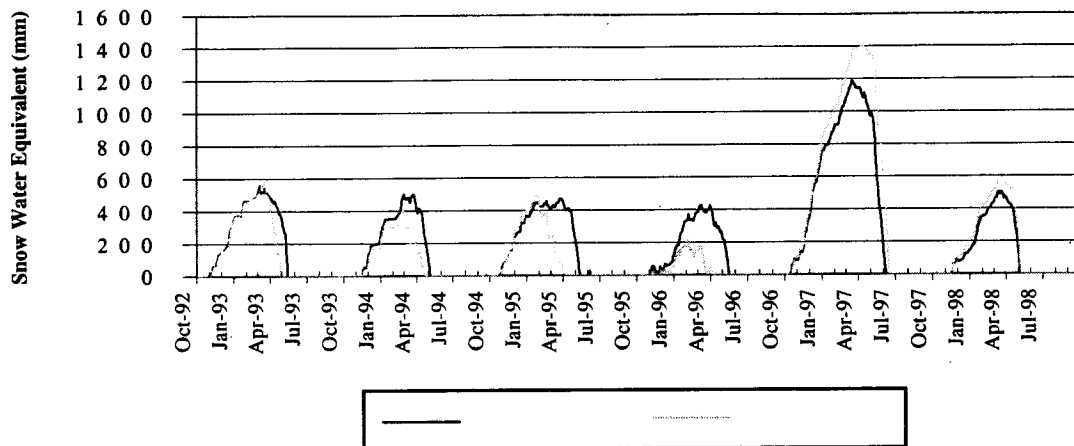


Figure 6-2: Mica SNOTEL Snow Water Equivalent (SWE) calibration / validation

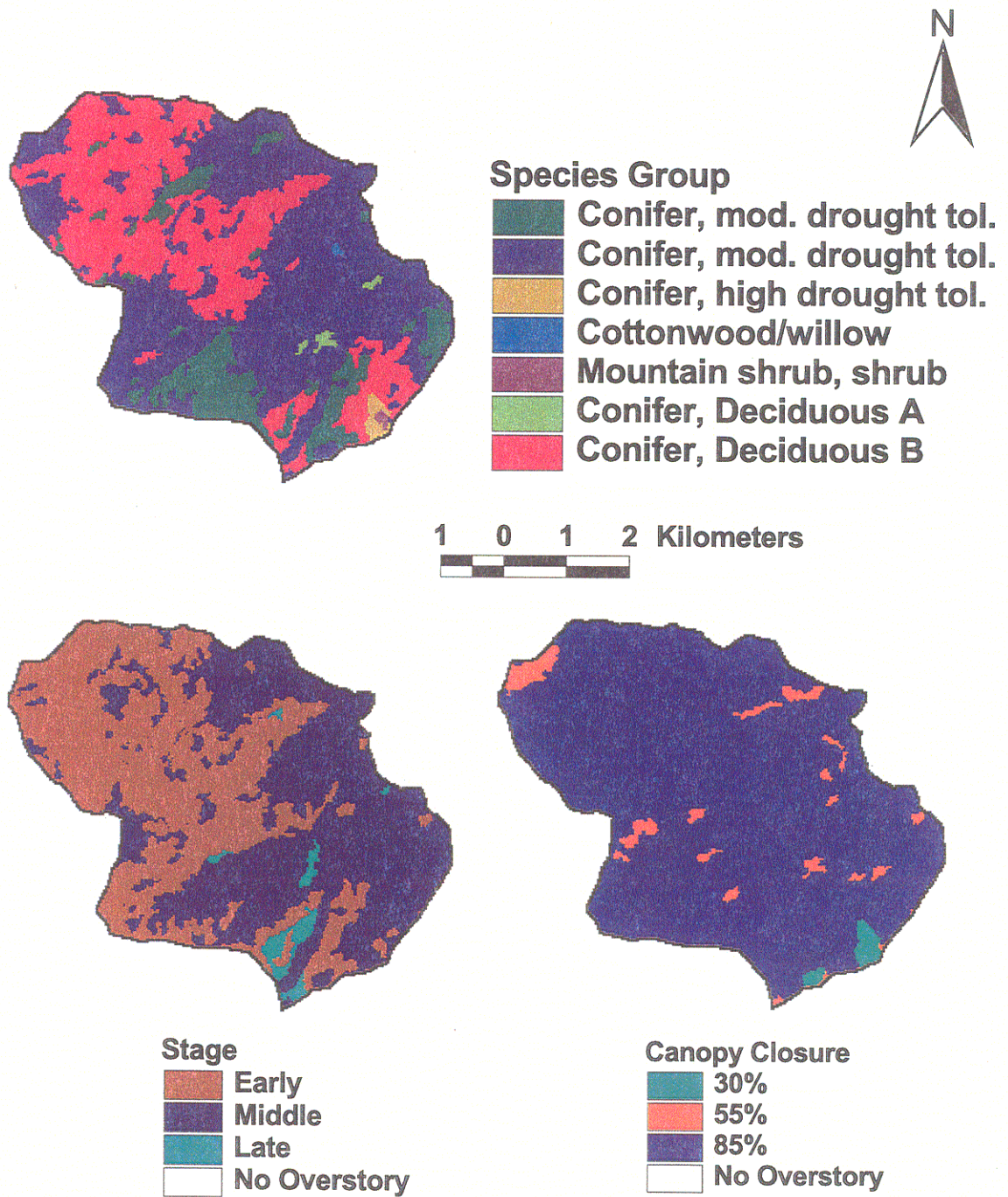


Figure 6-3: Mica Creek vegetation based on the UMT land cover data. Species group (top), stage (middle), canopy closure (bottom) are the characteristics defining each of 108 possible vegetation types.

considerable differences in LAI between the two (Figure 6-4). The LAI difference seen in the figure comes from two sources. First, a large portion of the catchment with middle stage in the Potlatch classification is assigned early in the TM UMT derived classification. Second, and more importantly, the LAI assigned for the Potlatch data are consistently higher than those provided for a given class according to the VIC-style classification used for the TM UMT classification (see Section 5-4). Beyond what is visible in the LAI map (prepared using summer LAI values) is the reduction of LAI in winter associated with Western Larch as classified into the “Conifer, Deciduous A” category.

Simulations were produced for the alternative land cover, results of which are shown in Figure 6-5 for flume 7 for water years 1995 and 1996. Although some portions of the hydrograph are similar, others are quite different. The higher flows in June for the TM UMT vegetation result from deeper snow packs ripening later and melting more rapidly as a consequence of lower LAI values. The Potlatch vegetation description was used for this study for two reasons. First, the model had been calibrated to the Potlatch data prior to developing the TM UMT classification. Second, the data provided by Potlatch as prepared for the paired watershed study is likely more accurate than the classification derived from Thematically Mapped imagery. Nonetheless, some model runs were made and reported (see Chapter 7) using the TM UMT data. The implications of diverging land classifications on calibration and results of a hydrologic model are left for future investigation.

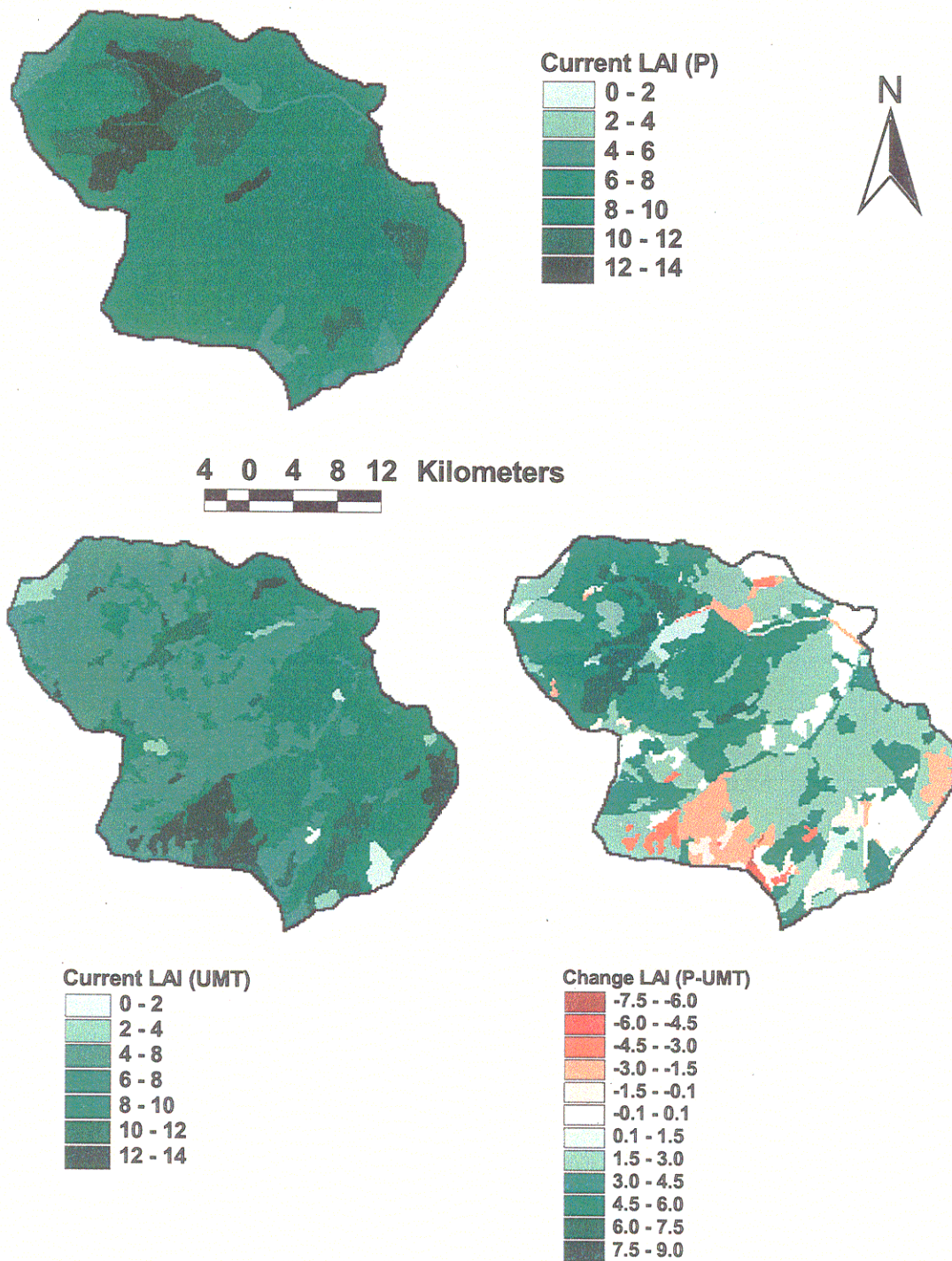


Figure 6-4: Mica Creek LAI. Calculated from current vegetation based Potlatch vegetation data (top), from current UMT vegetation data (bottom-left), and the change (current Potlatch – current UMT) in LAI (bottom-right)

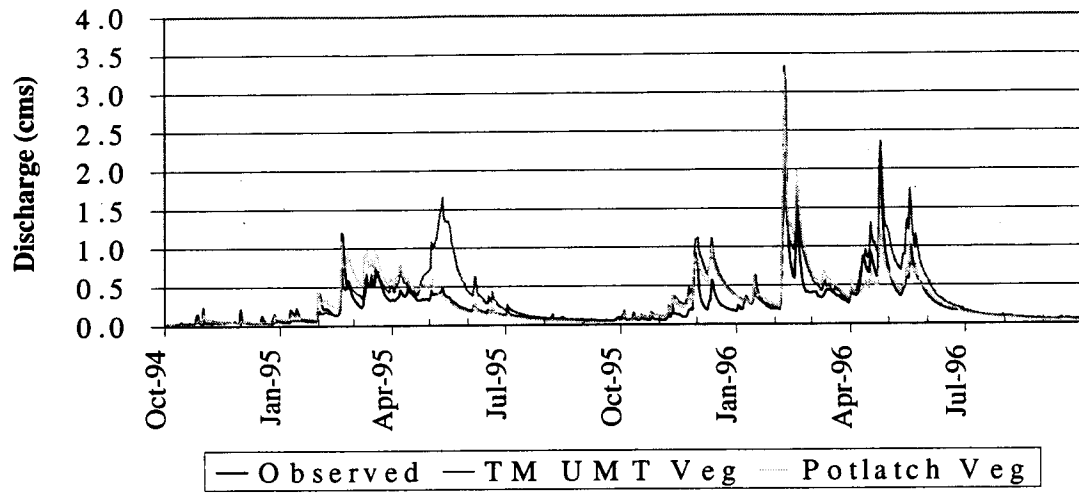


Figure 6-5: Mica Creek: Potlatch, UMT TM classification, and observed discharge hydrographs

6.2 Swan River

Sensitivity analysis prior to calibration showed the Swan River model was most sensitive to soil depth and stream channel depth, especially in the highest portion of the catchment. Lateral conductivity and exponential decay of soil conductivity with depth were also sensitive parameters. Forcing data and lapse rates also had an effect primarily through redistribution of precipitation.

The bulk of the spring runoff in the Swan catchment results from melting of snow at high elevations on the west side of the catchment. The land cover in this region as described by the University of Montana land cover classification ranged from rock, to mixed barren, to snow. This resulted in deep, relatively uniform snow packs that ripened and melted rapidly, generally according to elevation and aspect. Because of the geologic history and lack of extensive soil data in the wilderness area, the soil classification was also uniform with a very shallow estimated soil depth (0.4 and 0.8 m). Therefore, the model generally predicts rapid snowmelt and a quick runoff response to snowmelt—whereas the streamflow observations generally show a somewhat slower response.

To provide sufficient storage for this runoff, the soil depth and channel cut were increased to 1.4 and 1.395 m, respectively. This better represents the fractured rock condition which is not directly represented by DHSVM. Lateral saturated conductivity and exponential decrease with

depth was also adjusted. As shown in Figure 6-6 the runoff peaks still are generally over-simulated.

For the most part, the simulated flows in the calibration years follow the shape of observed hydrographs. There is some discrepancy in base- and early melt flows. The timing errors are, however, substantial. Problems in baseflow and early spring discharge may result from deep aquifer interaction with the glacial lakes, which are not represented in the model. Freezing conditions may also play a role through frozen soils underlying early snow melt—at low elevations (which might cause early peaks), frozen streams and gages—common in this area, and iced-over lakes. None of these processes are explicitly modeled by DHSVM. The calibration process tends to compensate for these mechanisms to some extent as the effects of increased soil depth demonstrate.

Snow accumulation patterns at Skylark Trail SNOTEL (see Figure 3-3) were calibrated by adjusting the rain / snow threshold and snow roughness. Figure 6-7 shows the time series of modeled and observed snow water equivalent. Excellent agreement was obtained for three of four years, while in 1988 the accumulation was underestimated by 25 percent—even though runoff volume was within 3 percent of observed. Unfortunately, this gage was discontinued in early 1990 and never recorded temperature.

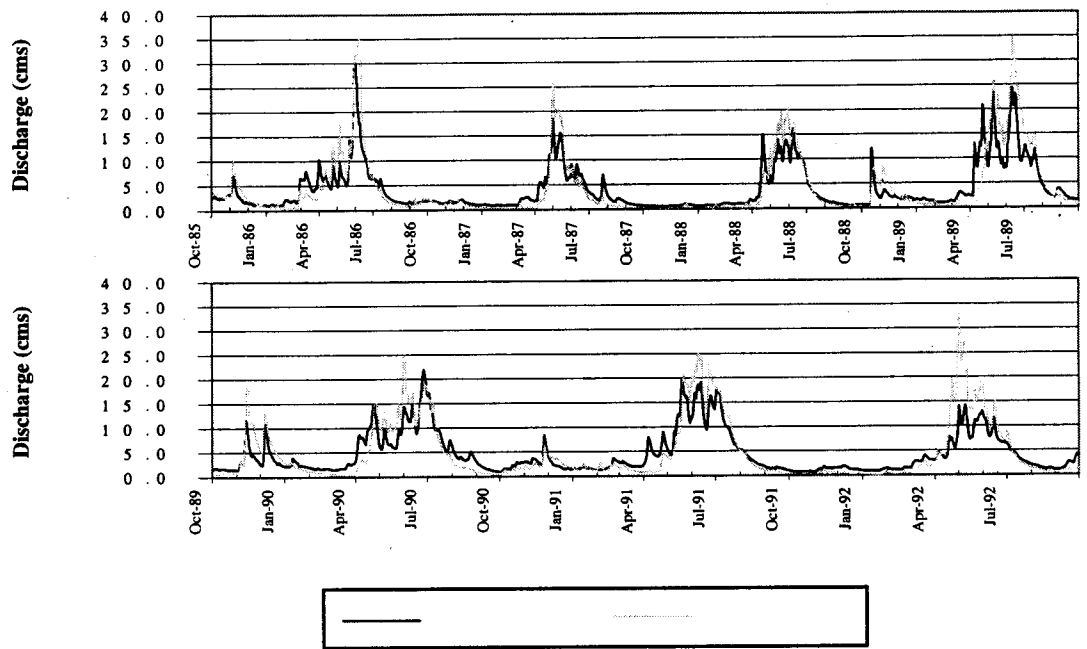


Figure 6-6: Swan River streamflow calibration and validation hydrographs

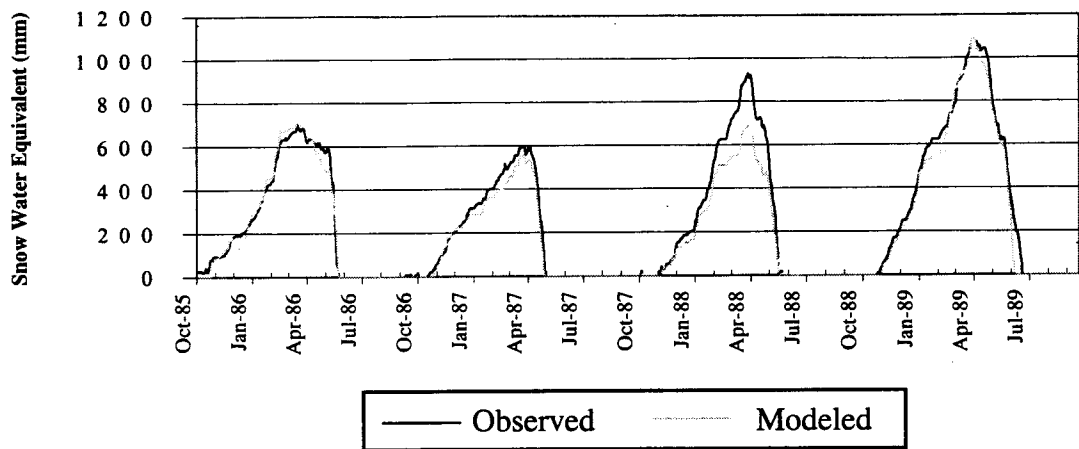


Figure 6-7: Skylark Trail SNOTEL SWE calibration / validation

The meteorological forcing data for the period of investigation of this catchment were available only at the Lindburgh Lake site. It is difficult to determine the extent to which forcing errors lead to difficulties with calibration. There is, however, considerable question as to the spatial distribution of precipitation within the catchment. Initially, PRISM (Daly, et al 1994) precipitation maps were used to distribute the precipitation spatially. Large snow packs high in the basin that melt rapidly late in the season motivated use of a precipitation elevation lapse rate. Monthly values for precipitation and temperature lapses were calculated using nearby gage data in an attempt to better represent precipitation and snow accumulation patterns. These values were adjusted somewhat in the calibration process. Also, monthly precipitation was adjusted upward to compensate for precipitation gage catch deficiencies reported by Legates and DeLiberty (1993). This adjustment generally improved the overall water balance and runoff volumes. Table 6-2 shows annual values of the basic catchment water balance and the agreement of modeled and observed runoff volumes.

6.3 Entiat River

The Entiat River was calibrated to daily observed streamflow hydrographs by varying lateral saturated hydraulic conductivity (K_s), exponential decrease of K_s with depth, snow roughness, soil and stream channel depths, and temperature lapse rates. The initial lapse rates were calculated as monthly means based on daily maximum temperatures at the Entiat Valley Fish Hatchery and Pope Ridge SNOTEL, and at Holden Valley paired with Lyman Lake SNOTEL.

This value was adjusted downward slightly in calibration. A similar lapse rate calculated from the daily minimum temperatures justifies this. Table 6-3 shows calculated lapse rates for

Table 6-2: Swan River: Annual flow volumes

Water Year	Observed Runoff (m)	Modeled Runoff (m)	Prec. (m)	ET (m)
Calibration				
1985	0.668	0.628	1.259	0.478
1986	0.767	0.861	1.470	0.496
1987	0.540	0.478	0.981	0.543
1988	0.527	0.539	1.079	0.413
Totals	2.502	2.507	4.789	1.931
Validation				
1989	0.933	1.078	1.797	0.550
1990	0.894	0.933	1.559	0.522
1991	0.853	0.870	1.490	0.513
1992	0.571	0.710	1.408	0.545
Totals	3.250	3.592	6.254	2.130

maximum and minimum temperatures. It also shows the monthly values used. The temperature lapse affects the freezing, and thus snowfall, elevation. This is most sensitive in the "middle" elevations where a slight shift may cause precipitation to fall as snow or rain, which affects the accumulation of snow.

Soil depths were increased by 25 cm above the STATSGO mean depth to rock, which was the starting point. Soil depths were also increased around high order streams to match their cut depths of 1.9 m, as estimated from field observations. The deep cut ensured drainage of the entire soil column maintaining baseflow. The resulting soil depth ranged from 1.2 m to 1.9 m.

The channel depths were adjusted from initial estimates based on field observation and expected

relative size of the channels. Low order stream depths were increased to intersect the entire soil column of the shallowest soil depth. These adjustments to low order channel depths provided increased soil moisture storage for snow melt.

Table 6-3: Entiat temperature lapses

	Lapse Rates from Maximum Temperatures			Lapse Rates from Minimum Temperatures			Value Used in Model
	Pope vs Hatchery	Lyman vs. Holden V	Average	Pope vs Hatchery	Lyman vs. Holden V	Average	
Jan	-0.0030	0.0000	-0.0015	0.0009	0.0025	0.0017	-0.0010
Feb	-0.0040	0.0002	-0.0019	-0.0011	0.0025	0.0007	-0.0012
Mar	-0.0062	-0.0020	-0.0041	-0.0018	0.0024	0.0003	-0.0026
Apr	-0.0076	-0.0045	-0.0061	-0.0025	-0.0003	-0.0014	-0.0043
May	-0.0068	-0.0064	-0.0066	-0.0017	-0.0006	-0.0011	-0.0046
Jun	-0.0064	-0.0071	-0.0067	-0.0020	-0.0004	-0.0012	-0.0047
Jul	-0.0065	-0.0079	-0.0072	-0.0017	0.0014	-0.0002	-0.0046
Aug	-0.0069	-0.0073	-0.0071	-0.0015	0.0020	0.0003	-0.0045
Sep	-0.0074	-0.0071	-0.0073	-0.0003	0.0044	0.0020	-0.0046
Oct	-0.0080	-0.0058	-0.0069	-0.0015	0.0007	-0.0004	-0.0044
Nov	-0.0057	-0.0027	-0.0042	-0.0019	0.0012	-0.0004	-0.0029
Dec	-0.0038	-0.0002	-0.0020	-0.0019	0.0022	0.0002	-0.0013

The soil conductivity parameters were adjusted uniformly throughout the basin. Attention was given to the peak flows, base flows and snow melt recession in adjusting these parameters. If additional stream gages were available, and / or if time allowed, these values could be adjusted independently based on soil type, which probably would improve the calibration.

Figure 6-8 shows the observed vs. modeled hydrographs for the calibration period—October 1988 through September 1992 and the verification period—October 1992 through September 1996. The figure shows good similarity in the shape of the hydrograph's peaks, recessions, and baseflow between the model predictions and observations. An overestimation of snow melt peaks and overall runoff is consistent throughout the hydrographs. This is likely attributable to error in precipitation volumes. However, the rate of snowmelt for high elevations and the amount of soil moisture storage in the soil column may also have an impact. Table 6-4 shows the annual totals of water balance components.

Table 6-4: Entiat River: Annual flow volumes

Water Year	Observed Runoff (m)	Runoff (m)	Modeled Prec. (m)	ET (m)
Calibration				
1989	0.067	0.091	1.122	0.367
1990	0.068	0.089	1.183	0.404
1991	0.102	0.140	1.616	0.413
1992	0.056	0.067	1.001	0.405
Totals	0.293	0.387	4.921	1.589
Validation				
1993	0.044	0.054	0.868	0.392
1994	0.046	0.054	0.786	0.327
1995	0.092	0.140	1.620	0.385
1996	0.117	0.163	1.829	0.420
Totals	0.299	0.410	5.103	1.523

The rain on snow (ROS) event in November of 1990 is greatly over-predicted both in terms of peak and volume discharge. Review of the meteorological records for the three stations forcing the model are in approximate agreement on the precipitation volumes. Review of the basin

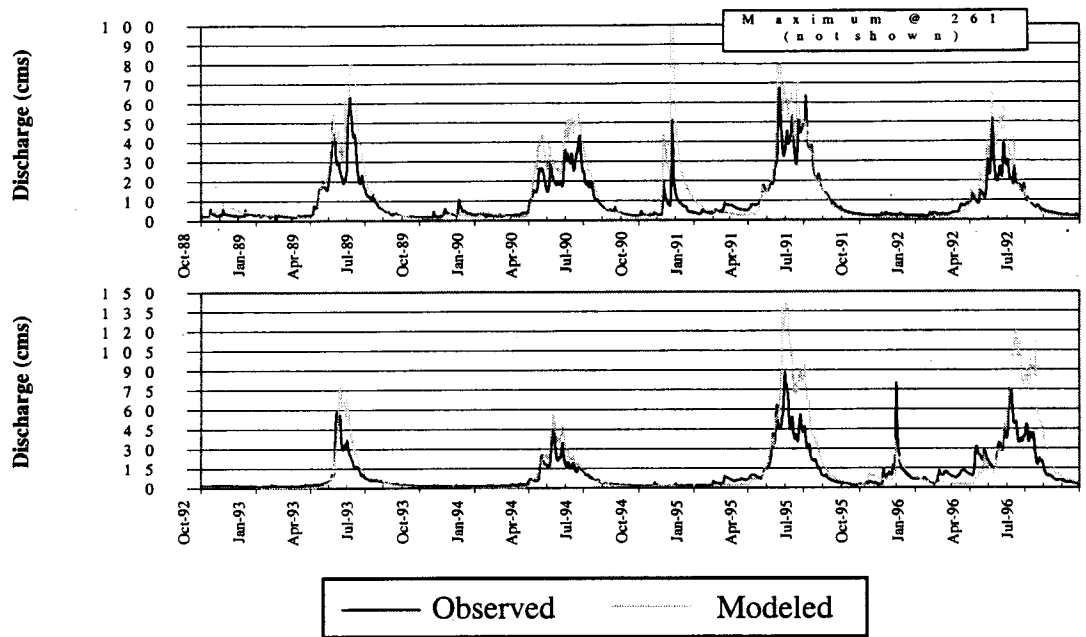


Figure 6-8: Entiat River streamflow calibration and validation hydrographs

average snow water equivalent during this period suggests that part of the basin was accumulating snow while other parts experienced snowmelt. Again, the monthly average temperature lapse rate may have partitioned snow and rain incorrectly. Pre-existent snow packs may also be over estimated, releasing too much water during the ROS event.

Although not used in calibration, Pope Ridge SNOTEL provides a time series of snow water equivalent. Figure 6-9 shows the modeled and the observed snow water storage at the SNOTEL site. Some of the discrepancy between the observations and model predictions are no doubt due to the physical conditions at the site as represented by the model. The snow pillow at Pope Ridge is in a small clearing, surrounded by trees. The model represents the entire pixel as a clearing and does not consider the aerodynamic or radiation shading effects of neighboring, forested pixels. Thus, the modeled wind and radiation may be somewhat misrepresented. Rain / snow partitioning errors associated with daily distribution of precipitation and diurnal temperature variation are also evidenced in the discrepancies. Nevertheless, no large bias develops.

6.4 Mores Creek

Mores Creek, the largest catchment modeled, provided unique challenges in the calibration phase. Lateral saturated hydraulic conductivity (K_s), exponential decrease of K_s with depth, soil and stream channel depths, wind speeds, snow roughness and temperature lapse rate were varied during the calibration period. During the process of calibration, stream density was increased

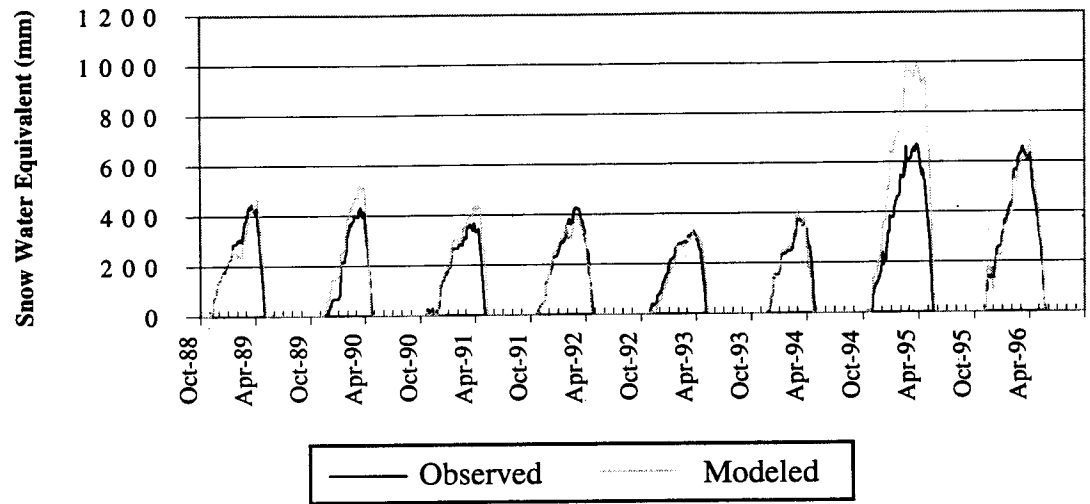


Figure 6-9: Pope Ridge SNOTEL SWE calibration / validation

significantly. The initial support area of 14.4 ha was changed to 4.3 ha (3 pixels) to reduce the extent of saturation and to mirror the small gully-like structures visible in the field. The temperature lapse rates, initially based on monthly average values calculated using the gages against Mores Summit SNOTEL, were replaced by lapse rates derived from soundings at Boise International Airport, when available.

Early calibration runs were plagued with large runoff volumes occurring days to weeks later than in the observations. This was caused by an excess of snow melting too rapidly too late in the season. This bias is related primarily to the quantity of snow accumulated in the model. The snow storage obviously affects how much water is available to affect the discharge volumes, but it also represents how much heat must be absorbed before the pack ripens and begins to produce melt water. Due to the spatial distribution of precipitation as inferred from PRISM maps (Daly, et al 1994) and the least-distance squared interpolation method used, the location of the apparently excessive snow packs (high in elevation) weren't readily susceptible to reduction. Because of the size of the catchment and the number of gages, conversion to a precipitation lapse as in Swan River seemed counterproductive. In general, the high elevation snowpack was relatively insensitive to the temperature lapse rate and rain / snow threshold adjustments.

Attention, therefore, was shifted from the accumulated spring snow pack volumes to snow ripening processes and adjustment of those parameters that affect the amount of heat available and absorbed by the pack. Snow albedo, which affects the absorption of radiation, is handled

internally by the model—using a decay function based on time since last snowfall—and therefore cannot readily be adjusted. Canopy radiation and wind attenuation factors were found to have relatively little influence on the high elevation snow pack predictions. These parameters were, therefore, not adjusted. Snow roughness also had a relatively modest effect. Due to the catchment's large extent, it was determined that wind speeds, modeled as daily averages over the basin, were likely the source of part of the problem. Convective snowpack heat exchange is influenced more by gusts of wind than longer-term average wind (Storck, personal communication). The spatial distribution and the diurnal temporal variability of wind was not available in the current wind time series. For this reason, the wind speed was scaled by 1.5, which resulted in a significant temporal shift of snowmelt.

In addition to scaling the wind, the snow roughness was also adjusted. The model is most sensitive to snow roughness in areas without canopy coverage. The resultant value, although seemingly high, is arguably appropriate to the sub-grid variability of terrain at high elevations.

With the time shift correction, attention was returned to the soil parameters. The Mores Creek model was sensitive to lateral conductivity, soil depth and channel cut. The limited number of soil units (3) limited how well the variety of conditions as seen in the field could be duplicated in the model. Soil and channel cut depths were therefore adjusted to provide sufficient soil storage to allow infiltration of snow melt. The cuts in higher order channels also penetrated the entire soil column which helped in replication of baseflow. The resulting calibration / validation

hydrographs (Figure 6-10) show good agreement of baseflow and recession, but over-simulation of peak flows for all but the driest year, with significant over simulation of late snow melt season flows. These late volumes dominate the annual runoff volumes shown in Table 6-5. The only nearby SNOTEL site (Mores Creek Summit) is outside the catchment, so snow accumulation/ablation comparisons were not possible.

Table 6-5: Mores Creek: Annual flow volumes

Water Year	Observed Runoff (m)	Modeled Runoff (m)	Modeled Prec. (m)	ET (m)
Calibration				
1985	0.359	0.448	1.045	0.464
1986	0.101	0.106	0.471	0.440
1987	0.100	0.130	0.570	0.354
1988	0.230	0.379	0.839	0.367
Totals	0.791	1.063	2.926	1.625
Validation				
1989	0.126	0.208	0.745	0.495
1990	0.090	0.138	0.668	0.469
1991	0.075	0.129	0.563	0.399
1992	0.273	0.476	0.980	0.431
Totals	0.564	0.951	2.957	1.795

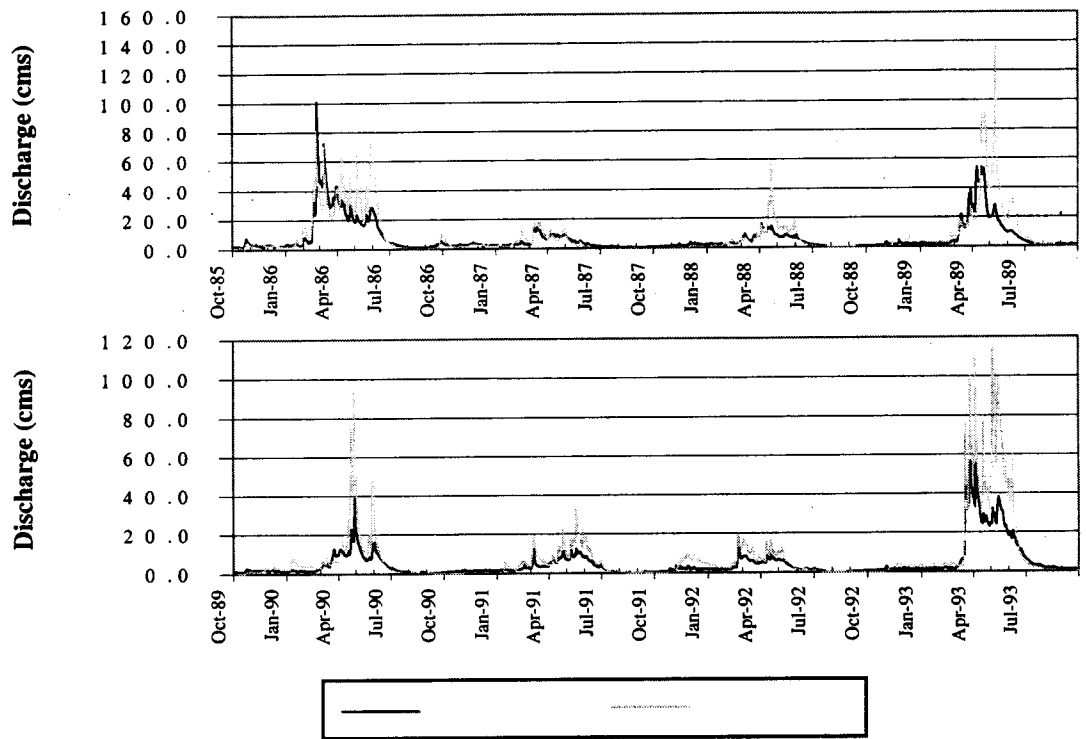


Figure 6-10: Mores Creek streamflow calibration and validation

Chapter 7: Results

The calibrated model for each catchment as described in Chapter 6 was used as the basis for an investigation of the hydrologic sensitivities of each of the catchments to vegetation change over the last century. The calibrated models simulated the periods shown in Table 7-1. For each catchment, the simulation period included one or more years of warm-up to eliminate errors associated with initial conditions. Model output variables archived included time-series of basin-averaged evapotranspiration and snow water equivalent, runoff hydrographs, and selected spatial images of hydrologic characteristics at pre-specified times. Following the initial runs with current vegetation, the simulations were repeated using the same initial condition but with alternative specifications of vegetation scenarios including the estimated 1900 condition. This chapter presents the findings of these simulations.

Table 7-1: Meteorological Data Time Periods

	Mores	Entiat	Swan	Mica
Warm-up Begin	10/01/84	10/01/86	10/01/84	10/01/90
Warm-up End	09/30/85	09/30/87	09/30/85	09/30/92
Investigation Period Begin	10/01/85	10/01/87	10/01/85	10/01/92
Investigation Period End	09/30/94	09/30/97	09/30/95	09/30/99
Number of Years Investig'd	9	10	10	7
ET Map Begin	06/11/87	07/01/96	07/21/86	07/01/96
ET Map End	06/17/87	07/07/96	07/27/86	07/07/96
SWE Map Date	03/01/86	03/01/88	03/01/86	03/01/91
	Winter	Spring	Summer	Fall
Soil Water Table Depth Dates	Jan-15	Apr-15	Jul-15	Oct-15

7.1 Annual Water Balance

The mean annual water balance was calculated for each model run scenario. For all runs, the meteorological forcings were the same. The mean annual runoff changes, expressed as depths over the catchments, are shown in Figure 7-1. Figure 7-2 shows the mean annual evapotranspiration (ET) depths. Table 7-2 provides more details of the current values and the residual series of current minus historical mean annual depths.

Table 7-2: Current minus Historic Residual Values

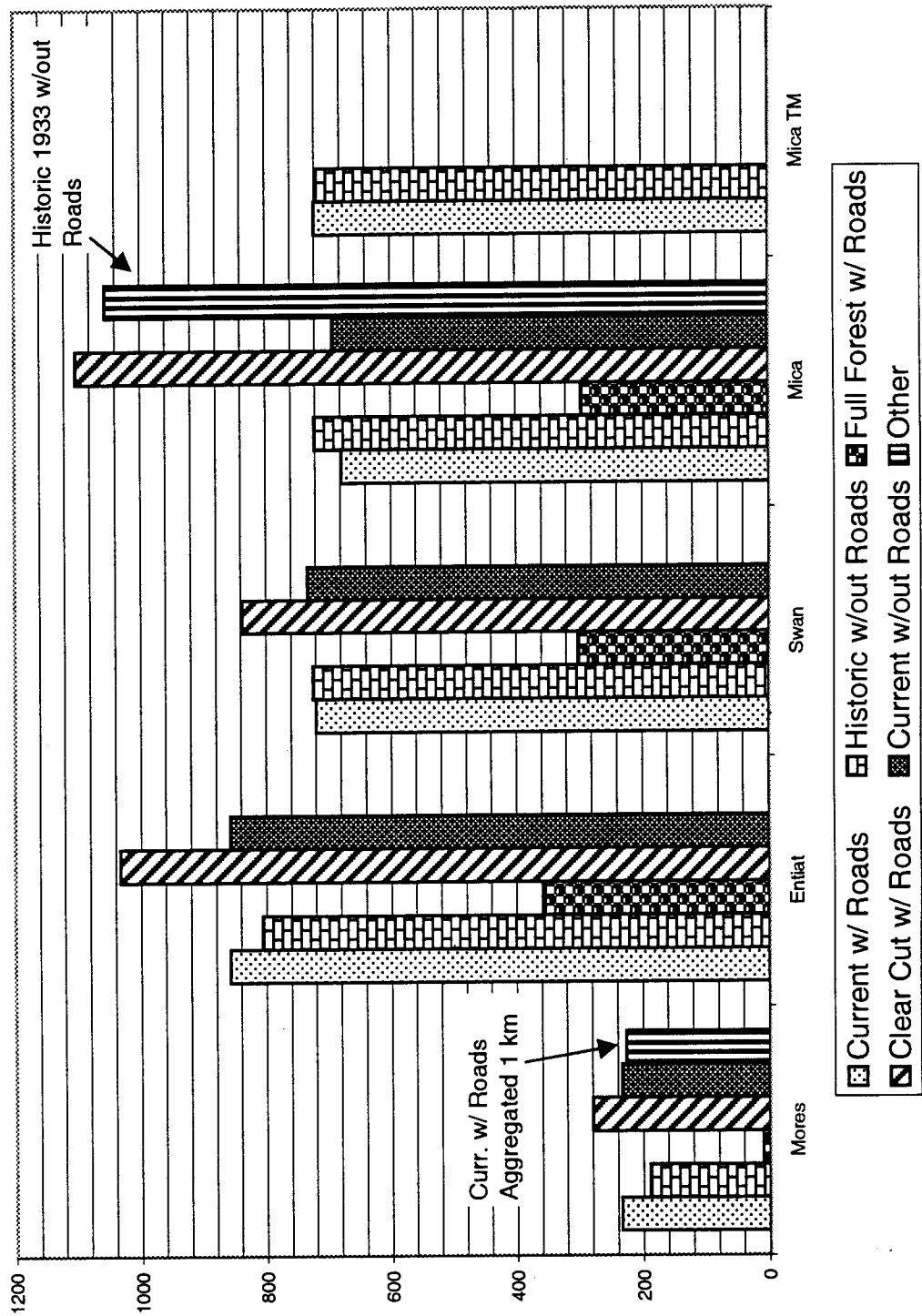
	Mores	Entiat	Swan	Mica	Mica Tmveg
Area (km ²)	1028	527	180	27	27
Avg Etot Current (mm)	419.5	386.9	505.2	683.4	683.8
Avg Runoff Current (mm)	233.8	858.2	720.1	679.4	721.6
Avg LAI change	-0.70	-0.60	0.32	2.71	0.76
Avg Etot Change (mm)	-41.98	-45.47	-5.62	4.13	-12.17
Avg Etot Change (%ofCurr)	-10.01	-11.75	-1.11	0.60	-1.78
Avg Runoff Change (mm)	45.02	51.99	-4.65	-43.26	3.34
Avg Runoff Change (%ofCurr)	19.25	6.06	-0.65	-6.37	0.46
Max Etot Change (mm)	-61.50	-62.30	-9.37	30.99	6.52
Max Etot Change (%ofCurr)	-14.66	-16.10	-1.86	4.54	0.95
Max Runoff Change (mm)	70.45	70.28	-21.93	-85.97	-4.76
Max Runoff Change (%ofCurr)	30.13	8.19	-3.05	-12.65	-0.66

7.1.1 Current vs. Historic Vegetation

For the Mores and Entiat catchments, long-term deforestation is reflected in the catchment-wide average LAIs (Table 7-2). The reduced LAIs are reflected in reductions in ET and increases in

streamflow. The difference in the runoff changes (Figure 7-1) for the Mores and Entiat catchments are a reflection of the non-linear

Figure 7-1: Mean annual runoff depths (mm) for all investigation runs



influence of aridity. Runoff in the Entiat catchment is almost four times larger than in Mores Creek. In semi-arid catchments like Mores Creek, runoff is more sensitive to changes in surface conditions and meteorological forcings than in more humid catchments, like Entiat River.

For Swan River, the overall vegetation change over the last century has been a slight afforestation (Table 7-2). Nonetheless, both runoff *and* ET drop (Figures 7-1 and 7-2). These changes are small relative to the precipitation. The LAI change for Swan River is small compared to the LAI changes for other catchments. Furthermore, some of these small changes may result from the interaction of roads with vegetation change. Although the changes are small, the water balance clearly cannot be maintained if both runoff and evapotranspiration increase, so there must have been some long-term change (increase) in subsurface storage over the simulation period.

For Mica Creek, the inferred changes likewise reflect a long-term inequilibrium in the water balance: runoff decreases much more than ET increases (Table 7-2). This inequality is greatly reduced, however, when the change in snow vapor flux is considered. Mica Creek experiences a large change in vapor flux (25.4 mm) which acts in the water balance in the same direction as ET. This is likely the result of high LAI vegetation unique to the Potlatch vegetation characteristics. In the other catchments the change in snow vapor flux is much closer to zero.

The information shown for the University of Montana TM vegetation classification for Mica Creek (see Section 6-1) is provided primarily for comparison with the classification derived from

Potlatch Corporation data. The results show a situation contrary to general expectation, where an increase in LAI resulted in a decrease in ET and a small increase in runoff (Table 7-2).

Nevertheless, most of the average change occurs during the wettest and second wettest year, and may have been related to particular interactions between the initial conditions and the meteorological patterns in those years. The small change in runoff (~3.3 mm) and the virtually uncalibrated condition does not merit extensive examination.

7.1.2 Extremes, Special Cases, and Roads

For most of the catchments, the response of both the current and historical conditions are more similar to the barren response than the fully forested (Figures 7-1 and 7-2). Mica Creek is the exception; the current and historical responses are nearly midway between the barren and fully forested responses. This can be easily understood by returning to Figures 5-2, 5-6, 5-8, and 5-10, which show large barren or shrub-covering areas over part of each of the catchments except Mica Creek. Considerable areas of forested low-canopy-closure exist and more drought resistant conifers (than used in the "Full Forest" condition) exist as well. The clear-cut condition water balance change should be analogous to that inferred from paired catchment experiments for mature and clear-cut conditions (Hibbert, 1967; Bosch and Hewlett, 1982; Sahin and Hall, 1995; Stednick, 1995).

For Mores Creek, the simulation (Figure 7-1) showed that clear cutting would result in an increased water yield of 45.8 mm (19.6 percent). For Entiat River, whose yield is dominated by

high elevation areas with little or no forest in the current condition, the change is much smaller—only 13.6 mm (1.59 percent). The Swan River increase of 118 mm (16.4 percent) is surprisingly high, compared to the Entiat River increase given that both have similar high elevation precipitation and vegetation conditions. For Mica Creek, the increase is quite large—423 mm (62.3 percent)—which reflects the current predominance of mature or nearly mature vegetation throughout the catchment. Re-examining the change in snow vapor flux for the clear-cut investigation shows an even greater imbalance of snow vapor change in Mica Creek (70.0 mm). There is also a noticeable imbalance in snow vapor flux in Mores Creek (10.0 mm), although again these changes are in the direction of the change in ET.

The sensitivity of simulated annual runoff to the scale of the vegetation data is small, as shown by comparison of Mores Creek current and the “Other” (120 m aggregation to 1 km resolution) condition (Figure 7-1). The change in runoff is a reduction of 7.3 mm (3.1 percent) for the aggregated (1 km) vs. 120 m resolution. This suggests that the fraction of coverage of a given vegetation type is more important than its spatial distribution, at least within some unknown range of proximity.

The reconstruction of Mica Creek post-harvest (1933) conditions, representing clear-cut of more than 80 percent of the catchment, resulted in slightly less runoff (Figure 7-1) than the hypothetical clear-cut condition (47 mm). In the historical context (i.e., in progression from 1900 vegetation), the 1930’s harvest increased runoff by 333 mm (46.1 percent) relative to the

simulated “natural” historical condition. Regrowth to a currently harvestable condition subsequently reduced the yield 377 mm or 44 mm lower than the historical condition. A small portion (13 mm) of this reduction could be the result of roads, as the 1933 simulation was run for a no-roads condition.

Although the question of how much effect forest roads have on peak flows has attracted considerable attention, comparison of the current with roads simulations with the current with no roads simulations for the catchments shows that roads have little effect on the change in average annual water balance (Figures 7-1 and 7-2). For Mores Creek and the Entiat River, less than one-half of a percent change in runoff was accounted for by roads. For Mica Creek and Swan River, the changes were likewise small—approximately 13 mm, or less than 2 percent. In both cases runoff for the roaded condition was higher than for no roads. This effect, in part, explains the counterintuitive changes in Swan River current with roads vs. historical without roads simulations. The effects of roads on annual maximum flows is addressed in Section 7-2.

7.1.3 Spatial patterns of ET

In addition to the effects of vegetation change on runoff, which represents the integrated effect of water balance changes over a catchment, effects on the spatial component of ET were investigated. For this investigation, maps were created showing the total ET throughout the catchment for one week of the simulation period. The residual ET values (current with roads – historic without roads) are shown in Figure 7-3. Mores Creek shows spatial correspondence with

the patterns of changed LAI (Figure 5-9). In the mountainous region to the north and east a small change in LAI (shown in light green in Figure 5-9) produces significant ET changes. These changes produce hill-slope scale patterns of increasing and decreasing ET as shown in dark greens and oranges. Comparison of ET from current 120 m and 1 km vegetation parameterizations shows that the effect of degraded spatial resolution is also greatest in these mountainous regions.

The Mica Creek ET maps (Figure 7-3) appear to follow the change in LAI (Figure 5-6) reasonably, with some interesting spatial variations related to topography. In fact, many of the prominent patterns are the reverse of what might be expected—higher LAI historically resulting in more ET historically. The large pink area in the central portion of the catchment (representing more ET in the current simulation) actually had substantially higher LAI in the historical condition. This reversal from expectation (although not an improbable outcome) apparently results from soil moisture limitation associated with the high extraction rates early in the season for the historical (high) LAI. This pattern repeats itself in part of the northwest portion of the catchment, where most of the light green area (historically more ET) has higher LAI currently. Review of the ET time series supports this; the period used to develop the maps is located on the

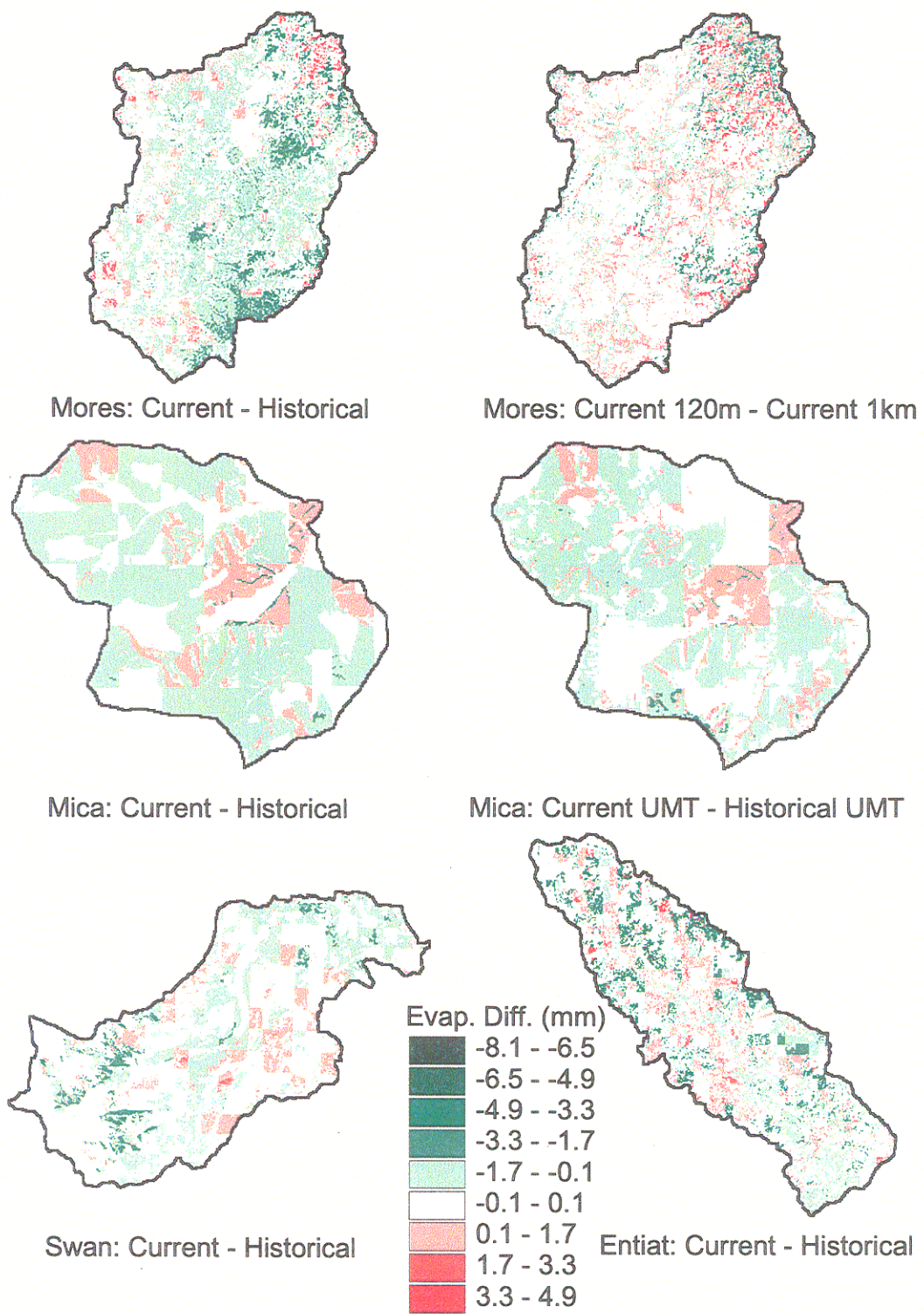


Figure 7-3: Catchment maps of residual ET

falling limb of the annual ET time series. While this result is unexpected, it is not improbable on an annual basis.

The effects of topography on ET are apparent in Mica Creek as shown in Figure 7-3. Downslope redistribution of soil moisture focuses the effects of vegetation change on the hillslope to the valley bottoms. This can be seen as the dark green lines (areas where considerably more ET occurred historically) in the central portion of the catchment. The same effects, but with more ET currently than historically, can be seen in some of the linear pink areas.

For both the Swan and Entiat catchments, ET spatial distribution (Figure 7-3) is closely related to the LAI change (see Figures 5-7 and 5-8) over most of the catchment. The lower, flatter, northeast region of Swan, however, shows a slight decrease in current ET (light green) with a moderate to considerable increase in current LAI. This irregularity is due to the historical change in overstory. In the 1900 vegetation maps, these regions have no overstory. The inverse relationship shown in the Swan ET maps suggests that if the water is available to the shallower root systems of understory vegetation, greater ET can occur.

7.2 Annual Peaks

The peak streamflows were extracted from each model run for each year of simulation. Figures 7-4, 7-5, 7-6, and 7-7 show these peaks along a time-series of water years, and against the peak flow rate for the current (baseline) condition. The Entiat River plots (Figure 7-5) confirm some

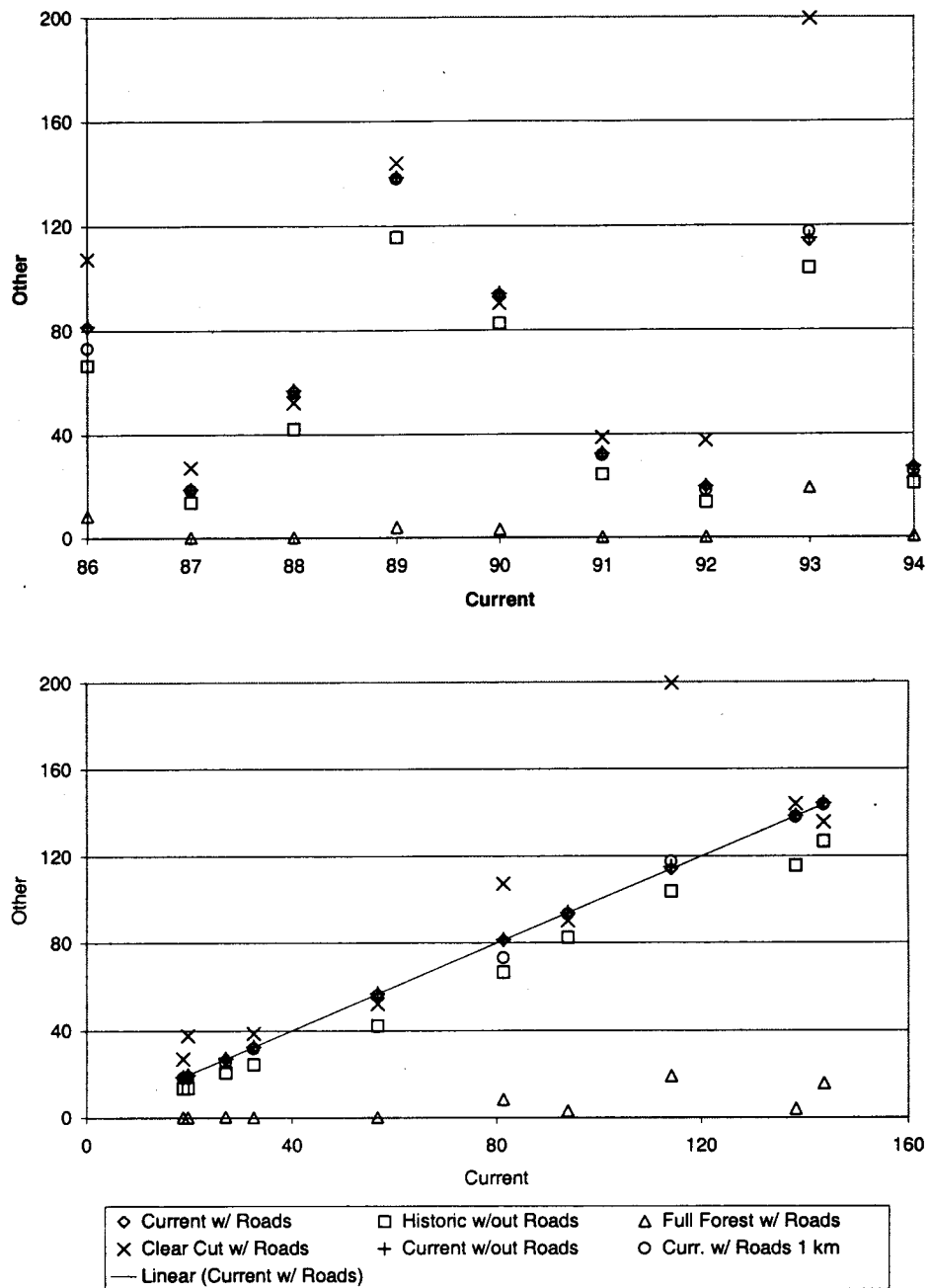


Figure 7-4: Annual peak flows: Mores Creek.

Top: Annual peak flows (cms) for each run, by year. Bottom: Current w/ roads (baseline condition) is displayed on the x-axis and comparable (by year) values for each of the other investigation runs are on the y-axis (cms). The one-to-one line is shown.

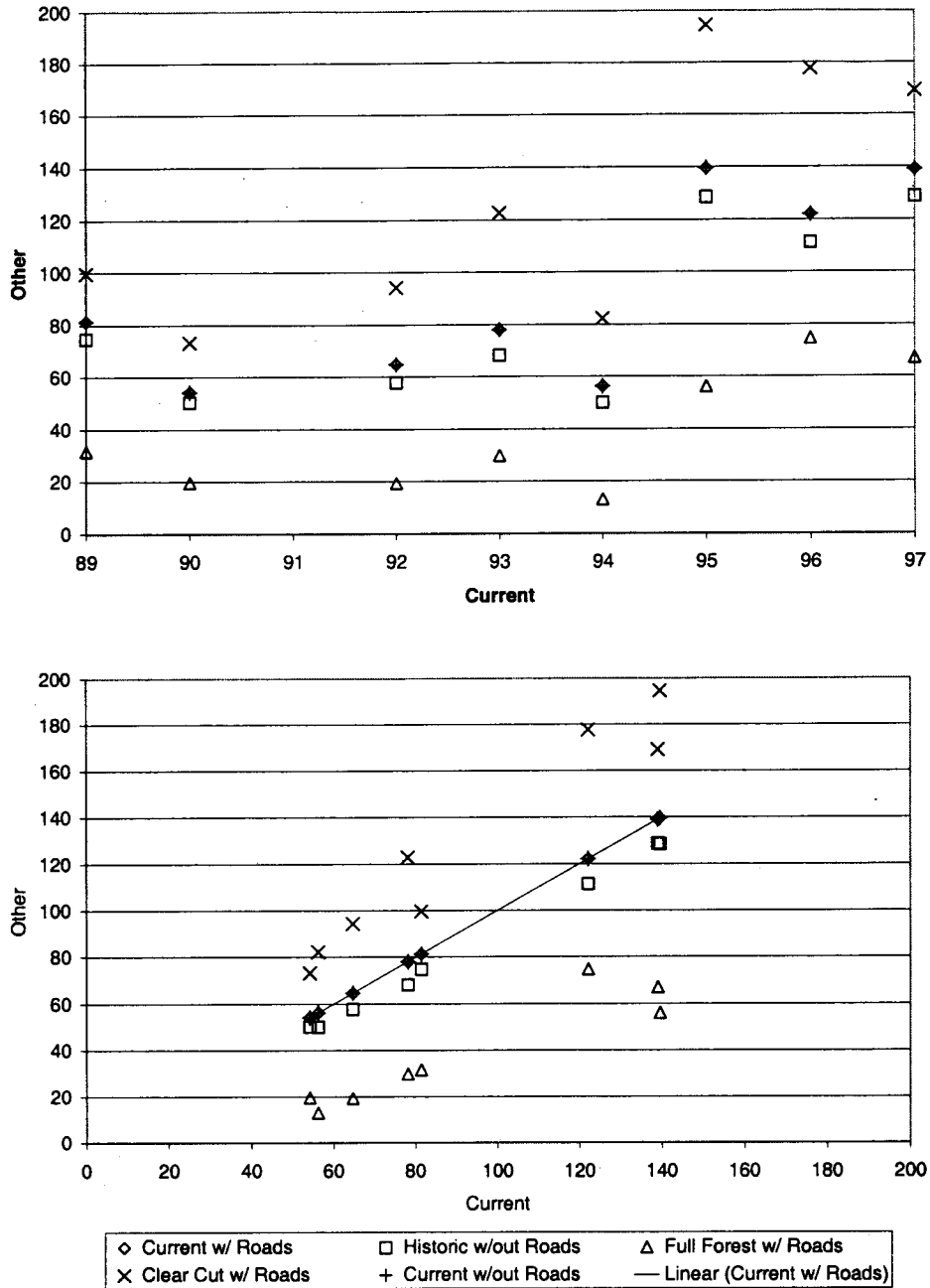


Figure 7-5: Annual peak flows: Entiat River.

Top: Annual peak flows (cms) for each run, by year. Bottom: Current w/ roads (baseline condition) is displayed on the x-axis and comparable (by year) values for each of the other investigation runs are on the y-axis (cms). The one-to-one line is shown.

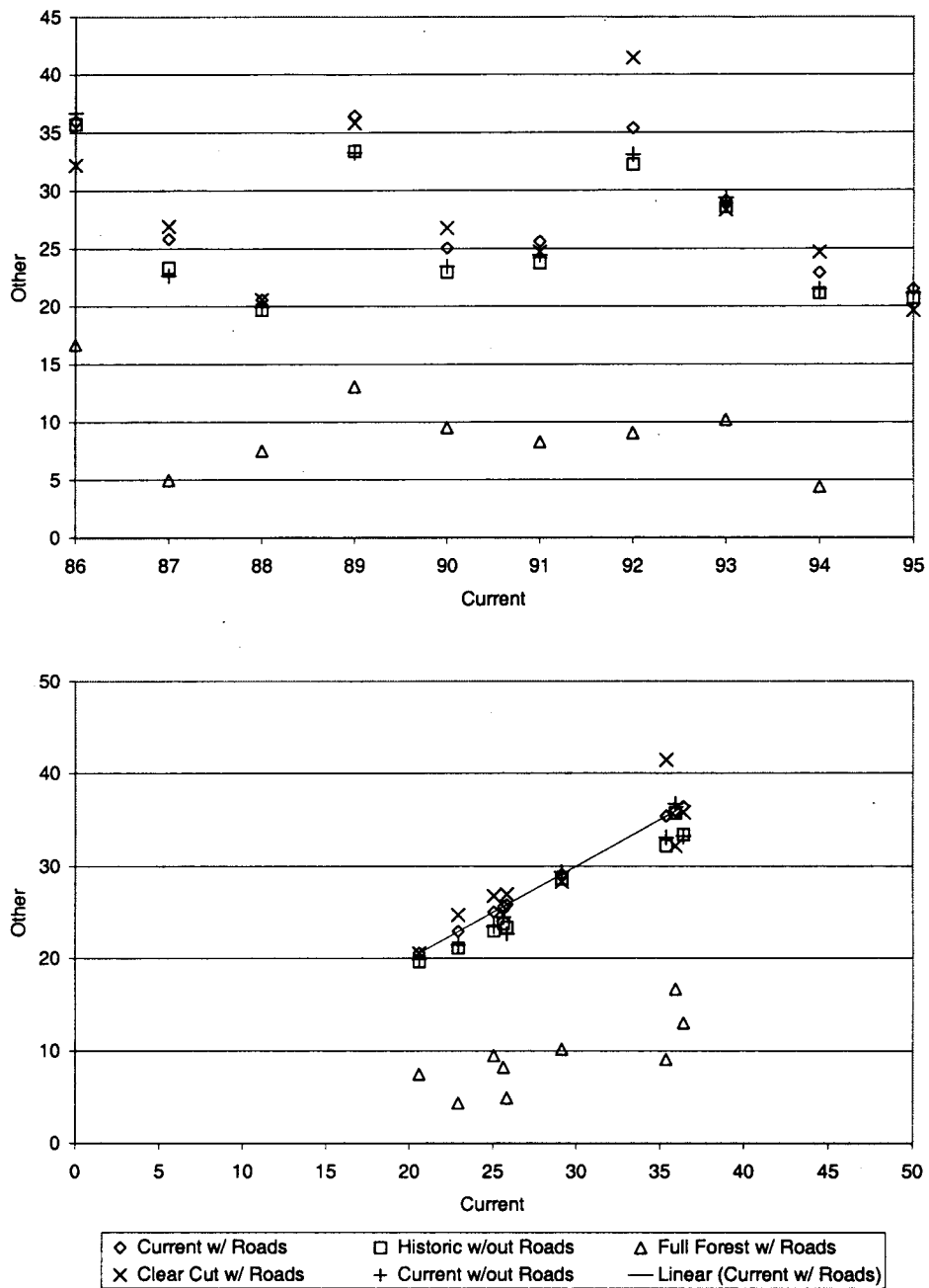
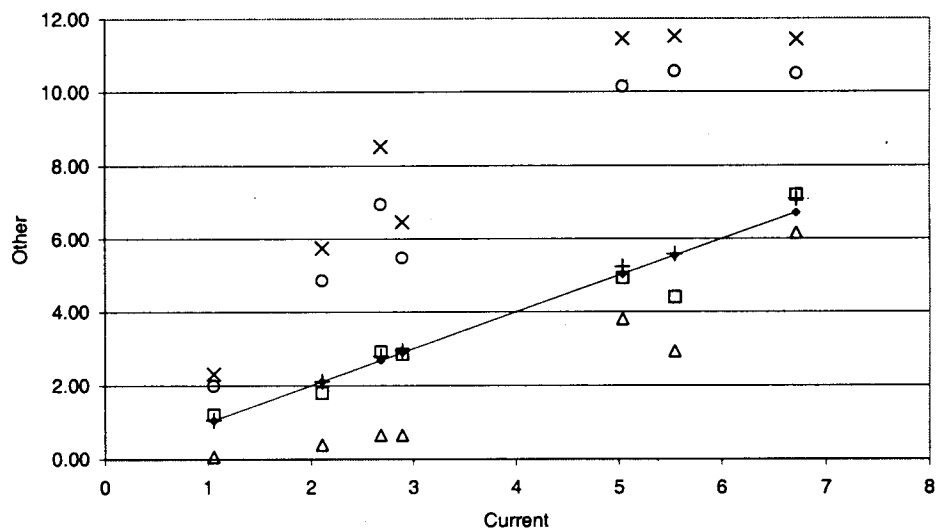
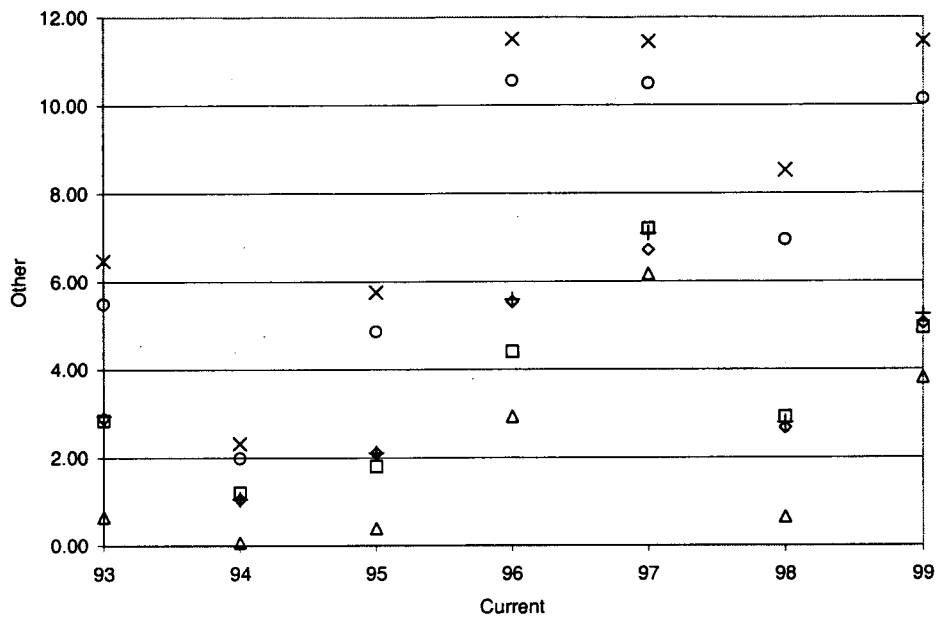


Figure 7-6: Annual peak flows: Swan River.

Top: Annual peak flows (cms) for each run, by year. Bottom: Current w/ roads (baseline condition) is displayed on the x-axis and comparable (by year) values for each of the other investigation runs are on the y-axis (cms). The one-to-one line is shown.



• Current w/ Roads □ Historic w/out Roads △ Full Forest w/ Roads
 × Clear Cut w/ Roads + Current w/out Roads ○ Historic 1933 w/out Roads
 — Linear (Current w/ Roads)

Figure 7-7: Annual peak flows: Mica Creek.

Top: Annual peak flows (cms) for each run, by year. Bottom: Current w/ roads (baseline condition) is displayed on the x-axis and comparable (by year) values for each of the other investigation runs are on the y-axis (cms). The one-to-one line is shown.

of the classic expectations. The barren condition streamflows were consistently highest. A more highly vegetated historical condition consistently produced flows lower than the current condition. The simulated flows for a fully mature, high water-demanding vegetation condition were lowest. In these simulations, however, roads had little influence on the annual peak flow. This is probably due to the location of roads (low elevations) with respect to the portion of the catchment contributing the largest amount of flow during the annual peak flows (high elevations). Reviewing the results with the work done by La Marche and Lettenmaier (in press) shows a considerable difference in road density: Entiat River catchment has less than 0.9 km/km^2 while the Deschutes River catchment has about 6 km/km^2 .

Alternatively, the plots for the other catchments demonstrate the cumulative effects of a catchment on timing of flows, snow ablation, and related processes by scrambling the points in somewhat less predictable ways. Positioning of the points relative to the one-to-one line are mixed in Swan River (Figure 7-6) for current with roads and clear-cut conditions, although historical without roads conditions are consistently at or below the line. Mica Creek (Figure 7-7) flows are relatively consistent with roads being at or above the one-to-one line, while the relationship of the historical flows fluctuates in both time and magnitude. The Mores Creek (Figure 7-4) historical condition consistently plotted below the one-to-one line. The aggregated vegetation case lay close to or slightly below the one-to-one line. Like Entiat River, Mores Creek showed only modest differences for the current vegetation condition with and without

roads. The effects of roads on intra-annual peaks are present, although the scope of this investigation prevents further examination of this issue.

Figure 7-8 shows the maximum flood during the period of investigation for each vegetation condition and the percent change in flood discharge relative to the current maximum flood. Note that the maximum floods reported here did not necessarily occur in the same year. The range and mean of percent changes from current conditions in the maximum flood can be seen in Figure 7-9.

7.3 Storage: Snow and Soil Moisture

In considering the effects of vegetation change on snow storage within the catchments, trends are not easily recognizable. Both catchment-average time series of snow water equivalent (SWE) and snapshot spatial plots were archived. Figure 7-10 shows the annual maximum SWE for the various sensitivity runs relative to the current (baseline) condition. In practically all cases, the direction of change is consistent from year to year, but the direction of change is not necessarily consistent from catchment to catchment. For instance, the current with roads vs. clear-cut with roads change for Mica and Entiat are above the one-to-one line while Swan and Mores are below the one-to-one line. While the direction of shift for individual pixels may be predicted, averaging over the basin and selecting a single moment in time may synchronize (as in Mica and Entiat) or de-synchronize (as in Swan and Mores) the total maximum SWE storage.

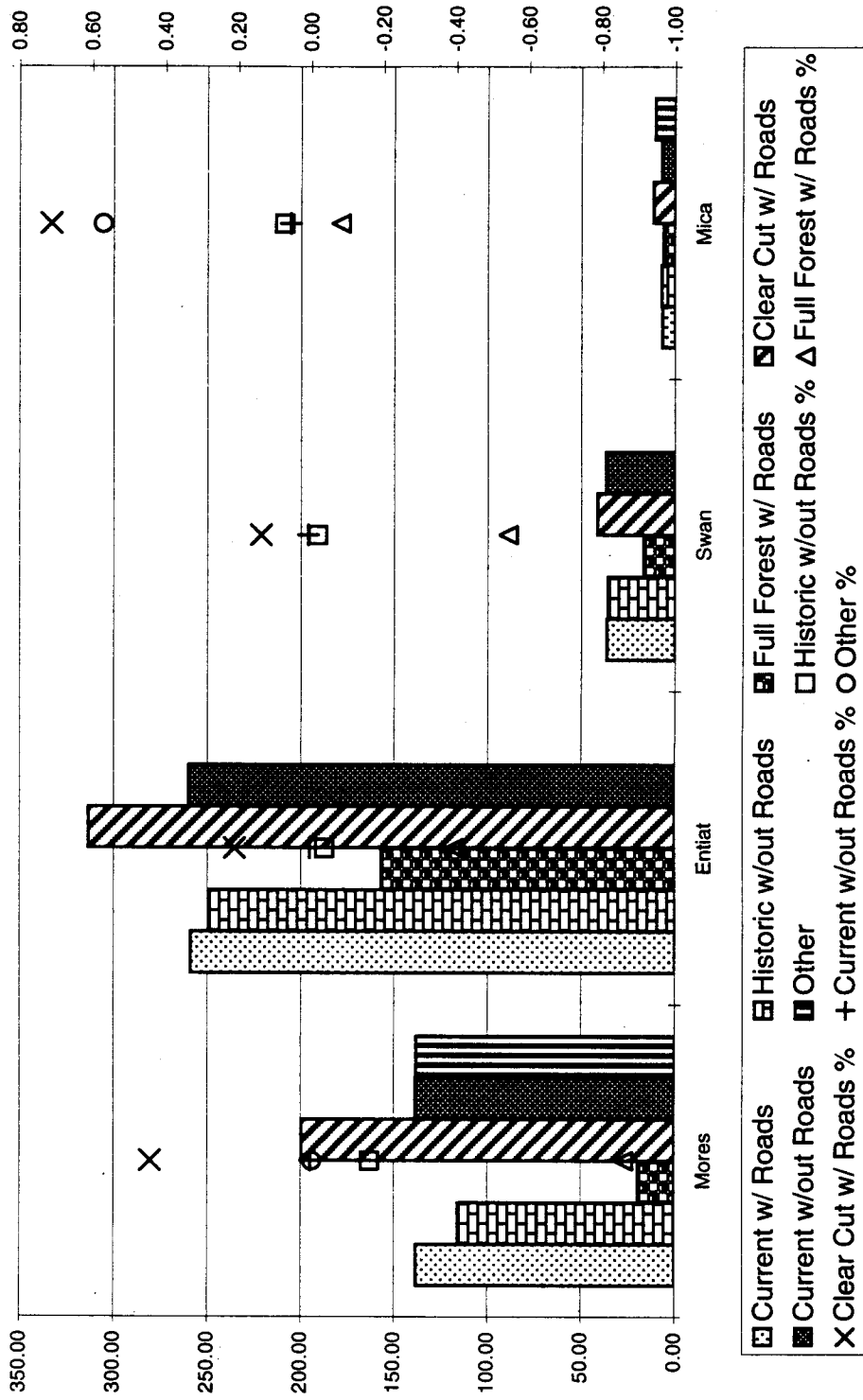


Figure 7-8: Maximum flood during investigation: Barchart (left axis) shows flowrate (cms) and x-y points (right axis) show percent change $(X - \text{Current w/ Roads}) / (\text{Current w/ Roads})$ where X is each vegetation scenario.

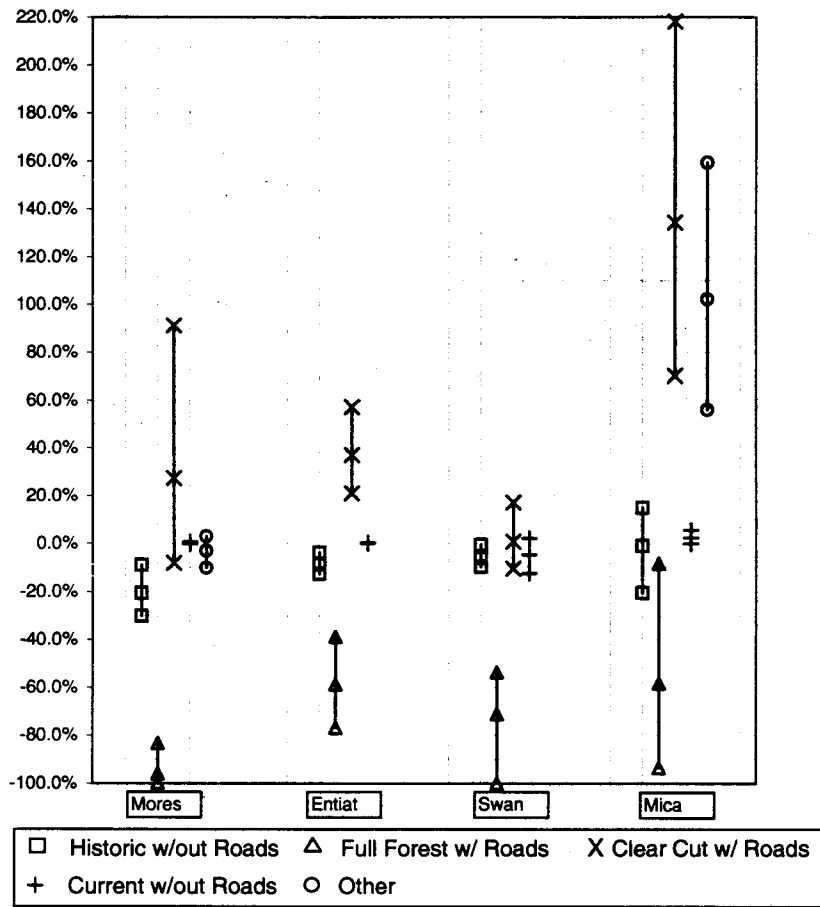


Figure 7-9: Range of percent change in annual maximum flood $(X - \text{Current w/ Roads}) / (\text{Current w/ Roads})$ where x is each vegetation scenario.

The timing of SWE accumulation and ablation averaged over the basin for each calendar date over the simulation period can be seen in Figure 7-11. Based solely on catchment average LAI, the changes cannot be readily predicted. Mores Creek has lower curves for both significantly higher and lower LAI values (fully forested with roads and clear-cut with roads). It appears, however, that within some unknown limit, a slight increase of LAI raises the curve, as seen comparing current with roads and historical without roads. Interestingly, the 1-km aggregation resulted in the highest curve. The Swan River results are similar to the Mores Creek results in the clear-cut and fully forested comparisons. Both have more LAI currently than historically, although the Mores Creek historical SWE curve plots above the current SWE curve while the Swan River historical SWE curve plots below the current SWE curve. The warm-season, fully forested SWE curve for Swan River predicts glacier snowpack growth at the highest elevations. This part of the prediction is unrealistic as the vegetation scenario assigns dense canopy above the natural tree-line, insulating the snowpack from radiation and sensible heat exchange (wind) and thus preventing its annual melt. In both the Entiat River and Mica Creek catchments, open areas accumulate more snow and have higher ablation rates than more densely forested areas.

The change in spatial distribution of SWE (meters) taken as a snapshot on March 1 (as reported in Table 7-1) can be seen in Figures 7-12 and 7-13. While patterns of SWE are evident and generally are related to vegetation change, change in LAI (Figures 5-6, 5-7, 5-8, and 5-9) alone is not a reliable predictor of the direction of change in SWE.

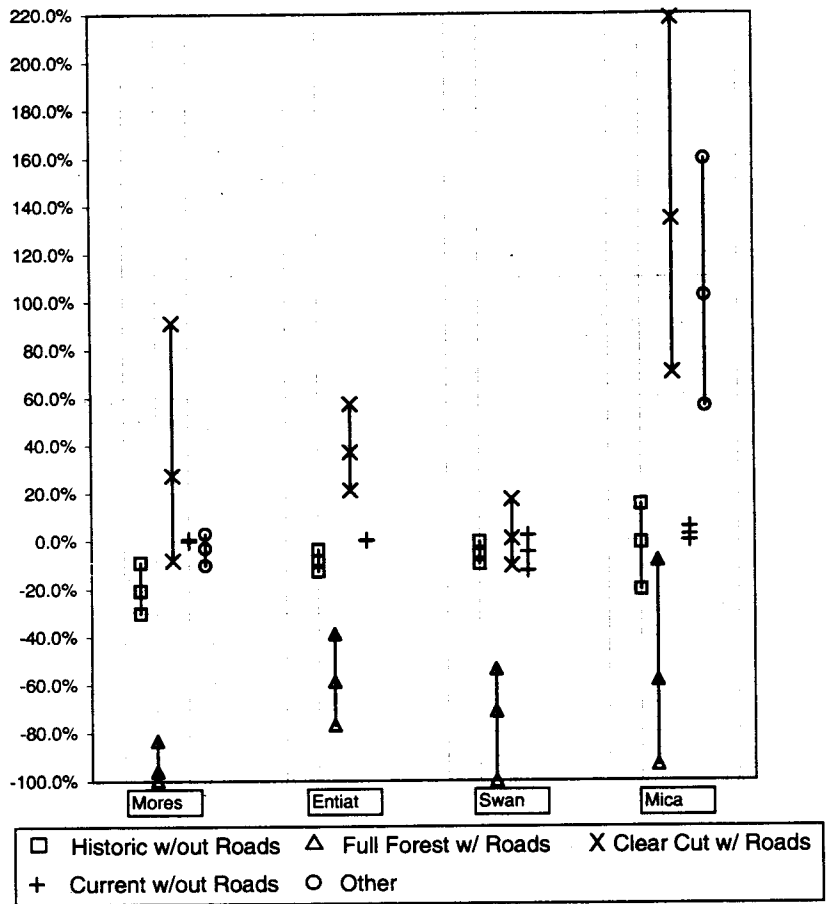


Figure 7-9: Range of percent change in annual maximum flood (X-Current w/ Roads)/(Current w/ Roads) where x is each vegetation scenario.

The timing of SWE accumulation and ablation averaged over the basin for each calendar date over the simulation period can be seen in Figure 7-11. Based solely on catchment average LAI, the changes cannot be readily predicted. Mores Creek has lower curves for both significantly higher and lower LAI values (fully forested with roads and clear-cut with roads). It appears, however, that within some unknown limit, a slight increase of LAI raises the curve, as seen comparing current with roads and historical without roads. Interestingly, the 1-km aggregation resulted in the highest curve. The Swan River results are similar to the Mores Creek results in the clear-cut and fully forested comparisons. Both have more LAI currently than historically, although the Mores Creek historical SWE curve plots above the current SWE curve while the Swan River historical SWE curve plots below the current SWE curve. The warm-season, fully forested SWE curve for Swan River predicts glacier snowpack growth at the highest elevations. This part of the prediction is unrealistic as the vegetation scenario assigns dense canopy above the natural tree-line, insulating the snowpack from radiation and sensible heat exchange (wind) and thus preventing its annual melt. In both the Entiat River and Mica Creek catchments, open areas accumulate more snow and have higher ablation rates than more densely forested areas.

The change in spatial distribution of SWE (meters) taken as a snapshot on March 1 (as reported in Table 7-1) can be seen in Figures 7-12 and 7-13. While patterns of SWE are evident and generally are related to vegetation change, change in LAI (Figures 5-6, 5-7, 5-8, and 5-9) alone is not a reliable predictor of the direction of change in SWE.

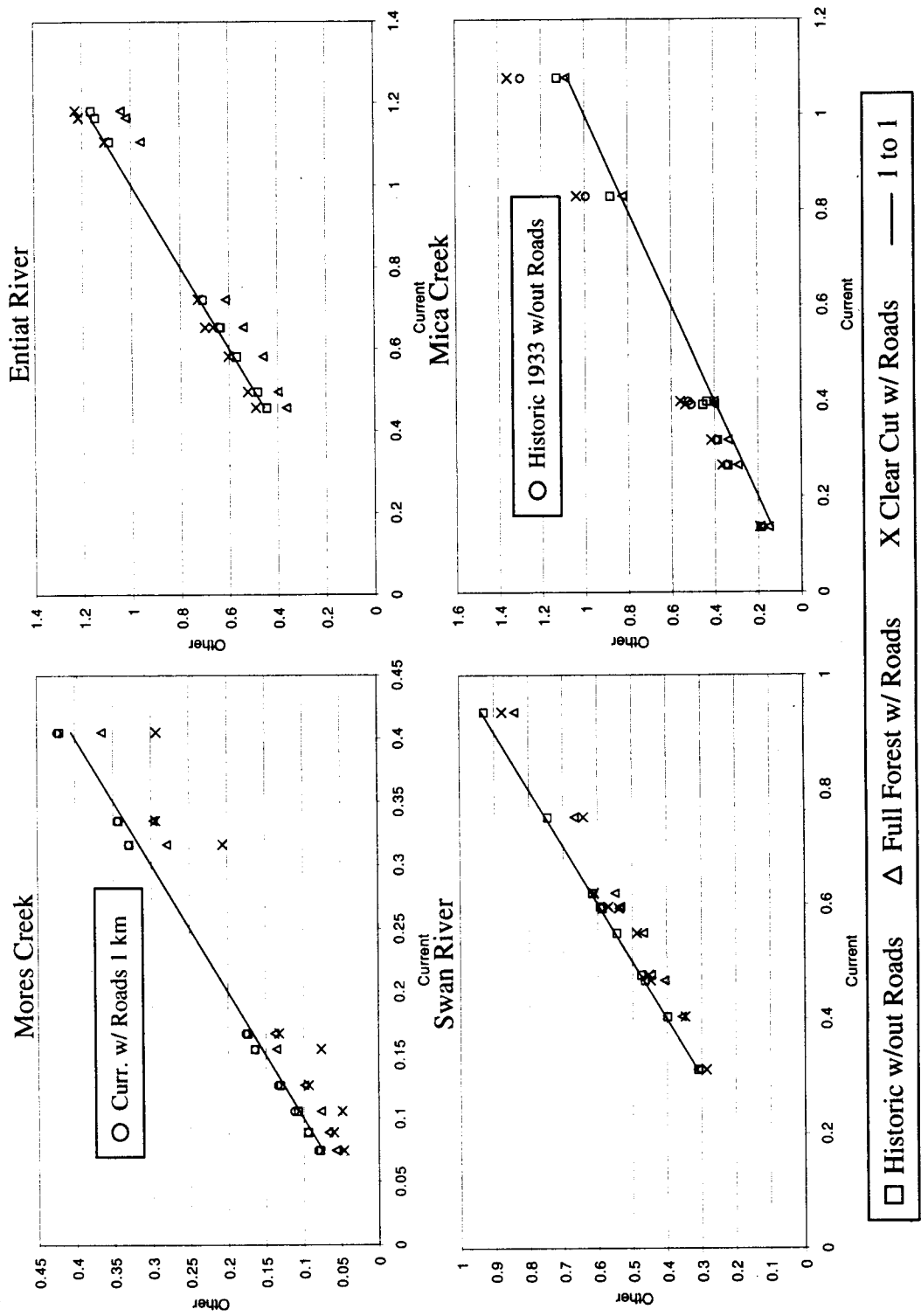


Figure 7-10: Current maximum annual SWE (m) vs. alternative vegetation maximum annual SWE (m) Current w/ roads on the x-axis and comparable (by year) values for other investigation runs on the y-axis (cms). The line is one-to-one.

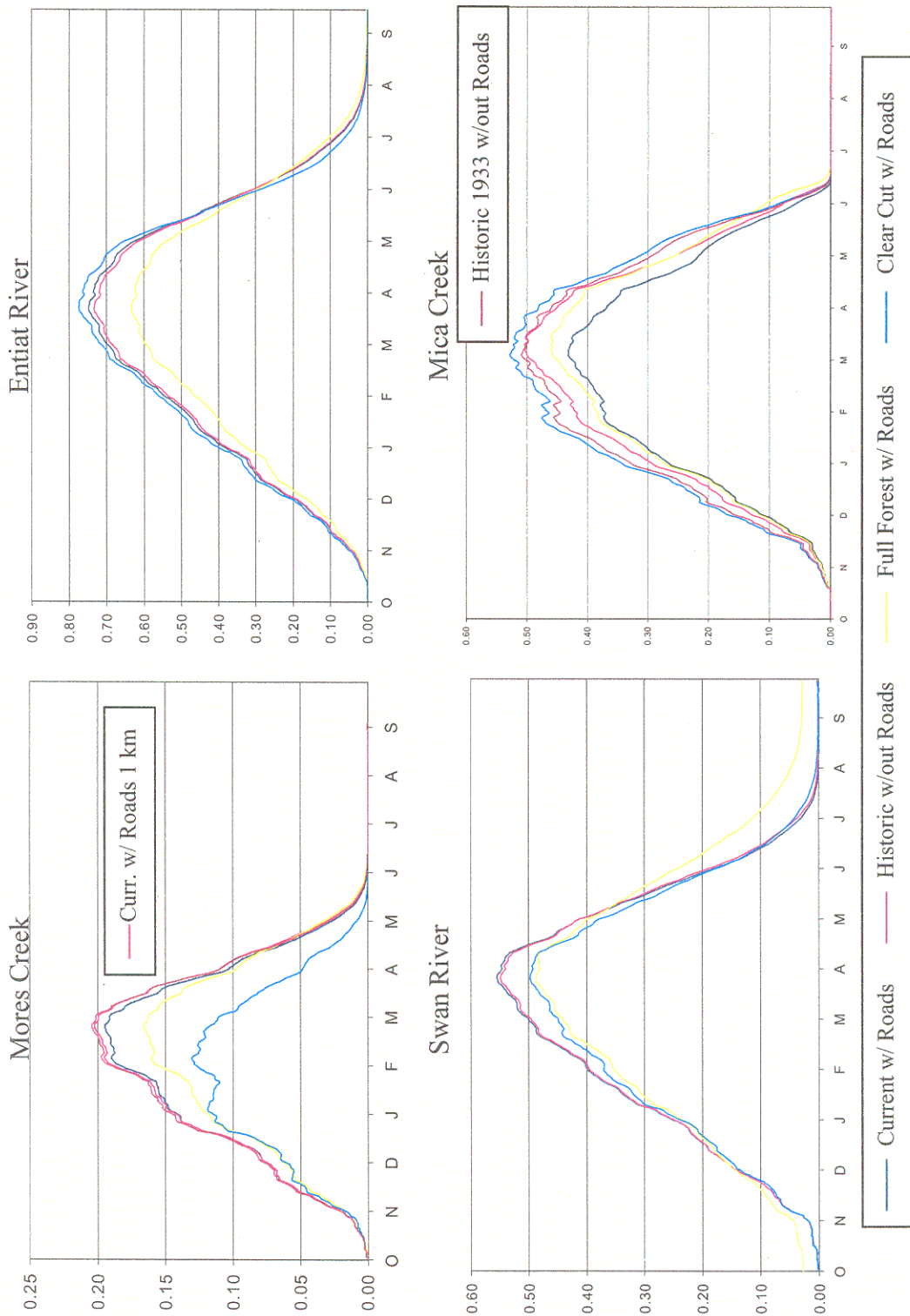
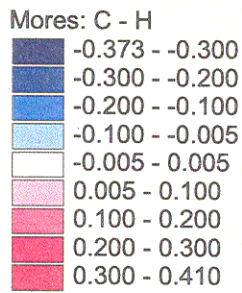
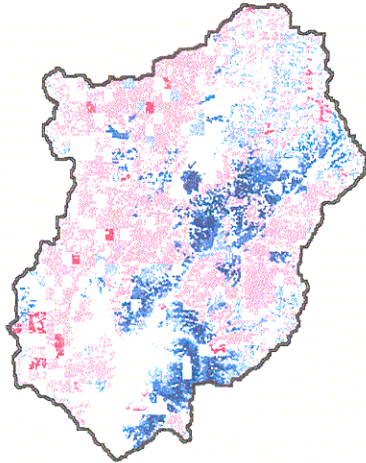
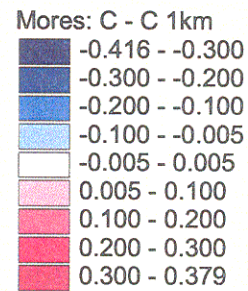
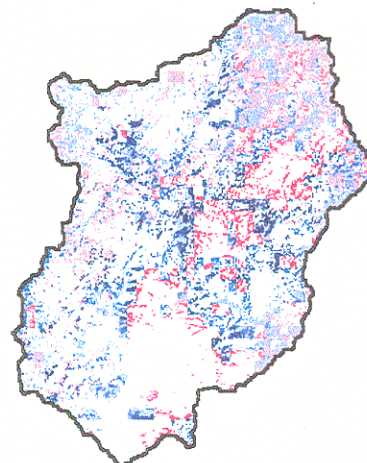


Figure 7-11: Catchment average annual SWE (m) time-series (month)

Mores: Current - Historical



Mores: Current - Current 1km



Swan: Current - Historical

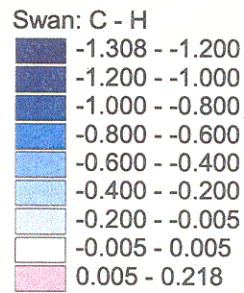
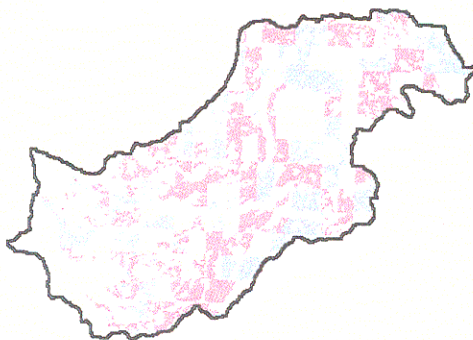
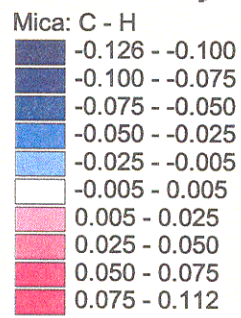
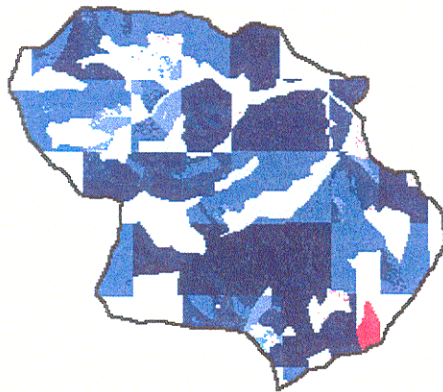
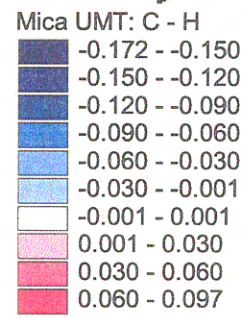
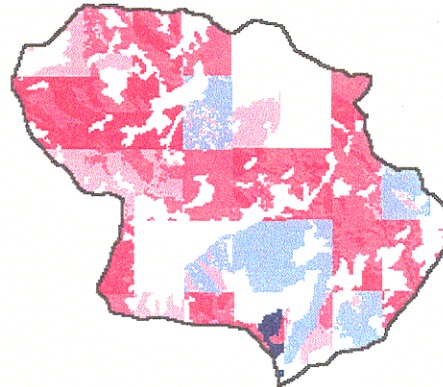


Figure 7-12: Spatial distribution of change in SWE: Mores Creek and Swan River (m)

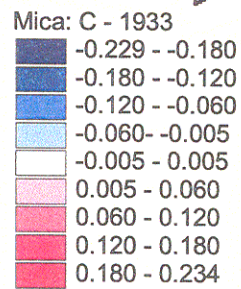
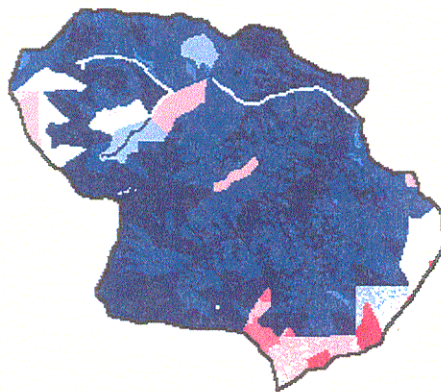
Mica: Current - Historical



Mica UMT: Current - Historical



Mica: Current - 1933



Entiat: Current - Historical

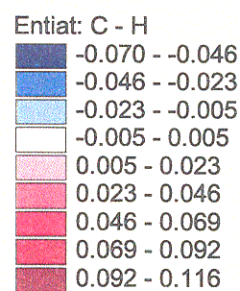
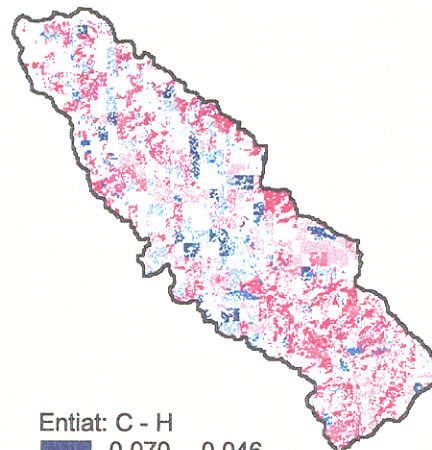


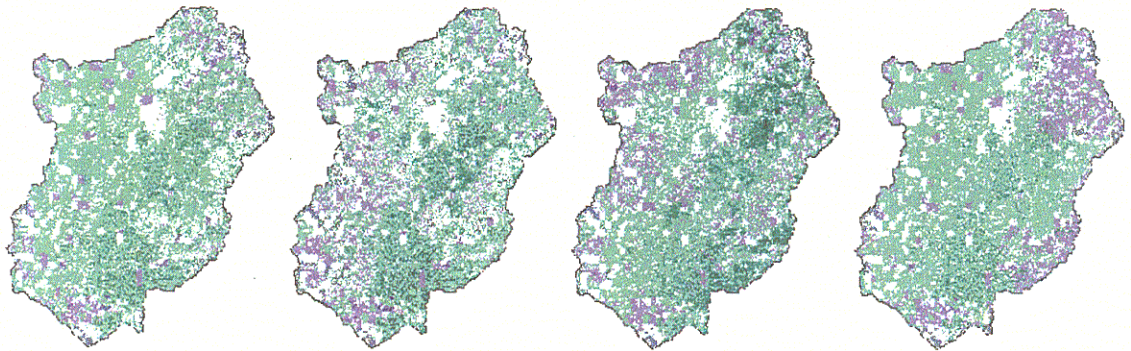
Figure 7-13: Spatial distribution of change in SWE: Mica Creek and Entiat River (m)

Elevation and aspect, which influence temperature and the amount of radiation input to a pixel, cloud the catchment-wide patterns related to vegetation. Likely, some function of change in LAI, elevation, and aspect could predict change in SWE (in spatial terms) more effectively than change in LAI alone. Change in overstory presence (not shown) is highly correlated to change in SWE. Change in soil moisture was evaluated by using depth to water table as a surrogate. Figures 7-14 and 7-15 show the seasonal average (over the years simulated) taken on January 15, April 15, July 15, and October 15. The patterns are clearly related to LAI, although the effects of LAI in conjunction with local topography are more readily visible. The changes in average soil moisture are most distinct in July, while October shows only general trends across the catchment.

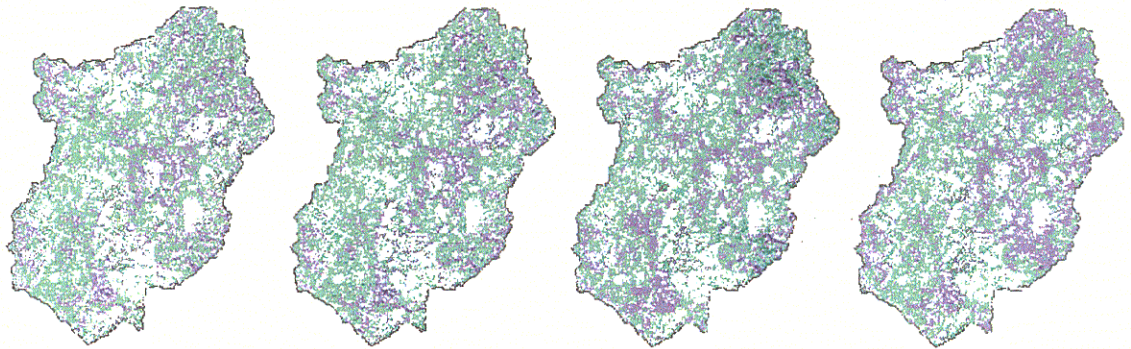
7.4 Comparison with VIC model pixel(s)

Results of the simulations reported here, based on DHSVM simulations at the catchment scale, were compared with previous results at one-quarter degree resolution of the entire Columbia River basin (Matheussen, et al, 2000). To make this comparison, one or more quarter degree VIC pixels were identified as representing each catchment. Figure 7-16 shows how these VIC grid cells correspond spatially with the catchments. For the VIC pixel(s) associated with each catchment, annual mean values were computed from 18 years of runoff and ET data (representing 1972-1990). Figure 7-17 shows the current and historical runoff with both models, as well as the current aggregated condition for Mores Creek (DHSVM). Figure 7-18 shows similar

Mores: Current - Historical



Mores: Current - Current 1km



Swan: Current - Historical

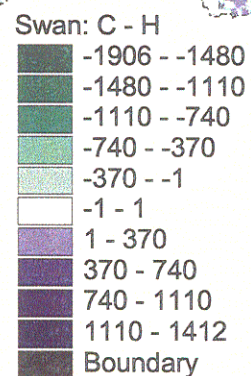
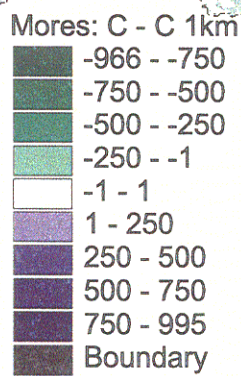
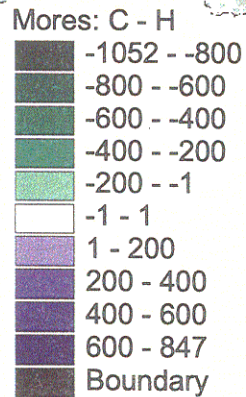
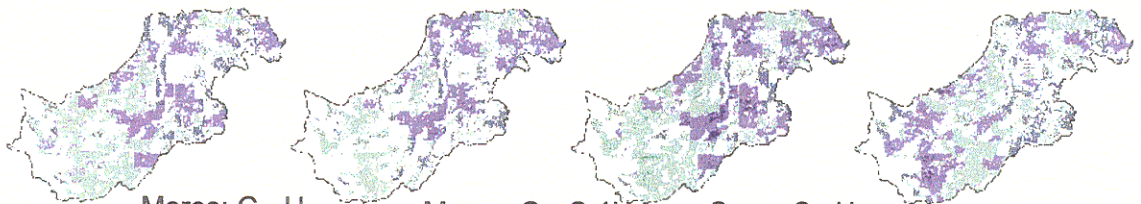


Fig. 7-14: Average seasonal spatial patterns of water table depth: Mores Creek and Swan River (mm). "Boundary" outlines the catchment

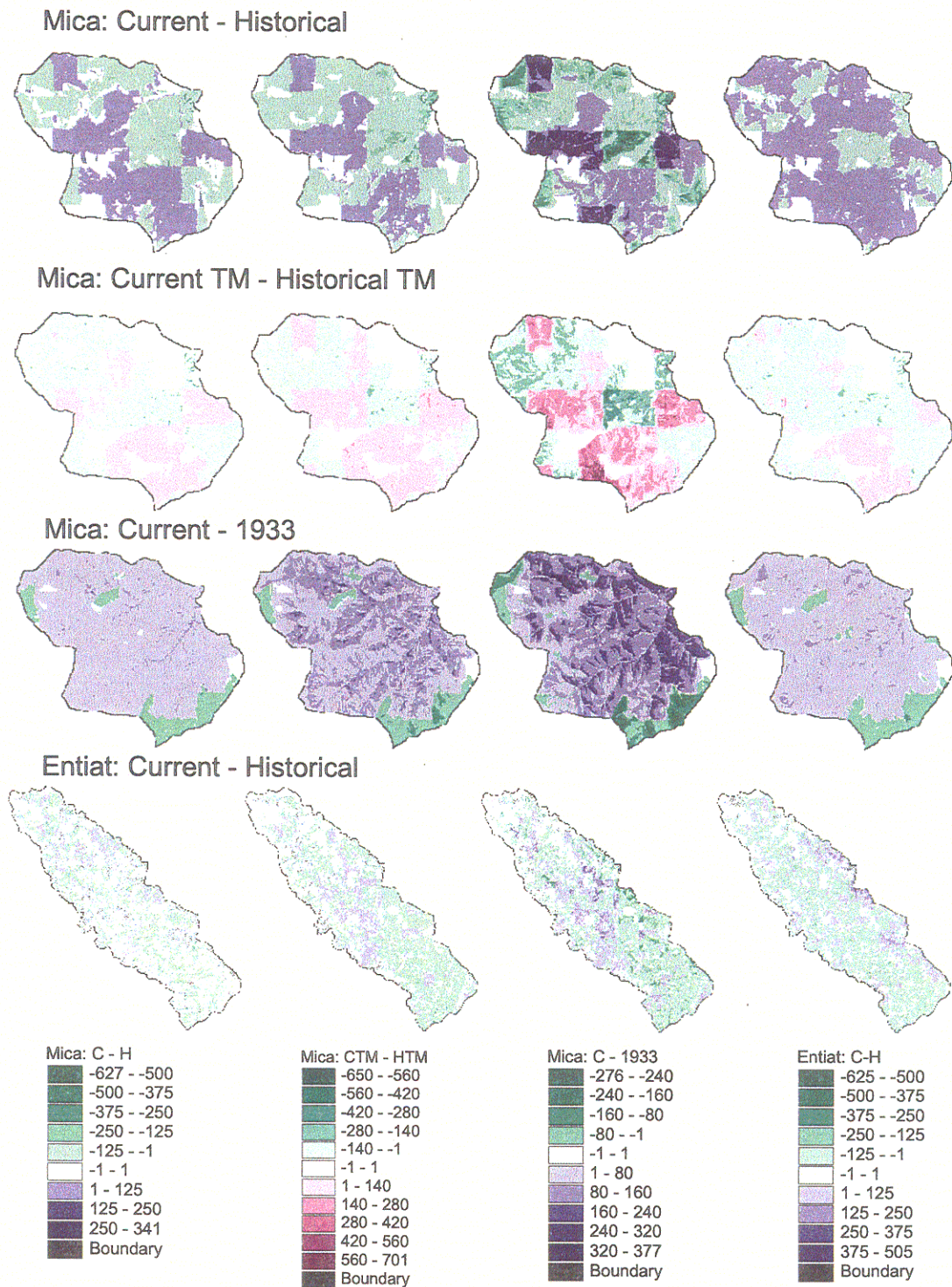
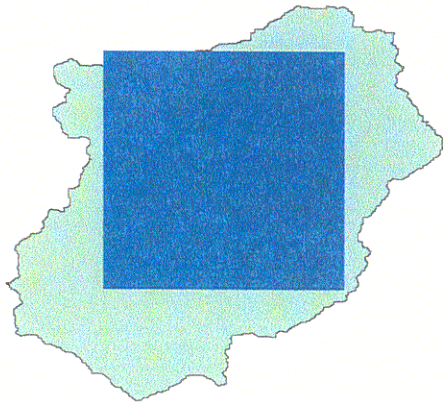
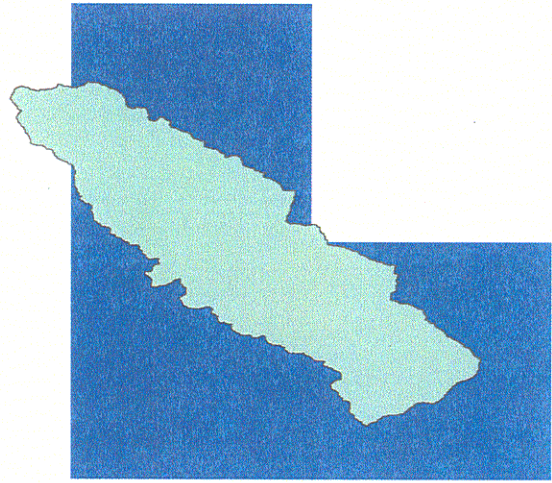


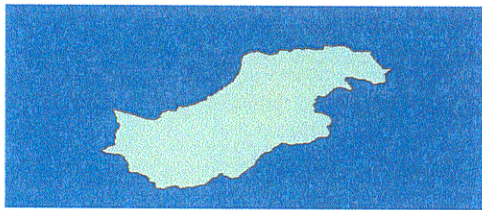
Figure 7-15: Average seasonal spatial patterns of depth to water table: Mica Creek and Entiat River (mm). "Boundary" outlines the catchment.



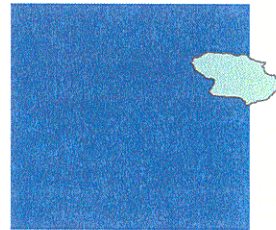
(A)



(B)



(C)



(D)

Figure 7-16: VIC $\frac{1}{4}$ degree pixels and catchment overlay
(A- Mores Creek, B- Entiat River, C- Swan River, D- Mica Creek)

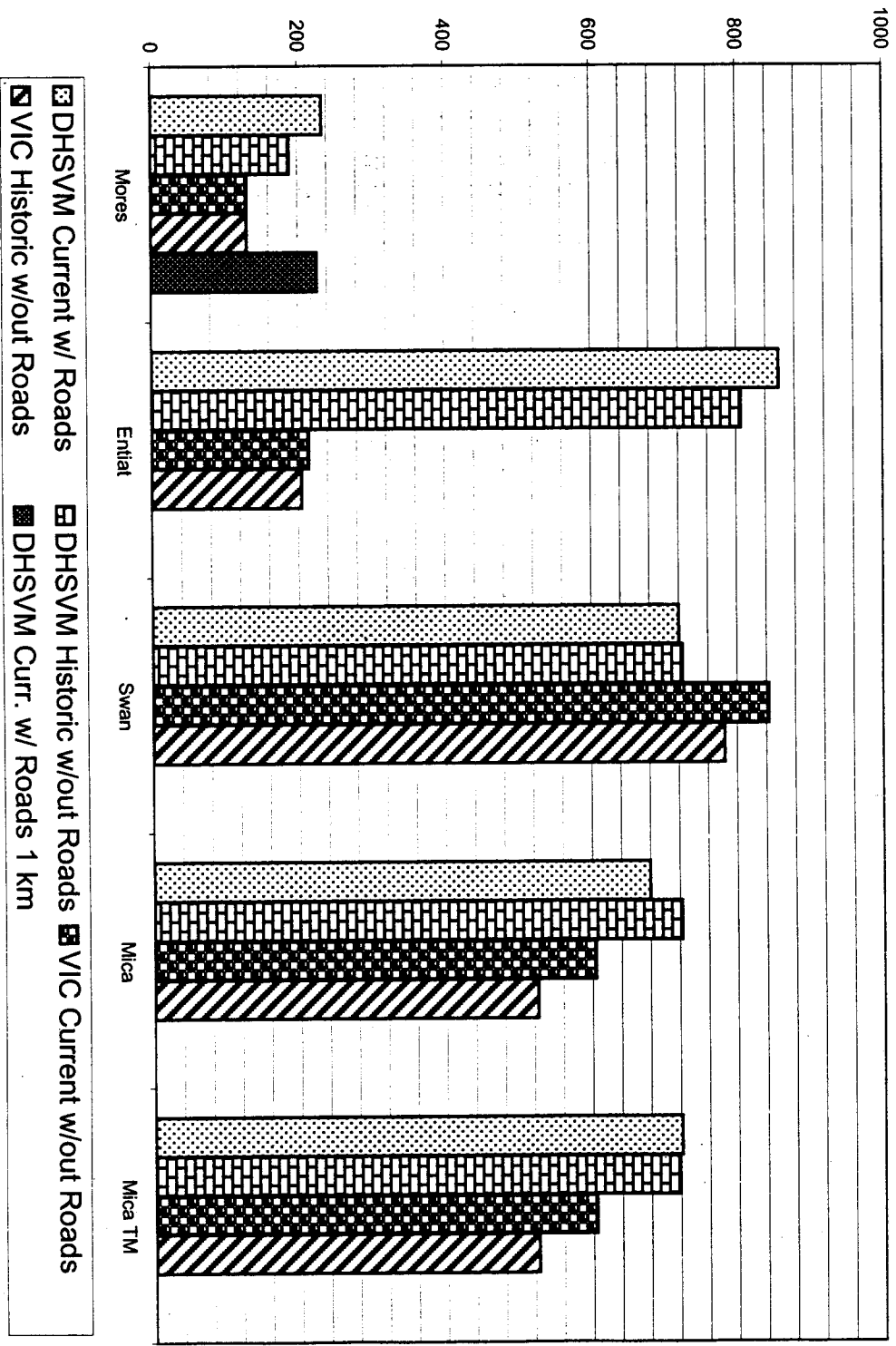


Figure 7-17: Average annual runoff (mm): VIC & DHSVM

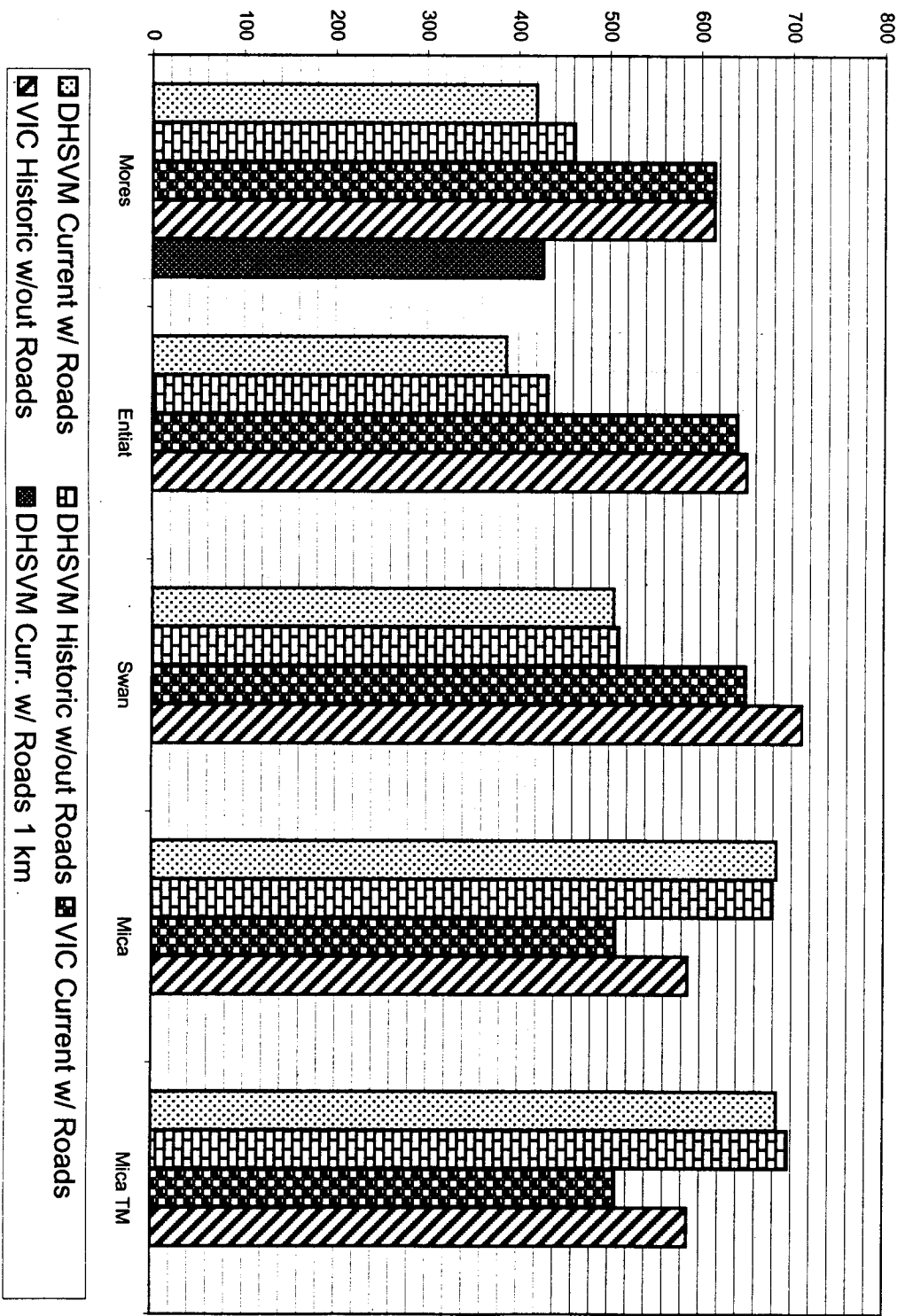


Figure 7-18: Average annual ET (mm): VIC & DHSVM

results for ET. The VIC change in LAI was calculated only within the grid cells themselves, and not for the catchment as outlined by higher resolution data used in DHSVM.

While these figures show relatively few similarities between the VIC and DHSVM runs, Table 7-3 helps explain why. Only in the Entiat River catchment are the LAI changes in the same direction. This is an artifact of the method used to develop historical vegetation for this study. The differences in results appear to be related more to differences in the coarse (1 km) data sets used by Matheussen, et al and the higher resolution data used here, than to differences between the DHSVM and VIC models.

Keeping the vegetation problems in mind, the following observations were made. While the magnitude of LAI change is similar in the Entiat catchment, the change in yield and ET are considerably larger in the DHSVM parameterization. The Entiat DHSVM and Swan VIC runs show similar changes in mean annual yield and ET for similar changes in LAI. In Mores Creek, changes in LAI similar in magnitude but opposite in direction resulted in no similarity in magnitude of either yield or ET changes. The Swan basin VIC results show on the order of 10 times more change over the DHSVM runs despite an increase in LAI of 2 times.

Table 7-3: Annual Water Balance: VIC vs. DHSVM

		# Pixels	Avg Etot Current (mm)	Avg Runoff Current (mm)	Avg LAI change	Avg Etot Change (mm)	Avg Etot Change (%ofCurr)	Avg Runoff Change (mm)	Avg Runoff Change (%ofCurr)
Mores	DHSVM	N/A	419.5	233.8	-0.7	-42.0	-10.0	45.0	19.3
	VIC	1	614.4	130.6	1.3	0.5	0.1	0.0	0.0
Entiat	DHSVM	N/A	386.9	858.2	-0.6	-45.5	-11.8	52.0	6.1
	VIC	3	214.6	640.0	-0.4	-9.9	-4.6	9.9	1.6
Swan	DHSVM	N/A	505.2	720.1	0.3	-5.6	-1.1	-4.7	-0.7
	VIC	2	638.4	843.3	0.5	-61.1	-9.6	60.6	7.2
Mica	DHSVM	N/A	683.4	679.4	2.7	4.1	0.6	-43.3	-6.4
	VIC	1	507.8	604.6	0.0	-78.7	-15.5	79.6	13.2
UMT	DHSVM	N/A	683.8	721.6	0.8	-12.2	-1.8	3.3	0.5

Chapter 8: Conclusions

This research investigated the extent of hydrologic changes over the last century that may have occurred due to land cover change in four geographically diverse catchments within the Columbia River basin. Effects of vegetation change were inferred for all four catchments using DHSVM, a spatially-distributed, physically-based hydrologic model, which was applied at spatial resolutions ranging from 30 to 120 m.

Prior to initiation of the model studies, field reconnaissance was undertaken in each of the four catchments. These field visits were used to map features such as culverts, and to observe first-hand the dominant processes affecting runoff generation. In addition, estimates of some model parameters that could not be obtained otherwise were made.

DHSVM, which is a high-resolution, spatially-distributed model, requires detailed land cover characteristics data in addition to climatological forcing time series over a multi-year period. Land cover classifications for current conditions were obtained from high-resolution land cover classifications extracted from remotely sensed imagery. Historical vegetation was developed by projecting the high-resolution current data back in time using the large scale estimate of historical (1900) vegetation produced by the Interior Columbia Basin Ecosystem Management Program, as modified by Matheussen, et al (2000). Additional hypothetical vegetation scenarios corresponding to entirely clear-cut and entirely mature forest conditions were prepared as logical bounding estimates. In addition, the effect of spatial resolution was tested via an aggregated

(from 120 m to 1 km resolution) current vegetation scenario for Mores Creek and a 1933 historical condition (based on aerial photography) was prepared for Mica Creek.

Following calibration of the model for each catchment model using current land cover conditions and recent streamflow records, multiple model runs were conducted corresponding to current vegetation with and without roads, historical vegetation without roads, fully forested with roads, and clear-cut with roads. Effects of land cover change alone was made by comparing runs for each vegetation scenario with the current condition with (or without) roads as appropriate.

Model simulations with the historical and current land cover conditions show that average annual runoff is predicted to have increased 19.2 and 6.1 percent in Mores Creek and Entiat River, respectively, and to have decreased 0.6 and 6.4 percent in Swan River and Mica Creek, respectively, over the period from 1900 to present. Predictions for clear-cut roaded conditions showed increases in annual runoff volumes by 19.6 percent in Mores Creek, 20.4 percent in Entiat River, 16.4 percent in Swan River, and 62.3 percent in Mica Creek relative to the current vegetation (with roads) condition.

Comparison of each catchment with similar regions from the much coarser Columbia basin-wide (one-quarter degree resolution) study by Matheussen, et al (2000) was clouded by inconsistencies in the vegetation data. Inferred changes appear to be primarily related to the method used to develop historical vegetation for this study at the differing resolutions used by

the two studies. Nevertheless, this study provides a basis to further pursue the scale dependence of vegetation change effects on hydrology.

Comparison of model simulations with the historical and current land cover conditions (without roads) shows that the mean annual flood was predicted to have increased 20.6 percent in Mores Creek, 8.5 percent in Entiat River, 6.0 percent in Swan River, and 0.9 percent in Mica Creek since 1900. Individual flood peaks within the range of years studied were predicted to have increased from 9.0 to 30.1 percent for Mores Creek, 3.7 to 12.5 percent for Entiat River, 0.5 to 9.6 percent for Swan River, and -15.0 to 20.5 percent for Mica Creek. Comparison of simulations with current vegetation and clear-cut conditions (both roaded) predicted that full harvest would increase the mean annual flood by 27.3, 37.1, 0.9, and 134 percent for Mores Creek, Entiat River, Swan River and Mica Creek, respectively.

Due to the relatively low density of roads (0.9 to 1.6 km/km²) in the catchments studied, simulations with and without roads showed little effect on annual runoff volumes—less than one-half percent in Mores Creek and Entiat, and less than two percent in Swan River and Mica Creek. Predicted increases in annual maximum flood were 0.7, 0.4, 2.1, and 5.7 percent in Mores Creek, Entiat River, Swan River, and Mica Creek respectively.

Sensitivity of the model to the scale of vegetation was investigated using a 1-km aggregation of 120 m data in Mores Creek. The aggregation resulted in a reduction of 3.1 percent in average

annual runoff volume for the aggregated scenario relative to the base (high resolution) case. The mean annual flood was predicted to have increased by 3.1 percent. Increases in mean annual flow and maximum flood for the aggregated vegetation case appeared to be related primarily to the fraction of coverage of a given vegetation type rather than its spatial extent.

List of References

- Arola, A., Effects of the subgrid scale spatial variability on mesoscale snow modeling, M.Sc. Thesis, University of Washington, Seattle, WA, 1993.
- Bates, C.G. and Henry, A.J., Second phase of streamflow experiment at Wagon Wheel Gap, Colorado. *Mon. Weather Review*, 56(3): 79-85, 1928.
- Berris, S.N. and R.D. Harr, Comparative snow accumulation and melt during rainfall in forested and clear-cut plots in the western Cascades of Oregon, *Water Resources Research*, 23 (1), 135-142, 1987.
- Bosch, J.M. and J.D. Hewlett, A review of catchment experiments to determine the effect of vegetation changes on water yield and evapotranspiration, *Journal of Hydrology*, 55, 3-23, 1982.
- Bowling, L.C. and D.P. Lettenmaier, Evaluation of the effects of forest roads on streamflow in Hard and Ware Creeks, Washington, *Timber Fish Wild Water Resources Ser., Tech. Resp. 155*, 189 pp., Washington Dept. of Nat. Resources. Olympia, 1997.
- Bowling, L.C., Storck, P. and D.P. Lettenmaier, Hydrologic effects of logging in Western Washington, USA, in press, 2000.
- Black, T.A., Chen, J.M., Lee, X. and R.M. Sagar, Characteristics of short wave and long wave irradiances under a Douglas-fir forest stand, *Canadian Journal of Forest Resources*, 21, 1020-1027, 1991.
- Bras, R.L., *Hydrology, An Introduction to Hydrologic Science*, 643 pp., Addison-Wesley, Reading, Mass., 1990.
- Bristow, K.L. and G.S. Campbell, On the relationship between Solar Radiation and Daily Maximum and Minimum Temperature, *Agricultural and Forest Meteorology*, v. 31, p. 159-166, 1984.
- Calder, I.R., Hydrologic effects of land-use change, In *Handbook of Hydrology*, D. R. Maidment editor, McGraw-Hill, Inc., San Francisco, 1993.

- Calder, I.R., Newson, M.D. and P.D. Walsh, The application of catchment, lysimeter and hydrometeorological studies of coniferous afforestation in Britain to land-use planning and water management, *Proceedings of the Symposium of Hydrological Research Basins, Sonderh. Landeshydrologie*, Bern, pp. 853-863, 1982.
- Conte, S.C. and C. de Boor, *Elementary Numerical Analysis, and Algorithmic Approach*, 432 pp., McGraw-Hill, 1980.
- Cundy, T., Research hydrologist, Potlatch Corporation, personal communication, Sept. 1998.
- Curtis, D.C. and P.S. Eagleson, Constrained Stochastic Climate Simulation, Cambridge, Mass.: MIT Department of Civil Engineering, Ralph M. Parsons Laboratory, Technical Report No. 274, 1982.
- Daly, C., A statistical topographic model for mapping climatological precipitation over mountainous terrain, *Journal of Applied Meteorology*, 33(2):140-158, 1994.
- Duan, Q., Sorooshian, S., and V.K. Gupta, Optimal use of the SCE-UA global optimization method for calibrating watershed models, *Journal of Hydrology*, 158(3-4), pp. 265-284, 1994.
- Dubin, A.M. and D.P. Lettenmaier, Assessing the influence of digital elevation model resolution on hydrologic modeling, Water Resources Series, Technical Report, 159, University of Washington, Seattle, 1999.
- Dubayah, R., Dozier, J. and F.W. Davis, Topographic distribution of clear-sky radiation over the Konza prairie, Kansas, *Water Resources Research*, 26, 679-690.
- Eberhardt, L.L. and J.T. Thomas, Designing environmental field studies, *Ecol. Monogr.*, 61(1), 53-73, March 1991.
- Gates, D.M., *Biophysical Ecology*, New York: Springer-Verlag, 1980.
- Gupta, H.V., Sorooshian, S., and P.O. Yapo, Toward improved calibration of hydrologic models: Multiple and noncommensurable measures of information, *Water Resources Research*, 34(4) pp. 751-763, 1998.
- Gupta, H.V., Sorooshian, S., and P.O. Yapo, Status of automatic calibration for hydrologic models: Comparison with multilevel expert calibration, *Journal of Hydrologic Engineering*, 4(2) pp. 135-143, 1999.

- Haddeland, I. and D.P. Lettenmaier, Hydrologic modeling of boreal forest ecosystems, Water Resources Series, Technical Report, 145, University of Washington, Seattle, 1995.
- Hann, W.J., Long, D.G. and J.P. Menakis, *Landscape ecology assessment and evaluation of alternatives data analysis record*. USDA Forest Service, USDI, Bureau of Land Management, Interior Columbia Basin Ecosystem Management Project, 112 E. Poplar, Walla Walla, WA 99362, 1997.
- Hardy, C.C., Burgan, R.E., Ottmar, R.D. and J.E. Deeming, A database for spatial assessments of fire characteristics, fuel profiles, and PM10 emissions. In *Compilation of Administrative Reports: Multi-scale Landscape Dynamics in the Basin and Portions of the Klamath and Great basins*, Keane, R.E., Jones, J.L, Riley, L.S., and W.J. Hann (eds); USDA Forest Service, USDI, Bureau of Land Management, Interior Columbia Basin Ecosystem Management Project, 112 E. Poplar, Walla Walla, WA 99362, 1996.
- Harr, R.D., Some characteristics and consequences of snowmelt during rainfall in western Oregon, *Journal of Hydrology*, 53, 277-304, 1981.
- Harr, R.D. and F.M. McCorison, Initial effects of clearcut logging on size and timing of peak flows in a small watershed in western Oregon, *Water Resources Research*, 15(1), 90-94, 1979.
- Hart, A.A., *Basin of Gold, Life in Boise Basin, 862-1890*, Idaho City Historical Foundation, Inc., 1986.
- Helvey, J.D., Watershed behaviour after forest fire in Washington. Proceedings of the Irrigation and Drainage Division Special Conference, Fort Collins, CO, pp. 402-422, 1973.
- Helvey, J.D., Effect of a north-central Washington wild-fire on runoff and sediment production. *Water Resources Bulletin*, 16(4), pp. 625-634, 1980.
- Hibbert, A.R., Forest treatment effects on water yield, in *Forest Hydrology*, edited by W.F. Sopper and H.W. Lull, pp.527-543. Pergamon, Tarrytown, N.Y. 1967.
- James, L.D., and Burges, S.J., Selection, calibration and testing of hydrologic models, In *Hydrologic Modeling of Small Watersheds*, Haan, C.T., Johnson, H.P. and Brakensiek, D.L. editors, American Society of Agricultural Engineers, Michigan, 1982.
- Jensen, S.K., and J.O. Domingue, Extracting topographic structure from digital elevation data for geographic information system analysis, *Photogrammetric Engineering and Remote Sensing*, 54(11), pp.1593-1600, 1988.

- Jones, J. A. and G.E. Grant, Peak flow responses to clear-cutting and roads in small and large basins, western Cascades, Oregon, *Water Resources Research* 32(4), 959-974, 1996.
- Kalnay, E., Kanamitsu, M., Kistler, R., Collins, W., Deaven, D., Gandin, L., Iredell, M., Saha, S., White, G., Woollen, J., Zhu, Y., Chelliah, M., Ebisuzaki, W., Higgins, W., Janowiak, J., Mo, K.C., Ropelewski, C., Wang, J., Leetmaa, A., Reynolds, R., Jenne, R., Joseph, D., The NCEP/NCAR 40-year reanalysis project. *Bulletin of the American Meteorological Society*, Boston, MA, 77(3): 437-471, 1996.
- Kattelmann, R., Effects of forest cover on a snowpack in the Sierra Nevada, *Watershed Planning and Analysis in Action*. American Society of Civil Engineers, New York, 1990.
- Kenward, T. and D.P. Lettenmaier, Assessment of required accuracy of digital elevation data for hydrologic modeling, *Water Resources Series, Technical Report, 153*, University of Washington, Seattle, 1997.
- Kenward, T., Lettenmaier, D.P., Wood, E.F., and E. Fielding, Effects of digital elevation model accuracy on hydrologic predictions, *Remote Sensing of Environment*, 2000.
- Kimball, J.S., Running, S.W. and R. Nemani, An improved method for estimating surface humidity from daily minimum temperature, *Agricultural and Forest Meteorology*, 85, 87-98, 1997.
- King, J.G. and L.C. Tennyson, Alteration of streamflow characteristics following road construction in north central Idaho. *Water Resources Research*, 20(8), 1159-1163, 1984.
- Kirschbaum R. and D. P. Lettenmaier, An evaluation of the effects of anthropogenic activity on streamflow in the Columbia River Basin, Washington, *Water Resources Series, Technical Report, 156*, University of Washington, Seattle, 1997.
- La Marche, J. and D.P. Lettenmaier, Forest road effects on flood flows in the Deschutes River basin, Washington, *Water Resources Series, Technical Report, 158*, University of Washington, Seattle, 1998.
- La Marche, J. and D.P. Lettenmaier, Effects of forest roads on flood flows in the Deschutes River basin, Washington, *Earth Surface Processes and Landforms*, in press.

- Legates, D.R. and T.L. DeLiberty, 1993. Removal of Biases in Precipitation Gage Measurement: An Example Using the United States Raingage Network. Proceedings, Eighth Symposium on Methods and Observing Instruments and the Eighth Conference on Applied Climatology, American Meteorological Society, Anaheim, California, pp. J48-J51.
- Liang, X., Lettenmaier, D.P., Wood, E.F. and S.J. Burges, A simple hydrologically based model of land surface, water, and energy fluxes for general circulation models, *Journal of Geophysical Research*, 99(D7), 14415-14428, 1994.
- Losensky, B.J., Historical vegetation types of the Interior Columbia Basin, completion report., INT-94951-RJVAUSDA, Forest Service Intermountain Research Station, Forestry Sciences Laboratory: Missoula, MT 59807, 1994.
- Loveland, R.R., Merchant, J.M, Ohlen, D.O. and J.F. Brown, Development of a land-cover characteristics database for the coterminous US. *Photogrammetric Engineering and Remote Sensing* 57, pp 1453-1463, 1991.
- Loveland, R.R. and D.O. Ohlen, Experimental AVHRR land data sets for environmental monitoring and modeling. In *Environmental Modeling with GIS*, Goodchild, M.F., Parks, B.O., and L.T. Steyaert (Eds.); Oxford University Press, New York, pp. 379-385, 1992.
- Luce, C.H. and T.W. Cundy, Parameter identification for a runoff model for forest roads, *WaterResources Research*, 30, 1057-69, 1994.
- Maidment, D.R., *Handbook of Hydrology*, McGraw-Hill Inc., New York, 1992.
- Matheussen, B., Kirshbaum, R.L., Goodman, I.A., O'Donnell, G.M. and D.P. Lettenmaier, Effects of land cover change on streamflow in the interior Columbia River Basin (USA and Canada), *Hydrologic Processes*, 14, 867-885, 2000.
- Megahan, W.F., Subsurface flow interception by a logging road in mountains of central Idaho, paper presented at Symposium on watersheds in transition, American Water Resources Association, Ft. Collins, Colorado, 1972.
- Megahan, W.F., Hydrologic effects of clearcutting and wildfire on steep granitic slopes in Idaho, *Water Resources Research*, 19(3), 811-19, 1983.

- Menakis, J.P., Lyon, J.G. and R.E. Keane, The development of key broad-scale layers and characterization files. In *Compilation of Administrative Reports: Multi-scale Landscape Dynamics in the Basin and Portions of the Klamath and Great basins*, Keane, R.E., Jones, J.L, Riley, L.S., and W.J. Hann (eds); USDA Forest Service, USDI, Bureau of Land Management, Interior Columbia Basin Ecosystem Management Project, 112 E. Poplar, Walla Walla, WA 99362, 1996.
- Miller, D.H. Interception processes during snowstorms. *Research Paper PSW-18*, USDA Forest Service, Pacific Southwest Forest and Range Experiment Station, Berkeley, CA 22 pp., 1964.
- Miller, D.H., Sources of energy for thermodynamically-caused transport of intercepted snow from forest crowns, in *International symposium on forest hydrology*, edited by W.F. Sopper and H. W. Lull, 201-211, Pergamon, New York, 1967.
- Nijssen, B., Haddeland, I. and D.P. Lettenmaier, Point evaluation of a surface hydrology model for BOREAS, *Journal of Geophysical Research-Atmospheres*, 102:29367-29378, 1997.
- Perkins, W.A., Wigmosta, M.S. and B. Nijssen, Development and testing of road and stream drainage network simulation within a distributed hydrologic model, *EOS Trans. AGU*, 77 (46), F232, Fall Meet. Suppl., 1996.
- Pomeroy, J.W. and K. Dion, Winter radiation extinction and reflection in a boreal pine canopy: measurements and modeling, *Hydrological Processes*, 10, 1591-1608, 1996.
- Quigley, T.M. and S.J. Arbelide (Eds.), An assessment of the ecosystem components in the Interior Columbia Basin and portions of the Klamath and Great Basins, vol. 2, General Technical Report, PNW-GTR-405. Portland, OR., 1997.
- Rawls, W.J., and D.L. Brakensiek, A procedure to predict Green Ampt infiltration parameters, *Adv. Infiltration, Am. Soc. Agric. Eng.*, pp 102-112, 1983.
- Redmond, R.L., Ma, Z., Tady, T.P., Winne, J.C., Schumacher, J., Troutwine, J., Holloway, S.W., Hart, M.M., McLaughlin, K.P. and W.W. Williams. Mapping existing vegetation and land cover across western Montana and northern Idaho. Unpublished Final Report, Contract #53-0343-4-000012. USDA Forest Service, Northern Region, Missoula, MT, 1996.
- Rothacher, J., Streamflow from small watersheds on the western slope of the Cascade range of Oregon. *Water Resources Research*, 1(1), 1245-134, 1965.

- Rothacher, J., Increases in water yield following clear-cut logging in the Pacific Northwest, *Water Resources Research*, 6(2), 653-658, 1970.
- Sahin, V. and M.J. Hall, The effects of afforestation and deforestation on water yields. *Journal of Hydrology*, (178), 293-309, 1996.
- Satterlund, D.R. and H.F. Haupt, Snow catch by conifer crowns. *Water Resources Research*, 3:1035-1039, 1967.
- Seyfried, M.S. and B.P. Wilcox, Scale and the nature of spatial variability: Field examples having implications for hydrologic modeling, *Water Resources Research*, 31(1), pp. 173-184, 1995.
- Stednick, J.D., Monitoring the effects of timber harvest on annual water yield. *Journal of Hydrology*, 176, 79-95, 1996.
- Storck, P., Trees, snow and flooding: an investigation of forest canopy effects on snow accumulation and melt at the plot and watershed scales in the Pacific Northwest, *Water Resources Series, Technical Report*, 161, University of Washington, Seattle, 2000.
- Storck, P., and D. P. Lettenmaier, Predicting the effect of a forest canopy on ground snow pack accumulation and ablation in maritime climates, in C. Troendle and K. Elder (Eds.), *proceedings of the Western Snow Conference*, pp 1-12, 1999.
- Storck, P., Bowling, L., Wetherbee, P. and D. Lettenmaier, Application of a GIS-based distributed hydrology model for the prediction of forest harvest effects on peak streamflow in the Pacific Northwest, *Hydrological Processes*, 12:889-904, 1998.
- Storck, P., Lettenmaier, D.P., Connelly, B.A. and T. W. Cundy, Implications of forest practices on downstream flooding, *Tiber Fish Wild. Ser., Rep. TFW-SH20-96-001*, 100 pp., Phase II final report, Washington Department of Natural Resources, Olympia, 1995.
- Sullivan, K.O. and S.H. Duncan, Sediment yield from road surfaces in response to truck traffic and rainfall, Weyerhaeuser Co. technical Report No. 042-4402/81/04, 1981.
- Tennessee Valley Authority, Heat and Mass Transfer Between a Water Surface and the Atmosphere, Norris, Tenn.: Tennessee Valley Authority, Laboratory report no. 14; *Water resources research report no. 0-6803*, 1972.

- Thomas, R.B. and W. F. Megahan, Peak flow responses to clear-cutting and roads in small and large basins, western Cascades, Oregon: A second opinion. *Water Resources Research* 34I(12) 3393-3403, 1998.
- Thornton, P.E. and J.D. White, Biogeochemical characterization of the CRB using the BGC model, ecophysical inputs and landscape descriptions, USDA Forest Service, Report RJVA-94933, Intermountain Fire Sciences Laboratory: PO Box 8089, Missoula, MT 59807, 1996.
- Troendle, C.A. and R.M. King, The effect of timber harvest on the Fool Creek watershed, 30 years later, *Water Resources Research*, 21(12) 1915-22, 1985.
- U.S. Army Corps of Engineers, *Snow Hydrology: Summary Report of the Snow Investigations*, North Pacific Division, Portland, OR, 1956.
- U.S. Department of Agriculture, Soil Conservation Service, *State Soil Geographic Data Base, Data use information*, Miscellaneous Publication Number 1492, 1994.
- U.S. Department of Agriculture, Forest Service, Status of the Interior Columbia basin: summary of scientific findings. Gen. Tech. Rep. PNW-GTR-385, Portland, OR: U.S. Department of the Interior Bureau of Land Management, 1996.
- U.S. Department of Agriculture Forest Service, Watershed Assessment Entiat Analysis Area, Wenatchee National Forest, 215 Melody Lane, Wenatchee, WA, 98801, 1996.
- U.S. Geological Survey, Digital Elevation Models, National Mapping Program Technical Instructions, Data Users Guide 5, National Mapping Program, Reston, Virginia, 1993.
- U.S. Geological Survey, National Elevation Dataset, Fact Sheet 148-99, Reston, VA, 1999.
- Utah State University Remote Sensing and GIS Laboratory and Utah Cooperative Fish and Wildlife Research Unit, *Intermountain Region Land Cover Characterization*, RS/GIS Laboratory, Utah State University, 9635 University Blvd., Logan, Utah, 84322-9635, 1995.
- Yapo, P.O., Gupta, H.V., and S. Sorooshian, Multi-objective global optimization for hydrologic models, *Journal of Hydrology*, 204(1-4) pp. 83-97, 1998.
- Wemple, B.C., Hydrologic integration of forest roads with stream networks in two basins, Western Cascades, Oregon, M.S. Thesis, Oregon State University, 1994.

- Wetherbee, P. and D.P. Lettenmaier, Application of the distributed hydrology-soil-vegetation model (DHSVM) to the little naches basin in the context of watershed analysis, Report to Plum Creek Timber Company and the National Council of the Paper Industry for Air and Stream Improvement, 1996.
- Wetherbee, P. and D.P. Lettenmaier, Cabin Creek hydrology assesment report using the distributed hydrology-soil-vegetation model (DHSVM), Report to Plum Creek Timber Company and the National Council of the Paper Industry for Air and Stream Improvement, 1997.
- Wigmosta, M.S. and W.A. Perkins, A GIS-based modeling system for watershed analysis, Final Report to the National Council of the Paper Industry for Air and Stream Improvement, 1997.
- Wigmosta, M.S., and W.A. Perkins, "Simulating the Impacts of Road Drainage in a Distributed Hydrologic Model", in Influence of Urban and Forest Land Use on the Hydrologic-Geomorphic Responses of Watersheds, Wigmosta and Burges ed., American Geophysical Union Water Resources Monograph, 2000.
- Wigmosta, M.S., Vail, L.W. and D. P. Lettenmaier, A distributed-hydrology-vegetation model for complex terrain. *Water Resources Research* 30(6) p 1665-1679, 1994.
- Ziegler, A.D. and T.W. Giambelluca, Importance of rural roads as source areas for runoff in mountainous areas of northern Thailand, *Journal of Hydrology*, 196, 204-229, 1997.
- Ziemer, R.R. Storm flow response to road building and partial cutting in small streams of northern California, *Water Resources Research*, 17, 907-917, 1981.

Appendix A: Vegetation Class Descriptive Parameter Estimation

For many of the vegetation classes, information completely describing the class in terms of DHSVM parameters was not available. Due to the time frame of interest, it was not possible to do an extensive literature search for these values. The author doubts that all these values are available in the literature even if one had the time to conduct an exhaustive search. It was then necessary to apply some methods for estimating these parameters. I have chosen to document this more extensively than others have for use in future work and to enable more knowledgeable persons to recommend improvements. Table 5-6 lists all parameters used. This attempts to describe how the values used for the parameters were determined.

Fractional Coverage:

Generally estimated as the midpoint of the bins as assigned by land classifications. Swan used 85% (70-100%), 55% (40-69%), and 30% (15-39%).

Trunk Space:

This was generally available from previous DHSVM parameterizations. The cases where this was not the case are shown below with values used.

Aspen: 0.2

Other Deciduous: 0.3

Conifers (including Larch): 0.5

Aerodynamic Attenuation:

This is a coefficient which shapes the decay function of wind through the upper canopy. Personal conversation with Pascal Storck suggested that the decrease of wind through the overstory should result in an understory wind of 10-50% of the wind over the canopy. Experimentation with this parameter suggested that the model was not very sensitive to this parameter in terms of evaporation, and snow accumulation & melt. The resulting decision attempted to reduce the attenuation for more open canopies.

85% closed canopy: 1.0

55% closed: 0.5

30% closed: 0.1

Radiation Attenuation:

Field experiments conducted by Pascal Storck suggest that short wave radiation beneath the canopy is on the order of 10-20% that of open space. The model uses this parameter in conjunction with the LAI value to estimate what percentage of incoming short wave radiation makes it through the canopy to the understory vegetation and / or soil. Using the model's equations, the Radiation Attenuation coefficient was back-calculated for 100% canopy coverage for 15 LAI values and percent transferred values ranging from 10% to 30%, according to:

$$RA = -\ln(F)/LAI$$

where F is the ratio of radiation transmitted through the canopy to radiation incident on the canopy. It was decided to use the higher percentages of transmission for the lower LAI values and the lower percentages for the higher values.

LAI	Desired Transmitted Fraction				
	0.3	0.25	0.2	0.15	0.1
1	1.20	1.39	1.61	1.90	2.30
2	0.60	0.69	0.80	0.95	1.15
3	0.40	0.46	0.54	0.63	0.77
4	0.30	0.35	0.40	0.47	0.58
5	0.24	0.28	0.32	0.38	0.46
6	0.20	0.23	0.27	0.32	0.38
7	0.17	0.20	0.23	0.27	0.33
8	0.15	0.17	0.20	0.24	0.29
9	0.13	0.15	0.18	0.21	0.26
10	0.12	0.14	0.16	0.19	0.23
11	0.11	0.13	0.15	0.17	0.21
12	0.10	0.12	0.13	0.16	0.19
13	0.09	0.11	0.12	0.15	0.18
14	0.09	0.10	0.11	0.14	0.16
15	0.08	0.09	0.11	0.13	0.15

Where variable LAI (for deciduous vegetation) values complicate the method, the coefficient was chosen corresponding to the rightmost column for the canopy closure given the summer LAI. This fixes the lower bound. The reduced winter LAI allows for considerably more radiation to pass.

Maximum Snow Interception Capacity:

Coniferous Evergreens, early: 0.02
Coniferous Evergreens, middle: 0.03
Coniferous Evergreens, late: 0.04
Deciduous: 0.005 m
Mixed Evergreen / Deciduous: 0.02

Snow Interception Efficiency:

Held constant at 0.6

Mass Release Drip Ratio:

Held constant at 0.4

Height:

Estimated from VIC parameters as Vegetation Roughness Height / 0.67

Summer LAI:

Maximum value of monthly VIC LAI

Winter LAI:

Average of monthly VIC LAI Sept.-May

Maximum Resistance:

Overstory fixed at 5000.0 s/m
Understory assigned value of 600.0 or 3000.0 following patterns of past modeling
The model is not expected to be sensitive to this parameter, particularly in the understory.

Minimum Resistance:

Value assigned in VIC parameters.

Moisture Threshold:

Constant at 0.33 and 0.13 for over- under-story values as used in past modeling

Vapor Pressure Deficit:

Constant at 4000.0 for both over- and under-story values as used in past modeling

Rpc:

Constant at 0.108 for both over- and under-story values as used in past modeling

Albedo:

Constant at 0.2 for both over- and under-story values as in VIC parameterization

Number of Root Zones:

Constant at 3

Root Zone Depths:

0.3, 0.2, 0.5 as values provided in the original MICA model prepared by Laura Bowling

Overstory Root Fraction:

Varied according to stage: 0.6, 0.3, 0.1; 0.5, 0.3, 0.2; 0.4, 0.3, 0.3.

Understory Root Fraction:

Fixed for herbaceous types at 0.9, 0.1, 0.0

Fixed for non-herbaceous types (and overstory defined types) as 0.7, 0.3.

Note:

The root zone depths and fractions were used by Wigmosta, et al (1994) as calibration parameters, although he had considerably fewer classes to work with.